The effects of cyanobacteria and dissolved organic carbon on marine trace metal cycling

by

Brendan Alexander Bishop

A thesis submitted in partial fulfillment of the requirements for the degree of

Master of Science

Department of Earth and Atmospheric Sciences
University of Alberta

Abstract

Trace metals have been estimated to be required in one-quarter to one-third of all proteins as cofactors in metalloenzymes which code for numerous crucial biological processes such as respiration, photosynthesis, DNA and RNA synthesis, nitrogen fixation, and electron transfer reactions. However, the marine bioavailability of these trace metals is affected by complexation with microbes and organic ligands. Microbial biomass is an important vector involved in the adsorption and cycling of marine biomass due to its negative surface charge at marine conditions and high surface area to volume ratio. Furthermore, the majority of trace metals in seawater are complexed with dissolved organic ligands. Most of these ligands are produced autochthonously by cyanobacteria who use these ligands to alter the bioavailability of nutrients. Therefore, studying the interplay between microbes, dissolved organic molecules, and trace metals is critical in understanding marine nutrient cycles. Gaining insights into the interplay between biomass and trace metals is also critical for understanding the evolution of metalloenzymes and long-term trace element bioavailability, since it has been hypothesized that metalloenzymes reflect marine nutrient availability at their time of evolution. Furthermore, biomass can also be a sink for trace metals, acting as a sink for trace metals into sediments with these signatures being preserved in the rock record.

This study explores the surface reactivity and adsorption of the bioessential trace elements Co, Ni, Cu, and Zn to the cell wall of the marine cyanobacterium *Synechococcus* sp PCC 7002 and *Synechococcus*-derived dissolved organic carbon using a surface complexation modelling approach. *Synechococcus* and its lysate, an analogue for DOC, have similar surface properties as determined by FTIR analysis and titration data in conjunction with SCM. Titration data for both was modelled using a 3-site protonation model, while FTIR analysis determined the presence of

carboxyl, phosphoryl, hydroxyl, and amine groups. Although the general properties of *Synechococcus* and its lysate were similar, the lysate exhibited lower pK_a values as well as significantly higher site concentrations for each of the sites. Metal binding experiments were performed by means of pH edges to determine the adsorption capacity of *Synechococcus,* followed by surface complexation modelling of the adsorption data to calculate thermodynamic binding constants for each of the metals. These thermodynamic binding constants were then used to predict the adsorption of the metals in a competitive system, where the adsorption pattern of Zn>Cu>Ni>Co was accurately forecasted. This study aims to increase our understanding of the importance of trace metal adsorption to marine organic ligands and their influence on trace metal cycling.

Acknowledgements

First and foremost, I would like to thank my supervisor Dr. Kurt Konhauser for welcoming me into his lab as an undergraduate student and allowing me to further pursue my research as a graduate student. It was an honour to work under such a well-respected scientist and great supervisor. I would also like to thank my co-supervisor Dr. Daniel Alessi for his input and guidance throughout my graduate career and Dr. Murray Gingras for his support.

I would also like to thank Dr. Shannon Flynn for selflessly giving me his time to show me the ropes when I first started in the lab and who taught me how to do "rigorous science", Dr. Samrat Alam for taking the time to teach me the most brutal aspect of surface complexation modelling: FITEQL, and my friends in the lab: Jamie, Tyler, Kaarel, Weiduo, Jason, Logan, Konstantin, Neil, and Salman for their input, support, and willingness to have a pint after a long day of science.

I would never have had the same interest in science from a young age if not for my parents who nurtured my curiosity, and that's undoubtedly why I pursued a career in science. I'll forever be grateful for their love and always pushing me to become better at whatever endeavor I pursued. I would also like to thank Leigha, Tory, countless friends I have met along the way, as well as the continued support from the rest of my family.

Table of Contents

List of Tables

List of Figures

List of abbreviations

BIF: Banded iron formation

BLM: Biotic ligand model

CCM: Constant capacitance model

CRAM: Carboxyl-rich alicyclic molecules

DLS: Dynamic light scattering

DOC: Dissolved organic carbon

DOM: Dissolved organic matter

ESI: Electro-spray ionization

FT-ICR-MS: Fourier transform ion cyclotron resonance mass spectrometry

FTIR: Fourier transform infrared spectroscopy

FIAM: Free ion activity model

g: Force of gravity

GC-MS: Gas chromatography mass spectrometry

ICP-MS: Inductively coupled plasma mass spectrometer

K: Thermodynamic stability constant

HMW: High molecular weight (>1 kDa)

HPLC: High-performance liquid chromatography

LMW: Low molecular weight (<1 kDa)

MCP: Microbial carbon pump

NPOC: Non-purgeable organic carbon

POC: Particulate organic carbon

PPM: Parts per million

pK_a: Acid dissociation constant

PZC: Point of zero charge

RDOC(M): Refractory (or recalcitrant) dissolved organic carbon (matter)

$RDOC_c$: Refractory dissolved organic carbon in context of concentration

$RDOC_t$: Intrinsically refractory dissolved organic carbon

SCM: Surface Complexation Model(ing)

SLDOC: Semi-labile dissolved organic carbon

SPE: Solid phase extractions

TC: Total carbon

TOC: Total organic carbon

TN: Total nitrogen

URDOC: Ultra-refractory dissolved organic carbon

Chapter 1

An introduction to trace metal cycling and surface complexation modelling

1.1 Cyanobacteria and marine trace metal cycling

It has been demonstrated that up to 60% of primary production in the oceans may be attributed to the growth of planktonic cyanobacteria (Fisher, 1985), with some genera, such as *Synechococcus*, reaching densities on the order of 10^4-10^6 cells/mL in the photic zone (Waterbury et al., 1979). Similar to other phytoplankton, these cyanobacteria play an important role in the cycling of trace metals (e.g., Mn, Fe, Co, Ni, Cu, Zn, and Cd) in the oceans through: (1) the generation of reactive organic ligands on their cell walls which adsorb ions from seawater (Dittrich and Sibler, 2005), (2) assimilation for enzymatic use (Bruland et al., 1991; Morel and Price, 2003), and (3) the production of extracellular ligands that complex trace metals and alter their bioavailability (Moffett and Brand, 1996; Worms et al., 2006; Fein, 2017). The net effect of these cellularly controlled processes is the development of seawater "nutrient-like profiles" where uptake by cyanobacteria depletes nutrients in the photic zone, with the nutrients returning to solution in deeper waters due to the degradation of dead bacterial biomass, and eventual replenishing of the photic zone via upwelling currents (Morel, 2008; Sunda, 2012).

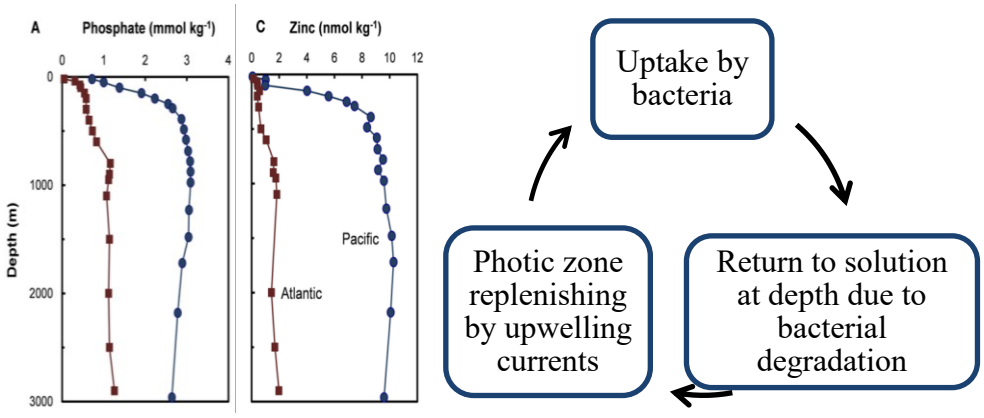

Figure 1.1: Nutrient profile of phosphate and zinc showing decreased surface concentrations due to uptake by bacteria and increasing concentrations with depth. Modified from Sunda et al. 2012.

Twining and Baines (2013) proposed that the assimilation of trace metals reflects both their environmental availability as well as the biochemical demands of phytoplankton. The cellular assimilation of metals occurs by a two-step process in which metals first bind to surface ligands through adsorption, followed by their active transfer across the cell membrane (Morel et al., 1991; Fein, 2017). The assimilation of trace metals from seawater is critical for the cell as it requires metals for various metalloenzymes which are utilized in processes such as photosynthesis, nitrogen fixation, respiration, the uptake of other trace metals, and for accessing organic macronutrients (Morel et al., 1991; Twining and Baines, 2013). In some cases, metals can substitute for one another depending on their environmental availability; for example, *Thalassiorsira weissflogii*, a marine diatom, can substitute Co and Cd for Zn (Price and Morel, 1990). In other cases entirely different proteins can be utilized if a required metal is biolimited (Twining and Baines, 2013).

Sañudo-Wilhelmy et al. (2004) found that phytoplankton are capable of adsorbing anionic trace nutrients such as phosphate, as well as cationic nutrients (e.g., Fe, Mn, and Mo) in laboratory settings using both simulated seawater and natural waters collected from the western Atlantic Ocean. The authors proposed that adsorption of cations to phytoplankton could be equally as important as uptake and assimilation by biological processes in controlling marine nutrient profiles. The ability of bacterial cell wall functional groups to react with protons and metal cations is well-established in the literature (Fein et al., 1997; Cox et al., 1999; Lalonde et al., 2008a; Alessi et al., 2010; Flynn et al., 2014). Although much of the current research has been directed at terrestrial microbes in order to better understand their potential for bioremediation, few studies have focused on planktonic marine cyanobacteria to determine their interactions with ions in seawater. In this regard, Dittrich and Sibler (2005) and Hadjoudja et al. (2010) demonstrated that marine cyanobacterial cell walls have low isoelectric points, as reflected by highly negative surface

charges and low hydrophobicity, and therefore, are capable of efficiently adsorbing trace metals. Cyanobacteria, specifically those of the *Synechococcus* genera, have also been found to be capable of adsorbing trace metals due to their high surface area to volume ratio and highly reactive cell walls (Azam et al., 1983; Fisher, 1985).

More recently, Liu et al. (2015), Martinez et al. (2016), and Gélabert (2018) investigated the surface reactivity of marine cyanobacteria, anoxygenic photosynthetic bacteria that oxidize dissolved iron (photoferrotrophs), and marine and freshwater diatoms, respectively, and demonstrated that they are capable of removing high amounts of metal cations from seawater. However, the Liu et al. (2015) study aimed to provide proof-of-principle, and as such focused only on a single cationic metals system (using Cd^{2+}), and did not consider competitive adsorption, which would be expected in more complex environmental systems. Since oceans are composed of a myriad of inorganic ions, consideration of the effects of competitive adsorption are needed to accurately represent trace metals adsorption in more realistic settings (e.g. Fowle and Fein, 1999; Du et al., 2016; Alam et al., 2017).

1.2 An introduction to bacterial surface reactivity

Since metal adsorption to the cell wall is the first interaction of a metal cation with the cell, the bioavailability of the metal is directly related to its speciation on the cell wall (Fein et al. 2017). Hence, it is important to develop a binding model for bacteria which accurately predicts the speciation, and therefore, bioavailability of metal cations with regards to the cell. Surface complexation modelling offers a method for predicting the adsorptive behaviour of metal cations in the presence of charged surfaces using equilibrium thermodynamics based on experimental metal adsorption data (Fein et al., 1997; Fowle and Fein, 1999). A surface complexation model

(SCM) treats the adsorbed metal as a chemical species whose stability can be quantified with an equilibrium constant, which can then be used to further predict the distribution of metal cations between reservoirs including bacterial surfaces, competing charged surfaces, or other ions in solution (Fein, 2006). For example, the thermodynamic stability constant (K) of a complex between a divalent cation M^{2+} and a negatively-charged surface functional group, $\equiv \mathrm{R-A^-}$, can be represented by:

$$K = \frac{[\equiv \mathrm{R-A-M^+}]}{[\equiv \mathrm{R-A^-}]\, a_{M^{2+}}} \quad (1)$$

where R represents the bacterial cell wall to which the surface functional site, A, is attached. The SCM approach requires information about the reaction stoichiometries, total metal concentration, as well as the type and concentration of surface functional sites and their corresponding pK_a values (Fein, 2006).

The major organic functional groups present in the cell wall that are involved in metal binding include carboxyl, phosphoryl, hydroxyl, and amino groups (Beveridge and Murray, 1980). In the case of *Synechococcus*, as with most bacteria, the cell wall becomes increasingly negatively charged with increasing pH due to the deprotonation of surface functional groups, specifically the carboxyl and phosphoryl sites. These deprotonated surface sites acting as locations for the binding of positively charged ions, but they can also act as nucleation sites for the formation and growth of authigenic mineral phases (Konhauser et al. 1993). The deprotonation of surface functional groups can be described by the following reaction:

$$\equiv \mathrm{R-AH} + OH^- = \mathrm{R} \equiv A^- + H_2O \quad (2)$$

The adsorption of metals to the bacterial surface is likely abiotically driven by the acid/base properties of the cell wall and the affinity of metals for specific surface functional sites (Fein et al. 1997), which is corroborated by evidence that the adsorption of metal cations to cell walls is

reversible (Fowle and Fein, 1999). However, Mullen et al. (1989) discovered that the total amount of metal bound to the cell wall is higher, on a molar basis, if there are multiple competing metals indicating stoichiometric binding to the cell wall is not the only sorption process occurring. Furthermore, different sites can have dissimilar affinities for metal cations depending on metal loading onto the bacterial surfaces. For example, Mishra et al. (2010) found that at very low metal concentrations, sulfhydryl groups dominate metal adsorption, followed by carboxyl and phosphoryl groups as metal loading increases.

Surface complexation modelling has inherent advantages over simpler adsorption models including empirical isotherm models, free ion activity models (FIAM), and biotic ligand models (BLM), because it can account for the effects of pH, metal speciation, complexation, and competing cations on trace metal bioavailability (Fein, 2017). Furthermore, SCMs can be used to predict the fate of metal species in multi-metal, multi-sorbent systems, which has important implications for studying realistic aqueous environments.

1.3 Dissolved organic carbon in seawater

Dissolved organic matter (DOM) is the largest reservoir of fixed carbon in the ocean, and therefore, has a profound influence on marine biogeochemical processes by playing an active role in the global carbon cycle (Hedges, 1987; Hedges, 1992). The dissolved organic carbon (DOC) component makes up approximately half of the marine DOM pool and is involved in various processes including modulating surface temperature, complexing metals, and serving as a precursor phase of fossil fuels (Hedges et al. 2000). The marine DOC pool contains approximately 200 times more carbon than oceanic biomass, acting as the main mediator for the flux of energy from autotrophs to heterotrophs in the ocean, and playing a major role in sustaining marine

bacterial communities (Dittmar and Stubbins, 2014). Previous models have indicated that the cycling of DOM in the ocean is almost entirely driven by marine production (Hansell et al., 2009), with the terrestrial inputs only making up a small fraction of the overall flux to the marine DOM pool (Hedges et al., 1997). Approximately 50% of photosynthetically produced particulate organic carbon (POC) is turned into DOC through processes such as viral lysis, extracellular release, and feeding (Anderson and Tang, 2010), with the major control on DOC production being primary production (Jiao et al., 2010; Carlson and Hansell, 2014). The released, dissolved compounds are up to 20 times more abundant than similar biochemicals in living organisms (Hedges, 1992; Hedges et al., 2000), and have an extremely diverse chemical composition (Moran et al., 2016).

Arguably the most important control on prokaryotic cell numbers which leads to the direct release of DOC in seawater is viral lysis. There are approximately 10^{30} viruses present in the ocean leading to 10^{23} viral infections per second, causing a microbial biomass turnover of 20-50% per day (Suttle, 2007). The release of DOM through lysis has been termed the "viral shunt" where approximately 25% of annual primary production is funneled, producing 3-20 Pg of DOC per year (Wilhelm and Suttle, 1999). The viral shunt returns carbon from particulate to dissolved forms by releasing biomolecules which were stored inside microorganisms. This also alters the Redfield ratio of the DOM, as the amount of carbon relative to nitrogen and phosphorus increase, causing the N and P to be selectively remineralized and released into solution to be used by other microorganisms (Clark et al., 1998; Hopkinson and Vallino, 2005). Furthermore, bacterial lysis can affect trace nutrient cycling, as the viral lysis of prokaryotes can release enough biologically available iron to meet the needs to phytoplankton (Poorvin et al., 2004). Overall, viral lysis can have a profound effect on the recycling of macro- and micro-nutrients in the pelagic zone by releasing assimilated and adsorbed nutrients back into the water column.

Extracellular release involves dissolved organic compounds being released into the surrounding seawater by phytoplankton, with two models having been proposed to explain this phenomenon. The first is the overflow model proposed by Fogg (1966, 1983) and Williams (1990) who hypothesized that when light and nutrient availability are uncoupled, a cell's photosynthate could be produced faster than it can be used by the cell. The second, coined the "passive diffusion model" by Bjørnsen (1988), argues that extracellular release is unintended and passive and is driven by a concentration gradient of low-molecular weight (LMW) photosynthate across the cell membrane. Although the two models are fundamentally different, some evidence exists for each, and it is therefore likely that the dominating model depends on environmental conditions (Carlson and Hansell, 2014).

DOM can also be produced as a consequence of direct excretory release, egestion, sloppy feeding, and leaching from fecal pellets from phytoplankton (Carlson and Hansell, 2014). Sloppy feeding involves the release of DOC by zooplankton that graze on phytoplankton, damaging the cell during the process (Lampert, 1978). Protozoan grazers can release unassimilated DOM such as colloidal material and enzymes through direct excretion and egestion, and up to 40% of ingested algal biomass can be released as DOC (Nagata, 2000).

The majority of the carbon produced from primary production is quickly moved through the food web, and since planktonic organisms have a short life span, they only account for a very small amount of the marine total organic carbon (TOC) pool (Benner and Amon, 2015). POC, which includes the living components such as bacteria, and nonliving suspended and sinking particles makes up less than 2% of TOC in the ocean (Gardner et al. 2006). The high-molecular weight (HMW) (sizes greater than 1 kDa) components of DOC including colloids and gels account

for approximately 22% of marine TOC, while 77% of TOC in the ocean can be attributed to LMW (< 1 kDa) dissolved molecules (Kaiser and Benner, 2009).

Generally, DOM is separated into three major categories. The first is labile DOM, which refers to organic molecules consumed by microbes within hours or days of production; semi-labile DOM is less reactive and has residence times varying from weeks to years, and refractory DOM persists in the ocean for potentially thousands of years, but remains the most poorly characterized fraction (Moran et al., 2016). Marine surface DOM is characterized by a higher DOC fraction and considerably higher amounts of labile compounds compared to the deeper, refractory DOM (Hopkinson et al. 2002); however, Ogawa et al. (2001) have shown that marine bacteria are capable of producing refractory DOM from simple sources. The bulk of the marine DOC is found in the deep-sea and has a high refractory background with residence times of thousands of years based on isotopic analysis (Williams and Druffel, 1987; Druffel et al., 2016).

Although the vast majority of compounds that comprise marine DOC have yet to be identified, recent studies are unravelling the composition of this important carbon pool. Early researchers used tangential flow ultra-filtration to isolate various components of DOM. For example, Benner et al. (1992) used this technique to demonstrate that polysaccharides could comprise up to 50% of the DOC found in surface waters and up to 25% in deeper samples in the North Pacific Ocean, whereas Tanoue et al. (1995) determined that proteins derived from cell membranes could contribute to the DOM pool. More recent techniques including electrospray ionization mass spectrometry (ESI-MS) coupled with Fourier transform ion cyclotron resonance mass spectrometry (FT-ICR-MS) are broadening our understanding of the basic composition of DOM and DOC (e.g. Kim et al., 2003; Koch et al., 2005; Schmidt et al., 2009; Dittmar and Stubbins, 2014; Zark et al. 2017). For example, Hertkorn et al. (2006) characterized ultra-filtered

DOM from waters in the mid Pacific Ocean and discovered a large amount of the refractory component was composed of carboxyl-rich alicyclic compounds (CRAM). However, FT-ICR-MS only provides information about the chemical composition of these molecules, and not their chemical structure. Accordingly, Fatayer et al (2018) employed the use of Atomic Force Microscopy in order to image the chemical structures of LMW DOC from the North Central Pacific and determined many of the compounds which compose DOC are polycyclic aromatic compounds with less than five aromatic rings.

1.4 Aims of this study

Since marine trace metal availability is strongly influenced by adsorption onto cyanobacteria and complexation by dissolved ligands in the water column, developing a model to quantify their partitioning in the water column is important for understanding marine chemistry. The aim of this study is to determine the metal binding capacity of the marine cyanobacterium *Synechococcus* sp. PCC 7002 and its lysate, an analogue for DOC, using a surface complexation modelling approach.

The first part of this work builds on a previous investigation by Liu et al. (2015) where the proton reactivity and Cd binding capacity of the *Synechococcus* cell wall was determined. Here, I examine the ability of *Synechococcus* to adsorb a suite of bioessential trace metals including Co, Ni, Cu, and Zn and develop a robust surface complexation model which is then used to predict the behaviour of these trace metals in systems containing multiple metals, where there exists competition among metals for sorption to cell wall functional groups. Furthermore, the potential for *Synechococcus* to behave as an exit pathway for these trace metals into ancient sediments is assessed.

In the second part of this study, I investigate the cell lysate from the marine cyanobacterium

Synechococcus sp. PCC 7002 as an analogue for marine DOC and compare the differences in surface reactivity between intact cells and cell lysates and study their effects on the cycling of bioessential trace elements using a complexation modelling approach. Consequently, this study will aim to assist in increasing our understanding of the importance of DOC in the cycling of marine trace metals.

By better understanding the processes which affect trace element cycles in the ocean, the fluxes of trace metals through the water column and their eventual incorporation into sediments can be better determined. Constraining the concentrations of marine elements through time is important for studying the evolution of the marine biosphere because it has been thought that trace elements in modern metalloenzymes reflect the availability of trace elements in seawater at their time of evolution (Robbins et al. 2016).

References

Alam Md. S., Swaren L., von Gunten, K., Cossio M., Bishop B., Robbins L. J., Hou D., Flynn S. L., Ok Y. S., Konhauser K. O., Alessi D. S. (2018) Application of surface complexation modeling to trace metals uptake by biochar-amended agricultural soils. *App. Geochem.* **88**, 103-112.

Alessi D. S., Henderson J. M., Fein J. B. (2010) Experimental Measurement of Monovalent Cation Adsorption onto Bacillus subtilis Cells. *Geomicrobiol. J.* **27**, 464–472.

Anderson T. R. and Tang K. W. (2010) Carbon cycling and POC turnover in the mesopelagic zone of the ocean: Insights from a simple model. *Deep. Res. Part II Top. Stud. Oceanogr.* **57**, 1581–1592.

Azam F., Fenchel T., Field J. G., Gray J. S., Meyer-Reil L. A. and Thingstad F. (1983) The Ecological Role of Water-Column Microbes in the Sea. *Mar. Ecol. Prog. Ser.* **10**, 257–263.

Benner R. and Amon R. M. W. (2015) The Size-Reactivity Continuum of Major Bioelements in the Ocean. *Ann. Rev. Mar. Sci.* **7**, 185–205.

Benner R., Pakulski J. D., Mccarthy M., Hedges J. I. and Hatcher P. G. (1992) Bulk Chemical Characteristics of Dissolved Organic Matter in the Ocean. *Science.* **255**, 1561–1564.

Beveridge T. J. and Murray R. G. E. (1980) Sites of metal deposition in the cell wall of Bacillus subtilis. *J. Bacteriol.* **141**, 876–887.

Bjørnsen P. K. (1988). Phytoplankton exudation of organic matter: why do healthy cells do it? *Limnol. Oceanogr.* **33**, 151-154.

Bruland K. W., Donat J. R. and Hutchins D. A. (1991) Interactive influences of bioactive trace metals on biological production in oceanic waters. *Limnol. Oceanogr.* **36**, 1555–1577.

Carlson C. A. and Hansell D. A. (2014) *DOM Sources, Sinks, Reactivity, and Budgets.* in Biogeochemistry of Marine Dissolved Organic Matter: 2nd ed. Elsevier Inc.

Clark L. L., Ingal E. D. and Benner R. (1998) Marine phorphorus is selectively remineralized. *Nature* **393,** 426

Cox J. S., Smith D. S., Warren L. A., Ferris F. G. (1999). Characterizing heterogeneous bacterial surface functional groups using discrete affinity spectra for proton binding. *Environ. Sci. Technol.* **33**, 4514–4521.

Dittmar T. and Stubbins A. (2014) Dissolved Organic Matter in Aquatic Systems. In *Treatise on Geochemistry 2nd ed*. 125-156. Elsevier Ltd.

Dittrich M. and Sibler S. (2005) Cell surface groups of two picocyanobacteria strains studied by zeta potential investigations, potentiometric titration, and infrared spectroscopy. *J. Colloid and Interface Sci.* **286**, 487–495.

Druffel E. R. M., Griffin S., Coppola A. I. and Walker B. D. (2016) Radiocarbon in dissolved organic carbon of the Atlantic Ocean. *Geophys. Res. Lett.* **43**, 5279–5286.

Du H., Chen W., Cai P., Rong X., Feng X. and Huang Q. (2016) Competitive adsorption of Pb and Cd on bacteria–montmorillonite composite. *Environ. Pollut.* **218**, 168–175.

Fatayer S., Coppola A. I., Schulz F., Walker B. D., Broek T. A., Meyer G., Druffel E. R. M., McCarthy M. and Gross L. (2018) Direct Visualization of Individual Aromatic Compound Structures in Low Molecular Weight Marine Dissolved Organic Carbon. *Geophys. Res. Lett.*, 1–9.

Fein J. B. (2017) Advanced biotic ligand models: Using surface complexation modeling to quantify metal bioavailability to bacteria in geologic systems. *Chem. Geol.* **464**, 127–136.

Fein J. B. (2006) Thermodynamic Modeling of Metal Adsorption onto Bacterial Cell Walls: Current Challenges. *Adv. Agron.* **90**, 179–202.

Fein J. B., Daughney C. J., Yee, N., Davis T. A. (1997) A chemical equilibrium model for metal adsorption onto bacterial surfaces. *Geochim. Cosmochim. Acta.* **61** (16), 3319-3328

Fisher N. S. (1985) Accumulation of metals by marine phytoplankton. *Mar. Biol.* **87**, 137–142.

Flynn S. L., Szymanowski J. E. S. and Fein J. B. (2014) Modeling bacterial metal toxicity using a surface complexation approach. *Chem. Geol.* **374**–**375**, 110–116.

Fogg G. (1983). The ecological significance of extracellular products of phytoplankton. *Bot. Mar.* **26**. 3-14

Fogg G. (1966). The extracellular products of algae. *Oceanogr. Mar. Bio. Annu. Rev.* **4**, 195-212

Fowle D. A. and Fein J. B. (1999) Competitive adsorption of metal cations onto two gram positive bacteria: Testing the chemical equilibrium model. *Geochim. Cosmochim. Acta.* **63**, 3059–3067.

Gardner WD, Mishonov AV, Richardson MJ. (2006). Global POC concentrations from in-situ and satellite data. *Deep-Sea Res. II.* **53,** 718–740

Gélabert A., Pokrovsky O. S., Schott J. and Feurtet-Mazel A. (2018) Surface complexation modeling of interactions between freshwater and marine diatom species and trace elements (Mo, W, Cr, Ge, Ga, Al). *Chem. Geol.* **494**, 117–126.

Hadjoudja, S., Deluchat, V. and Baudu, M. (2010). Cell surface characterization of *Microcystis aeruginosa* and *Chlorella vulgaris*. *J. Colloid Interface Sci.* **342,** 293-299.

Hansell D., Carlson C., Repeta D. and Schlitzer R. (2009) Dissolved Organic Matter in the Ocean: A Controversy Stimulates New Insights. *Oceanography* **22**, 202–211.

Hedges J. I. (1992) Global Biogeochemical Cycles - Progress and Problems. *Mar. Chem.* **39**, 67–93.

Hedges J. I. (1987) Organic matter in sea water. *Nature* **330**, 205–206.

Hedges J. I., Eglinton G., Hatcher P. G., Kirchman D. L., Arnosti C., Derenne S., Evershed R. P., K.ogel-Knabner I., de Leeuw J. W., Littke R., Michaelis W. and Rullkotter J. (2000) The molecularly uncharacter ized component of nonliving organic matter in natural environments. *Org. Geochem.* **31**, 945–958.

Hedges J. I., Keil R. G. and Benner R. (1997) What happens to terrestrial organic matter in the ocean? *Org. Geochem.* **27**, 195–212.

Hertkorn N., Benner R., Frommberger M., Schmitt-Kopplin P., Witt M., Kaiser K., Kettrup A. and Hedges J. I. (2006) Characterization of a major refractory component of marine dissolved organic matter. *Geochim. Cosmochim. Acta* **70**, 2990–3010.

Hopkinson C. S. and Vallino J. J. (2005) Efficient export of carbon to the deep ocean through dissolved organic matter. *Nature* **433**, 142–145.

Hopkinson C. S., Vallino J. J. and Nolin A. (2002) Decomposition of dissolved organic matter from the continental margin. *Deep. Res. Part II Top. Stud. Oceanogr.* **49**, 4461–4478.

Jiao N., Herndl G. J., Hansell D. A., Benner R., Kattner G., Wilhelm S. W., Kirchman D. L., Weinbauer M. G., Luo T., Chen F. and Azam F. (2010) Microbial production of recalcitrant dissolved organic matter: Long-term carbon storage in the global ocean. *Nat. Rev. Microbiol.* **8**, 593–599.

Kaiser K. and Benner R. (2009). Biochemical composition and size distribution of organic matter at the Pacific and Atlantic time-series stations. *Mar. Chem.* **113**, 63–77.

Kim S., Kramer R. W. and Hatcher P. G. (2003) Graphical Method for Analysis of Ultrahigh-Resolution Broadband Mass Spectra of Natural Organic Matter, the Van Krevelen Diagram. *Anal. Chem.* **75**, 5336–5344.

Koch B. P., Witt M., Engbrodt R., Dittmar T. and Kattner G. (2005) Molecular formulae of marine and terrigenous dissolved organic matter detected by electrospray ionization Fourier transform ion cyclotron resonance mass spectrometry. *Geochim. Cosmochim. Acta* **69**, 3299–3308.

Konhauser K. O., Fyfe W. S., Ferris F. G. and Beveridge T. J. (1993) Metal sorption and mineral precipitation by bacteria in two Amazonian river systems: Rio Solimoes and Rio Negro, Brazil. *Geology* **21**, 1103–1106.

Lalonde S. V., Smith D. S., Owttrim G. W., Konhauser K. O. (2008) Acid-base properties of cyanobacterial surfaces. II: Silica as a chemical stressor influencing cell surface reactivity. *Geochim. Cosmochim. Acta* **72**, 1269–1280.

Lampert W. (1978). Release of dissolved organic carbon by grazing zooplankton. *Limnol. Oceanogr.* **23**, 831-834.

Liu Y., Alessi D. S., Owttrim G. W., Petrash D. A., Mloszewska A. M., Lalonde S. V., Martinez R. E., Zhou Q. and Konhauser K. O. (2015) Cell surface reactivity of Synechococcus sp. PCC 7002: Implications for metal sorption from seawater. *Geochim. Cosmochim. Acta* **169**, 30–44

Martinez R. E., Konhauser K. O., Paunova N., Wu W., Alessi D. S. and Kappler A. (2016) Surface reactivity of the anaerobic phototrophic Fe(II)-oxidizing bacterium Rhodovulum iodosum: Implications for trace metal budgets in ancient oceans and banded iron formations. *Chem. Geol.* **442**, 113–120.

Mishra B., Boyanov M., Bunker B. A., Kelly S. D., Kemner K. M. and Fein J. B. (2010) High- and low-affinity binding sites for Cd on the bacterial cell walls of Bacillus subtilis and Shewanella oneidensis. *Geochim. Cosmochim. Acta* **74**, 4219–4233.

Moffett J. W. and Brand L. E. (1996) Production of strong, extracellular Cu chelators by marine cyanobacteria in response to Cu stress. *Limnology and Oceanography.* **41**(3), 388–395.

Moran M. A., Kujawinski E. B., Stubbins A., Fatland R., Aluwihare L. I., Buchan A., Crump B. C., Dorrestein P. C., Dyhrman S. T., Hess N. J., Howe B., Longnecker K., Medeiros P. M., Niggemann J., Obernosterer I., Repeta D. J. and Waldbauer J. R. (2016) Deciphering ocean carbon in a changing world. *Proc. Natl. Acad. Sci.* **113**, 3143–3151.

Morel, F. M. M. (2008) The co-evolution of phytoplankton and trace element cycles in the oceans. *Geobiology* **6**, 318–324.

Morel F.M. M. and Price N. (2003) The biogeochemical cycles of trace metals in the ocean. *Science* **300**, 944–947.

Morel, F. M. M., Hudson, R. J. M., Price, N. M. (1991) Limitation of productivity by trace metals in the sea. *Limnology and Oceanography.* **36** (8), 1742–1755.

Mullen M. D., Wolf D. C., Ferris F. G., Beveridge T. J., Flemming C. A. and Bailey G. W. (1989) Bacterial sorption of heavy metals. *Appl. Environ. Microbiol.* **55**, 3143–3149.

Nagata T. (2000). Production mechanisms of dissolved organic matter. In: *Microbial Ecology of the Oceans*. Wiley-Liss, New York, 121–152.

Ogawa H., Amagai Y., Koike I., Kaiser K. and Benner R. (2001) Production of refractory dissolved organic matter by bacteria. *Science.* **292**, 917–920.

Poorvin L., Rinta-Kanto J. M., Hutchins D. A. and Wilhelm S. W. (2004) Viral release of iron and its bioavailability to marine plankton. *Limnol. Oceanogr.* **49**, 1734–1741.

Price, N. M., Morel, F. M. M. (1990) Cadmium and cobalt substitution for zinc in a marine diatom. *Nature* **344**, 658–660.

Robbins L. J., Lalonde S. V., Planavsky N. J., Partin C. A., Reinhard C. T., Kendall B., Scott C., Hardisty D. S., Gill B. C., Alessi D. S., Dupont C. L., Saito M. A., Crowe S. A., Poulton S. W., Bekker A., Lyons T. W. and Konhauser K. O. (2016) Trace elements at the intersection of marine biological and geochemical evolution. *Earth-Science Rev.* **163**, 323–348.

Sañudo-Wilhelmy, S. A., Tovar-Sanchez, A., Fu, F., Capone, D. G., Carpenter, E. J., Hutchins, D. A. (2004). The impact of surface-adsorbed phosphorus on phytoplankton Redfield stoichiometry. *Nature*. **432**, 897-901.

Schmidt F., Elvert M., Koch B. P., Witt M. and Hinrichs K. U. (2009) Molecular characterization of dissolved organic matter in pore water of continental shelf sediments. *Geochim. Cosmochim. Acta* **73**, 3337–3358.

Sunda, W. G. (2012) Feedback interactions between trace metal nutrients and phytoplankton in the ocean. *Frontiers in Microbiology.* **3** (1-22).

Suttle C. A. (2007) Marine viruses - Major players in the global ecosystem. *Nat. Rev. Microbiol.* **5**, 801–812.

Tanoue E., Nishiyama S., Kamo M. and Tsugita' A. (1995) Bacterial membranes: Possible source of a major dissolved protein in seawater. *Geochim. Cosmochim. Acta* **59**, 2643–2648.

Twining B. S. and Baines S. B. (2013) The trace metal composition of marine phytoplankton. *Annual Review of Marine Science.* **5**, 191–215.

Waterbury J. B., Watson S. W., Guillard R. R. L. and Brand L. E. (1979) Widespread occurance of a unicellular, marine, planktonic, cyanobacterium. *Nature* **277**, 293–294.

Wilhelm S. W. and Suttle C. A. (1999) Viruses and Nutrient Cycles in the Sea. *Bioscience* **49**, 781–788.

Williams P. J. L. B. (1990). The importance of losses during microbial growth: commentary on the physiology, measurement and ecologe of the release of dissolved organic material. *Mar. Microb. Food Webs.* **4**, 175-206.

Williams P. M. and Druffel E. R. M. (1987) Radiocarbon in dissolved organic matter in the central North Pacific Ocean. *Nature* **330**, 246–248.

Worms I., Simon D. F., Hassler C. S. and Wilkinson K. J. (2006) Bioavailability of trace metals to aquatic microorganisms: importance of chemical, biological and physical processes on biouptake. *Biochimie.* **88**, 1721–1731.

Zark M., Christoffers J. and Dittmar T. (2017) Molecular properties of deep-sea dissolved organic matter are predictable by the central limit theorem: Evidence from tandem FT-ICR-MS. *Mar. Chem.* **191**, 9–15.

Chapter 2

Adsorption of biologically critical trace elements to the cyanobacterium *Synechococcus* sp. PCC 7002: Implications for marine trace metal cycling

2.1 Introduction

Major nutrients such as phosphorus are thought to control primary productivity throughout much of the ocean, however, trace nutrients including Fe, Co, Ni, Cu, and Zn play important physiological roles in biogeochemical cycles and can also affect primary productivity. Whereas macronutrients are important for macro-molecular synthesis (Zehr and Ward, 2002), trace metals are important as cofactors in metalloenzymes (Morel and Price, 2003). Trace metals have inherent differences in their speciation, reactivity, and complexation than do macronutrients, and therefore, their cycling in the oceans differ due to adsorption to organic ligands and changes in oxidation state which alter their solubility and bioavailability (Bruland et al. 2014). Macronutrients can occur in different forms; for example, in the case of nitrogen, *Prochlorococcus* targets for ammonium whereas *Synechococcus* targets for nitrate to meet their cellular quotas (Boyd et al., 2017). However, these preferences are less understood for trace metals because of uncertainties in how metal-binding ligands influence their bioavailability (Bruland and Lohan, 2003).

In order for these trace metals to be cycled through the oceans, they must initially be retained through both biotic and abiotic mechanisms (Boyd et al. 2017), with external supply mostly occurring during the winter (Tagliabue et al. 2014). However the interactions between these mechanisms remains largely unknown, although the crucial linkage between the two may be organic ligands (Boyd et al., 2017). Since micro-organisms account for the majority of exposed biotic surface area in the ocean (Jiao et al., 2010), they can have a significant impact on the cycling of trace elements through adsorption. Although previous studies such as Liu et al. (2015) attempted

to characterize the metal binding of Cd to *Synechococcus* over a range of ionic strengths, it neglected to consider adsorption of bioessential trace metals and the effects of competitive adsorption. Accordingly, this chapter explores the adsorption of Co, Ni, Cu, and Zn to the cyanobacterium *Synechococcus* sp. PCC 7002 using a surface complexation modelling approach. Site pK_a and concentration values were determined by modeling potentiometric titration data using the computer software FITEQL 4.0 (Hebelin and Westall, 1999). These values were then combined with metal adsorption pH edge data to solve for the thermodynamic metal binding constants for the *Synechococcus* cell wall-metal complexes, with these constants then being used as the basis for a model which was able to accurately predict the behaviour of the trace elements when all four were tested in a competitive system. This is one of the first studies to quantitatively explore the effects of metals adsorption to cyanobacteria and its effects on trace metal cycling and is also among the first to demonstrate the value of surface complexation modelling for predicting the behaviour of trace metals in marine systems when multiple sorbates are present.

2.2 Methods

2.2.1 Bacterial growth

The cyanobacterial strain *Synechococcus* sp. PCC 7002 (referred to hereafter as *Synechococcus*) was aerobically cultured on A+ medium (Stevens and Van Baalen, 1973; Stevens and Porter, 1980) agar plates with a light intensity of 50 mmol photons m^{-2} s^{-1} at 30°C for 14 days. Once a suitable colony developed on the plate, cells were harvested using an inoculation loop and inoculated in 50 mL of A+ media at 30°C for 3 days. Cells were then transferred to a 1 L Erlenmeyer flask with an additional 350 mL of A+ media and rotated at 100 rpm for 10 days until the stationary growth phase was reached. Aeration was provided throughout by bubbling with filtered, humidified air. The cells were harvested by centrifugation at 10000 g for eight minutes and washed with 0.56 M

NaCl (a representative seawater concentration) five times to remove any residual growth media and competing metals from cell wall surface sites. Following each wash, the bacteria were resuspended in a fresh electrolyte solution and a new pellet of bacteria was formed by centrifugation and the supernatant decanted. After the final wash, the bacteria were centrifuged twice for 30 min to remove as much water from the biomass as possible. The wet mass of bacteria was then determined, and the pelleted cells were suspended in 0.56 M NaCl to the desired concentration.

2.2.2 Potentiometric titrations

Potentiometric titrations were conducted for comparison with the Liu et al (2015) study in accordance with previously established protocols in our laboratory (e.g., Petrash et al., 2011; Warchola et al., 2017; Alam et al., 2018), in which the addition of aliquots of base induce the progressive deprotonation of organic functional groups at the bacterial surface. All plastic and glassware used for the titrations were soaked in 10% HCl for a minimum of 24 h, rinsed three times in 18.2 MΩ•cm water, and allowed to air-dry while inverted. Before each titration, 0.05 g (wet mass) of washed *Synechoccocus* cells were suspended in 50 mL of 0.56 M NaCl, to achieve a final concentration of 2.5 g L^{-1}. The titrations were conducted under a N_2 atmosphere and titration solutions were purged with N_2 gas for 30 min prior to commencement of the titration to establish and maintain a CO_2 free environment in the titration vessel. Throughout the titration, pH was measured using a glass electrode (Metrohm), calibrated in advance using commercially available buffers (Thermo Fisher Scientific). Titrations were performed alkalimetrically from pH 3 to 10 by initially acidifying the solution to pH 3 with 0.1 M HCl, followed by incremental additions of 0.1 M NaOH until pH 10 was reached. The volume of base added, and the corresponding pH change,

were recorded for each titration step. A "down-titration" was then performed with the addition of 0.1 M HCl to pH 3 to determine the reversibility of proton binding and if hysteresis between the "up" and "down" titrations had occurred, which would be an indicator for titration-induced cell damage. All titrations were performed in dynamic addition mode whereby the titrator adds a variable amount of either HCl or NaOH depending on the instantaneous buffering capacity, as per Alam et al. (2018). Subsequent additions of acid or base were only made once the pH electrode achieved a stability of 0.2 mV s^{-1}. Blank titrations of the 0.56 M NaCl background solution were conducted to quantify the background proton buffering capacity, which was then subtracted from the *Synechococcus* titration data before modeling to determine cell wall functional group concentrations and proton binding constants (pK_a values).

The titration data was evaluated in terms of excess charge, where the reactivity of the background electrolyte was subtracted from the total reactivity of the solution so only the reactivity of the *Synechococcus* was modelled (Lalonde et al., 2008a; Lalonde et al., 2010). A least-squares optimization method was then applied using FITEQL v. 4.0 (Herbelin and Westall, 1999) to determine surface site acidity constants and ligand site concentrations based on the titration data.

2.2.3 Metal adsorption experiments

Adsorption experiments were conducted by measuring the change in the aqueous trace metal concentrations before and after exposure to pre-washed *Synechococcus* cells. The metal stock solutions were prepared by diluting a 1000 ppm standard solution of either Co, Ni, Cu, or Zn in 0.56 M NaCl to achieve a concentration of 10 ppm. A known mass of *Synechococcus* cells were suspended in the metal solution to achieve a wet mass concentration of 5 g L^{-1}. Aliquots of 10 mL of the bacteria-metal solution were then partitioned into 50 mL polypropylene test tubes and the

pH of each was adjusted twice using aliquots of 0.01 M HCl or NaOH to bring the samples within the desired pH range of 3 to 9, at approximately 0.5 pH unit intervals. Each sample was mixed via end-over-end rotation at 40 rpm for 6 h to allow for equilibration between the metal-containing solution and the cellular surfaces.

Following equilibration, the final pH of each experiment was measured, and the solutions were centrifuged at 10000 g for 5 min to remove the cells. The supernatant was filtered through 0.2 μm nylon membranes and diluted 1:10 in 2% nitric acid before trace metal analysis by Inductively Coupled Plasma Mass Spectrometry (ICP-MS/MS) using an Agilent 8800 Triple Quad. Before each analysis, a series of external standards prepared from commercially available ICP-MS standards were run. Controls containing the metal and 0.56 M NaCl background solutions were also analyzed to determine whether metal was lost by adsorption to the experimental apparatus.

Multi-element pH edges were performed using the same protocol as described above. However, to maintain a similar total metal concentration, 2.5 ppm of each of the four tested metals (Co, Cu, Ni, and Zn) were added, for a total of 10 ppm trace metal.

2.3. Results/Discussion

2.3.1 *Synechococcus* surface reactivity

Figure 1.1 shows the titration data for 2.5 g L^{-1} (wet mass) *Synechococcus* in 0.56 M NaCl electrolyte, plotted in terms of mmol of deprotonated sites (excess charge) per gram of bacteria. The slope at any point of the titration curve gives the instantaneous buffering capacity of the *Synechococcus* suspension at that specific pH, which corresponds to the rate of deprotonation of the surface ligands.

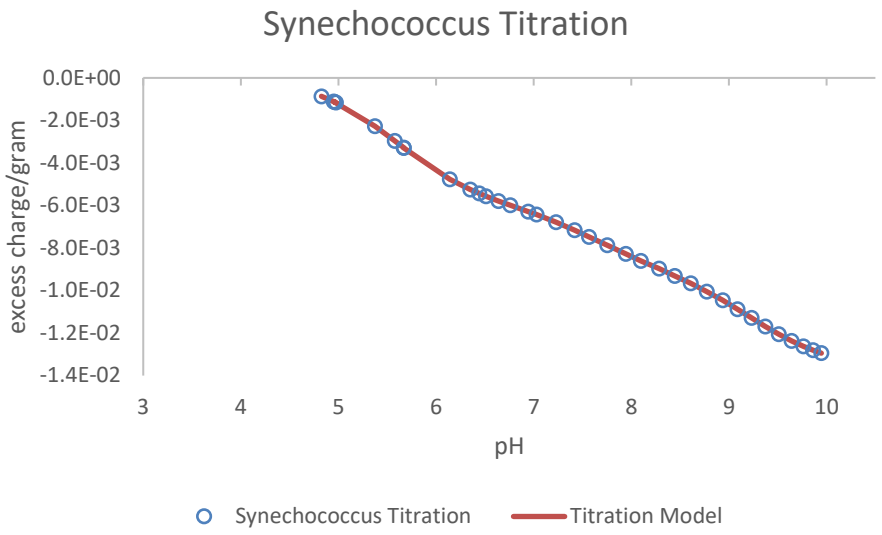

Figure 2.1 Titration data in terms of excess charge per gram of *Synechococcus* cells plotted with the FITEQL protonation model.

The titration data indicate that *Synechococcus* has a high buffering capacity over the pH range measured, with greatest changes in excess charge occurring at low (<4.5) and high (>8) pH values. Bacterial ligand concentrations and acid neutralizing capacity were determined from titration data using a pK_a spectrum approach similar to Lalonde et al. (2008b). The number of potential pK_a values is fixed in FITEQL 4.0 (Herbelin and Westall, 1999), which then optimizes for both the pK_a values and their corresponding site concentrations. The regions of the titration curve with the greatest slope represent regions in which the buffering capacity of the cells is greatest, and therefore, correlate with the functional group pK_a values. Minimal hysteresis was observed between the up and down titrations, indicating there was no measurable cell damage and that the protonation and deprotonation of cell wall functional groups was highly reversible.

Protonation models with 1-4 sites were tested, and a model employing three proton active sites provided the best statistical fit to the titration data based on the FITEQL variance parameter V(Y). This result, combined with previous Fourier transform infrared (FTIR) spectroscopy performed on bacteria (Jiang et al., 2004; Yee et al., 2004; Liu et al., 2015), suggests that the

bacterial cell surfaces have four primary types of proton-active functional groups, carboxyl groups which deprotonate at acidic pH values, phosphoryl groups which deprotonate at circumneutral pH, and amino and hydroxyl groups, both of which deprotonate at alkaline pH values.

The mass action equations for the deprotonation of each type of surface ligand can be described by the following balanced chemical reactions:

$$\equiv R\text{-}COOH + OH^- = R\equiv COO^- + H_2O \quad [1]$$

$$\equiv R\text{-}PO_4H_2 + OH^- = R\equiv PO_4H^- + H_2O \quad [2]$$

$$\equiv R\text{-}NH_3^+ + OH^- = R\equiv NH_2 + H_2O \quad [3]$$

$$\equiv R\text{-}OH + OH^- = R\equiv O^- + H_2O \quad [4]$$

where ≡R represents the cell wall of the *Synechococcus* cell to which a proton-active surface functional group is attached. Equations 3 and 4 both correspond to site 3, as these two sites have been found to have similar pK_a values (Fein et al., 1997), however it is best interpreted as an amine site, as hydroxyl sites with pK_a values ~10 generally occur only for phenol groups (Cox et al., 1999).

Previous studies have shown that the surface charge of the cell wall is strongly pH dependent; increasing pH drives the deprotonation of the organic ligands on the cell wall, leaving the cell wall with a net negative charge (e.g., Fein et al., 1997; Cox et al., 1999). Indeed, zeta potential measurements by Liu et al (2015) determined that *Synechococcus* has a point of zero charge (PZC) below pH 4, and hence a net negative surface charge at marine pH. The negatively charged surface is composed of discrete surface sites that can bind metal cations, or act as nucleation sites for the growth of authigenic mineral phases (e.g. Konhauser et al. 1998).

The trend towards a net negative surface charge with increasing pH is mainly caused by the deprotonation of carboxyl and phosphoryl surface sites (reactions 1 and 2) below circumneutral

pH. The positively charged amino groups are generally less abundant and have a smaller impact on the overall surface charge of the cell than either carboxyl or phosphoryl groups. This has been corroborated by titration results that indicate higher site densities for both the carboxyl (Site 1) and phosphoryl (Site 2) ligands relative to the amino/hydroxyl groups (Site 3).

Site	pKa	Site concentration (mol/gram)	Functional group
1	5.59	2.389×10^{-3}	Carboxyl
2	7.61	1.244×10^{-3}	Phosphoryl
3	9.24	1.860×10^{-3}	Amino/Hydroxyl

Table 2.1 Potentiometric titration data in terms of site pK_a, site concentration (mol/g), and proposed functional group from Liu et al. (2015).

2.3.2 Single metal adsorption experiments

2.3.2.1 Surface complexation modelling

The negatively charged, deprotonated sites on the cyanobacterial cells resulting from an increased pH act as loci for the binding of metal cations. Site pK_a values and ligand densities determined from the titration data were combined with pH edge metal adsorption data to calculate the equilibrium metal binding constants using FITEQL. In this regard, a model that invoked metal binding to the carboxyl and phosphoryl groups best explains the experimental metal adsorption edge data. Metal binding to amino/hydroxyl groups were not important, as the pK_a value (9.24) was outside of the experimental range of the pH edge experiments, and even at pH 9, approximately 70% of these functional groups remain protonated. Mass action equations corresponding to each ligand can be used to predict the equilibrium state in more complex systems, including those in which multiple metals compete for adsorption to bacterial surface functional groups (Fowle and Fein, 1999). The balanced chemical reactions for divalent cation (M^{2+}) adsorption onto carboxyl and phosphoryl groups, respectively, are:

$$\equiv R\text{-}COO^- + M^{2+} = R\equiv COO\text{-}M^+ \qquad [5]$$

$\equiv R\text{-}PO_4H^- + M^{2+} = R\equiv PO_4H\text{-}M^+$ [6]

with ≡R representing the cellular surface to which functional group A is attached, and M representing the divalent metal cation. The metal binding constants (K) can be determined for each of the 2 sites in equations (5) and (6) above as follows:

$$K = \frac{[R\equiv COO-M^+]}{[[R\equiv COO^-]a]_{M^{2+}}} \quad [7]$$

$$K = \frac{[R\equiv PO_4H-M^+]}{[[R\equiv PO_4H^-]a]_{M^{2+}}} \quad [8]$$

2.3.2.2 Metal adsorption to *Synechococcus*

Adsorption edges for trace metals to *Synechococcus* were generated for a pH range between 3 and 9 at an ionic strength of 0.56 M. Figure 1.2 shows the percentage of each trace metal removed from solution by the bacteria, plotted with the corresponding best-fit surface complexation model calculated in FITEQL. In all cases, at low pH, the organic cell wall functional groups are nearly completely protonated, hence minimal adsorption of metal cations occurs. However, as pH increases, and functional groups progressively deprotonate, the now negatively-charged sites become available for cation binding. All metals investigated in this study reached maximum adsorption as pH approached 8.

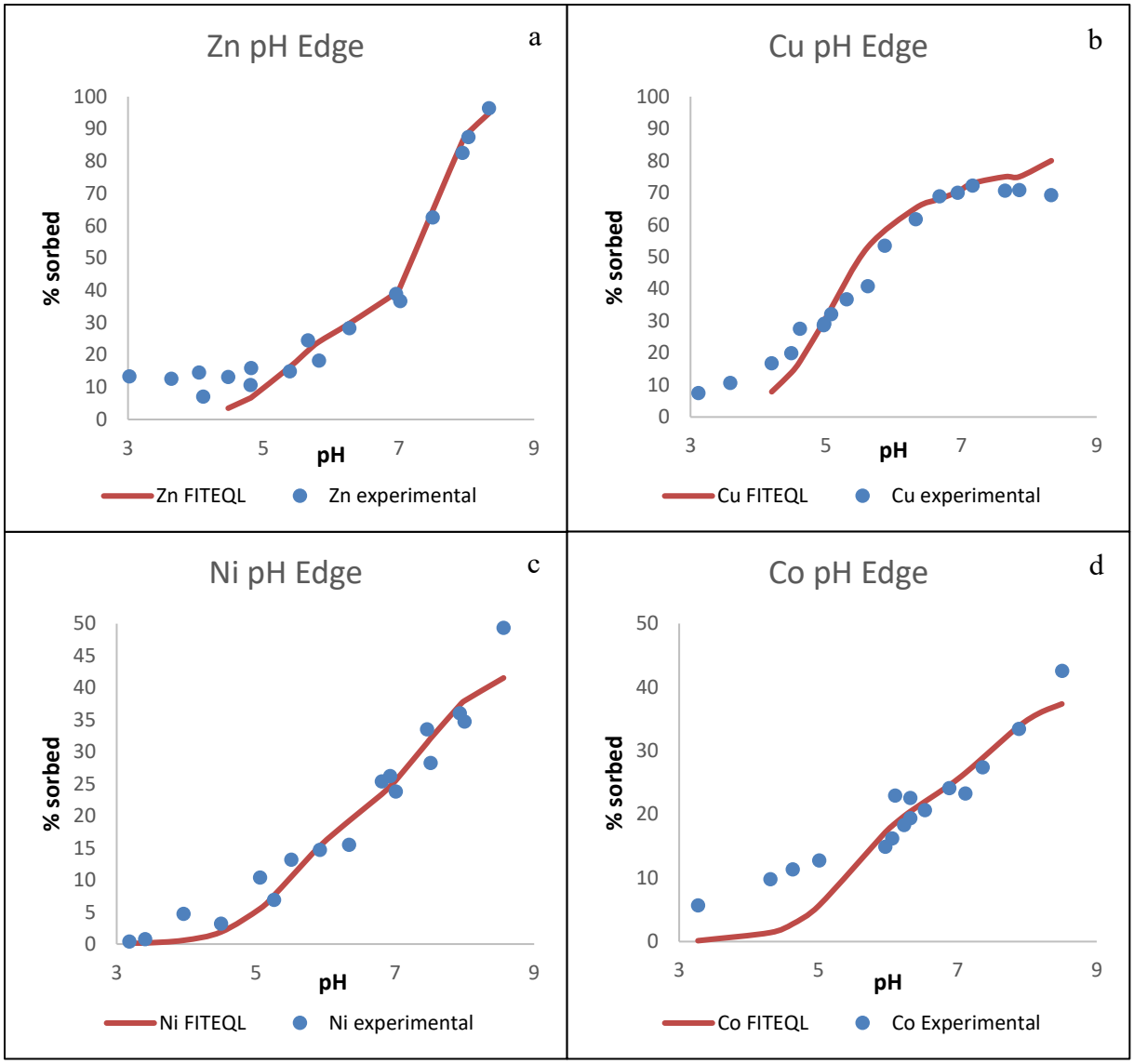

Figure 2.2(a-d) Metal adsorption pH edges in terms of percent adsorption vs pH for each of the metals studied plotted alongside the best-fit SCM.

Geochemical modelling using the programs PHREEQC and Geochemist's Workbench indicated that limited Cu and Co phases were above saturation, and no Ni or Zn phases occurred above saturation. These phases (malachite, azurite, tenorite, Co_3O_4), however, are characteristic of phases produced during the weathering of ore deposits or synthetic phases formed at high-temperature. Accordingly, we consider that these phases are likely to be kinetically facile at our

experimental conditions and exert minimal influence on the adsorption of these trace metals by *Synechococcus*.

Synechococcus has differing affinities for each metal cation. Zn and Cu were most removed from the simulated seawater, followed by Ni and Co. This is consistent with the Irving-Williams series that describes the stability of complexes formed by divalent first-row transition metal cations, and how the stability generally increases across the period to a maximum stability at copper: Mn(II) < Fe(II) < Co(II) < Ni(II) < Cu(II) > Zn(II) (Irving and Williams, 1953). With regards to *Synechococcus*, we similarly observe that Zn and Cu form stronger biological complexes than do Ni and Co. Based on the calculated metal binding constants (Table 1.2), phosphoryl groups form stronger metal-ligands complexes with the cell wall than carboxyl groups. Interestingly, Co and Ni form stronger bonds with the carboxyl groups than Zn and Cu, however, Zn and Cu complexes form stronger bonds with phosphoryl groups. Overall, the results suggest that removal of Zn and Cu would be favoured under marine conditions, a finding corroborated by studies of the Northeast Pacific Ocean, where over 99% of Cu and >95% of Zn are organically complexed (Bruland, 1980; Coale and Bruland, 1988; Bruland et al., 2014).

Metal	Site 1 logK	Site 2 logK
Zn	4.365	7.863
Cu	3.726	7.412
Ni	4.667	6.097
Co	4.612	6.262

Table 2.2: Thermodynamic binding constants for each metal-cell wall complex.

Differing adsorption edge results were obtained for each individual metal cation, indicative of the relative affinity of each cation for cell surface functional groups. Comparing metal removal from solution at pH 8, which is representative of modern marine conditions, Zn adsorption reached nearly 100% (Figure 2.2a), Cu reached approximately 75% (Figure 2.2b), Ni approximately 40% (Figure 2.2c), and Co *ca.* 35% (Figure 2.2d). Importantly, the FITEQL models track well with the

experimental data through pH 5-8, which is the key range for metal binding as the pK_a values for the carboxyl and phosphoryl groups that form the basis for the thermodynamic metal binding constants lie within that range. Although these experiments were performed at a high ionic strength, similar to that of seawater, the work by Liu et al. (2015) indicated that ionic strength has a limited effect on Cd binding by *Synechococcus*. Furthermore, previous work has demonstrated that metal adsorption onto bacterial cell walls is a fully reversible process, and that the irreversible transport of the metals into the cell wall or cytoplasm does not occur to a meaningful extent over the time period of the adsorption reactions (Mullen et al., 1989; Fowle and Fein, 2000; Liu et al., 2015). Therefore, the values determined by the SCM are indicative of only metal adsorption to the surface, not assimilation by *Synechococcus* cells.

2.3.3 Competitive metal adsorption

The protonation constants, corresponding site concentrations, metal binding constants determined from models of single-metal adsorption experiments (Section 2.3.2), and the aqueous speciation of each metal (SI Table 1 a&b) were combined into one SCM. It was then used to predict the extent of adsorption in systems containing *Synechococcus* cells and all of the four metals. FITEQL models, along with the binding constants for the hydrolysis reactions, were utilized to solve for metal adsorption as a function of pH. The SCM predictions were then compared with the adsorption data from the experiments conducted at the same conditions to test the predictive rigor of the SCM. The competitive, multi-metal adsorption experiments were conducted using 2.5 ppm of each of the four metals in order to maintain a similar overall metal concentration (10 ppm) as the single element adsorption experiments and can be seen in Figure 2.3.

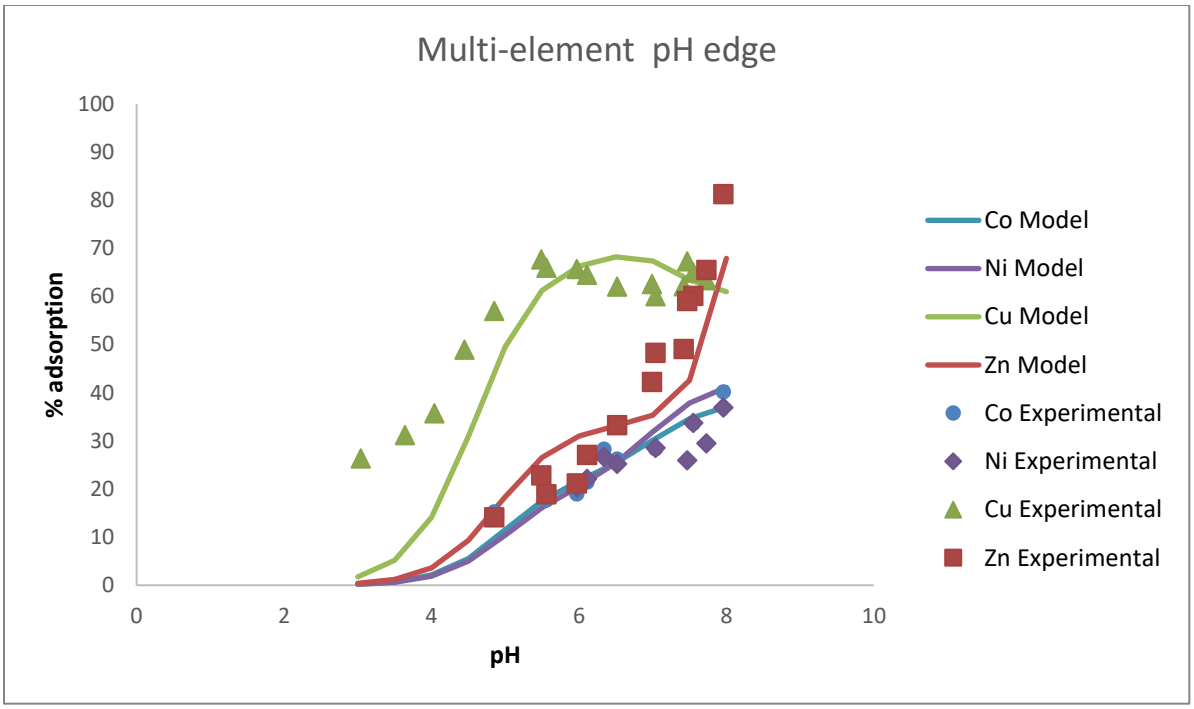

Figure 2.3: Competitive adsorption pH edge of the 4 metals studied in terms of % adsorption plotted alongside the predicted adsorption.

The trends in cation affinity for *Synechococcus* observed in the competitive metal adsorption experiments are similar to those of the single metal experiments, with Zn showing the highest adsorption at pH 8 followed by Cu, Co and Ni. However, Cu removal appears to plateau at pH 7 in the single element pH edge, while in the multi-element system, adsorption plateaus at approximately pH 5.5, and subsequently drops below the Zn curve at pH 8. Based on the modeling output from FITEQL, this pattern reflects decreased Cu adsorption on each of the two functional sites, carboxyl and phosphoryl groups, which could be due to competition with other cations as pH increases. The SCM accurately predicts Co, Ni, and Zn adsorption in the multi-metal system, while for Cu it predicts slightly weaker adsorption than is observed experimentally. The competitive sorption analysis provided here indicates that the relative sequestration of metals from the water column by *Synechococcus* was not significantly influenced by the presence of other trace metal ions, and that models based on single ion adsorption accurately predict the binding behaviour of *Synechococcus*.

2.4 Marine trace elements and their implications for the Precambrian

2.4.1 The importance of marine bioessential elements

Many of the trace elements in modern seawater are affected by the production and excretion of dissolved organic ligands, with many having a cyanobacterial origin (e.g., Coale and Bruland, 1988; Dupont et al. 2004; Bruland et al, 2013). Once excreted, these ligands can complex metal cations, keeping them in solution and thus bioavailable. For example, extracellular, ferric iron-chelating ligands, such as siderophores, can scavenge and solubilize iron from seawater, making it available for microbial cells (Neilands, 1995; Boiteau et al., 2016). Similar ligands also exist for metals, such as Co, Cu, Mo, and Zn (Bruland et al., 2014). In contrast, other organic ligands are produced to reduce trace metal concentrations to below toxic levels (Bruland et al., 1991). For example, in the northeastern Pacific ocean, Cu binding ligands have been found to complex up to 99.7% of free Cu, significantly reducing its bioavailability and limiting its toxicity (Coale and Bruland, 1988).

Each of the metals chosen for this study represent important cofactors in metalloenzymes required for various important cellular processes including photosynthesis, respiration, and DNA and RNA synthesis. Zn is a component in an array of metallo-peptides and polymerases, and many zinc metalloenzymes are involved in DNA and RNA synthesis (Lipscomb and Sträter, 1996). Nuclear bound Zn is also important for eukaryotes in the so-called Zn-fingers, small protein structural motifs which act as signaling agents within the nucleus (e.g., Dupont et al., 2006; Dupont et al., 2010). However, there is a significant difference in the utilization of Zn between prokaryotes and eukaryotes; up to 30% of known Zn-binding proteins are found in eukaryotes (Dupont et al., 2006). Cu is found in more than thirty enzymes including those involved in metabolism and methanogenesis (Chi Fru, 2011), as electron carriers in the thylakoid membrane during

photosynthesis in cyanobacteria (Cavet et al., 2003), as well as in plastocyanin, ferrous oxidase, and amine oxidase (Morel et al., 2014). Ni is critical for most bacteria, and it is particularly vital in metalloenzymes associated with methanogenic and acetogenic bacteria. The Ni containing metalloenzymes methyl-coenzyme M and acetyl-CoA synthase are both required for methane production, while acetyl-CoA synthase can also be used by acetogens to obtain energy from acetate (Hausinger, 1987). In non-methanogenic bacteria, Ni can also be found in hydrogenase, urease, and superoxide dismutase (Dupont et al., 2008). The foremost role of Co in biological utilization is as a cofactor in vitamin B12 (cobalamin), where a central cobalt atom is coordinated by four nitrogen ligands (Banerjee and Ragsdale, 2003). Eukaryotes use cobalamin in methionine synthesis (Swanner et al., 2014), while bacteria and archaea use cobalamin in enzymes for anaerobic metabolisms such as fermentation, dehalogenation, one-carbon compound electron transfers (Banerjee and Ragsdale, 2003), and in carbonic anhydrase (Morel et al., 2014).

In modern seawater, each of these metals show "nutrient-like" profiles, with decreased concentrations in the photic zone due to biological uptake, and increasing concentrations with depth as the metals are solubilized and returned to seawater as a consequence of cell biomass degradation (Bruland et al., 2014). Zinc concentrations in marine surface waters range from ~0.04 to 0.5 nM (Bruland et al., 2014), however, speciation and complexation with dissolved organic ligands significantly affects the bioavailability of Zn in marine waters (Morel and Price, 2003). The vertical concentration profile for marine Zn is coupled to that of Si (Bruland, 1980), implying that Zn is taken up and sequestered into the exoskeleton of coccolithophores and diatoms (Hunter et al., 1997). Although some studies of marine cyanobacteria, including *Synechococcus,* have found they have little to no measurable Zn requirement (Sunda and Huntsman, 1995), other studies have shown that phytoplankton growth rates are reduced when the activity of Zn^{2+} falls below a

certain threshold, however, this limitation associated with low Zn concentrations may be overcome by Cd substitution (Price and Morel, 1990). Due to the importance of Zn in metalloenzymes, it has been proposed that Zn may limit oceanic production, which can, in turn, influence the global carbon cycle (Morel et al., 1994). The proliferation of Zn metalloenzymes has been previously suggested to have contributed to the delayed rise of eukaryotes in the Proterozoic (Dupont et al., 2010), although ancient chemical sedimentary records for Zn abundances are at odds with this assertion and postulate marine Zn concentrations have been consistent throughout time (Scott et al., 2013; Robbins et al., 2013; 2016).

Similar to Zn, the distribution of Cu in modern oceans is strongly influenced by both recycling and scavenging processes, with uptake by biological processes depleting the surface waters to values as low as 10^{-9} M (Bruland et al, 2013). Also similar to Zn, Cu is heavily complexed by organic ligands in natural waters, causing the bioavailable Cu^{2+} concentration to be much lower than the total Cu concentration (Hunter et al., 1997; Leão et al., 2007). The complexation of Cu by organic ligands, which reduces Cu bioavailability, may be beneficial to some species, such as *Synechococcus* where the excretion of ligands serve as a means of detoxifying surface waters with elevated Cu concentrations (Saito et al., 2003).

There is a marked contrast between Ni in comparison to Cu and Zn where >90% of Cu and Zn are found as dissolved species bound by organic complexes. While only 10-30% of dissolved Ni is bound by organic complexes (Van den Berg and Nimmo, 1987; Donat et al. 1994; Achterberg and Van den Berg, 1997); approximately 10% of Ni exists as chloride complexes and 50% exists as the inorganic Ni^{2+} cation (Byrne, 2002). Similar to other trace metals examined in this study, Ni exhibits a nutrient-like vertical sea-water profile with low concentrations between 10^{-8}-10^{-9} M

near the surface due to biological uptake, with concentrations increasing with depth as Ni returns to seawater via remineralization (Bruland and Franks, 1983; Bruland et al, 2013).

Cobalt concentrations in modern seawater vary from 4-300 pM (Bruland et al, 2013). Saito and Moffett (2002) postulated that Co can behave as nutrient-like element at the surface due to biological uptake, however, with increasing depth, Co behaves as a scavenged type element as it does not show deep-water enrichment due to the oxidation of Co(II) to Co(III). Approximately 90% of marine Co is organically complexed (Saito and Moffett, 2001; Ellwood and van den Berg, 2001). Cobalt concentrations within phytoplankton are comparable to amounts for Cd and Cu (Ho et al., 2003). *Synechococcus* has the ability to produce copper binding ligands, analogous to siderophores, which can increase Co solubility by complexing Co^{2+} cations and preventing their scavenging by particles, oxidation, and precipitation, thereby increasing the bioavailability of Co (Leão et al., 2007; Morel et al., 2014). Swanner et al (2014) found that high organic ligand concentrations in simulated seawater can complex Co(II), decreasing the amount available for adsorption to ferrihydrite.

Using realistic marine concentrations of trace metals and cyanobacterial cell densities, the amount of each cation that was adsorbed to *Synechococcus* can be estimated for the marine photic zone and compared to our experimental results to assess the effects of trace metal adsorption to *Synechococcus* on marine trace metal cycling. Seawater trace metal concentrations were acquired from Bruland et al. (2014) as follows: 300 pmol/kg Co, 12 nmol/kg Ni, 4.5 nmol/kg Cu, and 9 nmol/kg of Zn; while the seawater *Synechococcus* cell density was assumed to be 10^6 cells/mL. In the experiments, it was determined that 5 g/L wet mass contained approximately 1.2×10^{10} cells/mL based on cell counting using a haemocytometer. Based on the adsorption experiments at pH 8, the *Synechococcus* culture of this density has the ability to adsorb approximately 5.9×10^{-5}

mol of Co, 6.2 x 10^{-5} mol of Ni, 1.3 x 10^{-4} mol of Cu, and 1.3 x 10^{-4} mol of Zn. By dividing the amount of each metal adsorbed during the adsorption experiments by 1.2 x 10^{10} cells, it was determined that each *Synechococcus* cell had the ability to adsorb 4.92 x 10^{-16} mol of Co, 5.17 x 10^{-16} mol Ni, and 1.08 x 10^{-15} mol of both Cu and Zn. Based on these values and multiplying them by 10^{6} cells mL^{-1} to simulate a marine *Synechococcus* bloom, the hypothetical amounts of the bioessential trace elements adsorbed in the water column could be calculated, which corresponds to removals of 4.92 x 10^{-7} mol of Co, 5.17 x 10^{-7} mol Ni, and 1.08 x 10^{-6} mol of Cu and Zn per L of seawater. It is important to point out that the values for trace metal sequestration by the surface ligands of *Synechococcus* presented here are elevated compared to those for those recently in determined for *Rhodovulum iodosum* in Konhauser et al. (2018). This discrepancy could be due to one of several factors including, (i) the *R. iodosum* values modeled by Konhauser et al. (2018) were for cellular-mineral aggregates, i.e., cell biomass and ferrihydrite mineral grains; (ii) binding constants in Konhauser et al. (2018) were extrapolated using a linear free energy approach, but for *Synechococcus* they were generated through surface complexation modeling; (iii) adsorption experiments performed here were at much higher levels of metal loading – 10 ppm as opposed to seawater concentrations; and (iv) Konhauser et al. (2018) assumed only carboxyl groups were binding the transition metals under paleomarine pH conditions, while here we also consider phosphoryl groups. When viewed in terms of metal absorbed per unit of biomass, differences between values generated herein and Konhauser et al. (2018) are within approximately two orders of magnitude, which may be accounted for in differences between extrapolated and modeled binding constants.

The values calculated here demonstrate that *Synechococcus* can adsorb significantly higher proportion of trace elements than present in marine waters. These results also show that

Synechococcus absorbs slightly higher, although similar amounts of these trace metals relative to Cd, which shows adsorption of approximately 10^{-16} mol per cell (Liu et al. 2015). This suggests that *Synechococcus* can potentially be a significant sink for these bioessential trace metals in the photic zone. Furthermore, our surface complexation modelling results were used to the predict the adsorption of the trace metals to *Synechococcus* using the trace element concentrations from Bruland et al (2013), the site concentrations present in 10^6 cells, considering Cl^- and CO_3^{2-} complexation, and using the binding constants derived from the SCM. This model calculated an inexplicably low degree of adsorption to the surface functional groups of the *Synechococcus*, even though the concentration of sites were magnitudes higher in concentration than the metal concentrations. Unexpectedly, the majority (>70% Cu and Zn and >90% Co and Ni) of the trace metals remained in solution as free cations and were not complexed with either Cl^- or surface functional groups. This could be explained by competition with protons in solution which have higher concentrations than the trace metals themselves in seawater and could out-compete the cations for the surface functional groups. However, there could also be a low concentration ligand site that has a higher affinity for the trace metals, such as sulfhydryl groups (Mishra et al., 2010). Nell and Fein (2017) determined that sulfhydryl functional groups represent only 5-10% of the total available binding sites on bacterial surfaces, yet they exhibit much higher binding affinities than other types of surface functional groups. Furthermore, they found that sulfhydryl surface functional groups become the important metal-binding ligands under low metal loading conditions (Nell and Fein, 2017). Hence, due to the drastically lower amount of metal binding between the experiments performed in this study and the concentrations found in seawater, metal loading onto the surface of *Synechococcus* may be controlled by sulfhydryl groups and could account for the low metal removal predicted by the seawater SCM. It is certainly clear that future studies

investigating metal-ligand interactions at sub-micromolar concentrations must integrate the low concentration, high affinity functional groups into their models, as these could control metal adsorption under low metal concentrations.

2.4.2 Implications for trace metal cycling and ancient ocean chemistry

The ability of cyanobacteria to effectively adsorb metal cations from seawater owes to their large surface area to volume ratio and rapid growth rates (Fisher, 1985). On average, phytoplankton biomass turns over once per week (Falkowski et al., 1998); consequently, trace metal cycling in the ocean is necessarily a rapid process in order to meet the trace metal demands of the oceanic biosphere. Although metals bound to the cell wall may eventually return to seawater at depths in the open ocean due to the bacterial degradation of organic matter (Sunda, 2012), it is possible that a fraction will settle to the relatively shallow continental shelves, carrying with them the adsorbed metals. This notion was postulated by Konhauser et al. (2002) for ancient iron rich sediments, where it was believed that trace metals would be immobilized with dead biomass and vectored to the accumulating sediment forming the precursor to banded iron formations (BIF). Each layer of dead biomass would be isolated by sedimenting Fe-rich particles, and therefore, trace-metal mobility would have been limited. As time progressed, the buried biomass would be respired, and the adsorbed metals would subsequently be released and adsorbed onto Fe-particles and thereby become incorporated into the rock record. Konhauser et al. (2018) subsequently suggested that most of the trace element assemblage preserved in BIF was biologically processed in the water column and, hence, phytoplankton may have controlled the trace-metal inventories of ancient seawater and sediment. Therefore, by constraining the quantitative effects that cyanobacteria exert

on trace element cycling, and their ability to transfer trace metals into sediments, a better understanding of trace metal fluxes in the ancient and modern oceans can be achieved.

Understanding the possible exit fluxes for trace metals is a crucial component for predicting how trace metals were sequestered into ancient marine settings, and how this ultimately affected their expression in the rock record. With regards to BIF, numerous studies have utilized those iron-rich chemical sediments as proxies for the evolution of trace metal abundances in the ancient ocean (e.g., Bjerrum and Canfield, 2002; Chi Fru et al., 2016; Konhauser et al., 2007; 2009; 2011; 2015; Partin et al., 2013a; Robbins et al., 2013; Swanner et al., 2014; Warchola et al. 2018). Similarly, shales have also proven to be a useful record for trace elements from the Archean through to the modern (e.g., Chi Fru et al., 2016; Scott et al., 2008; Partin et al., 2013b; Playter et al. 2017). When these studies are combined with proteomic studies (e.g Dupont et al., 2006; Dupont et al., 2010; David and Alm, 2011) they can help to determine the timing of the emergence of organisms such as cyanobacteria. To accurately assess the potential for cyanobacterial surfaces to act as an exit channel for trace metals in seawater to modern and ancient sediments, it is necessary to quantify the adsorptive capacity in dynamic, multicomponent systems. Thus, the surface complexation models developed here contribute to the understanding of adsorption of Zn, Cu, Co, and Ni to *Synechococcus,* and because *Synechoccocus* can act as a sink for trace metals, trace element deposition in the BIF and shale record.

Furthermore, despite the wealth of knowledge gleaned from these trace metal records, the primary exit channel for trace elements to the sediments remains a debated, and critically studied topic. One of four possible scenarios can be envisioned for the removal of trace metals from the water column: (1) adsorption to sinking biomass, such as *Synechococcus* cells, (2) adsorption to ferric iron minerals such as ferrihydrite, $Fe(OH)_3$, which formed the precursor phase of BIF

(Konhauser et al., 2018), (3) adsorption to clay particles which form shales and fine grained siliciclastics in modern and ancient marine settings (e.g.: Playter et al., 2017), or (4) complexation with dissolved organic carbon which can either decrease trace metals' bioavailability or form aggregates which then settle to the seafloor (Engel et al., 2004). These four mechanisms need not be mutually exclusive, and a combination of one or more may contribute to the formation of ancient or modern sediments. This study demonstrates that cyanobacteria can adsorb appreciable amounts of bioessential trace metals from seawater. It also demonstrates that surface complexation modelling can be used to accurately predict the adsorption behaviour of cations in competitive systems, which is important for building predictive models to study the fluxes of metals in the marine water column. These two findings, taken together, serve to increase our understanding of trace metal fluxes in seawater by constraining the major trace nutrients cycling pathways.

Although this study shows that surface-bound organic ligands on *Synechococcus* can adsorb trace elements from seawater, their binding constants are lower than those of dissolved organic compounds in the ocean. For example, Whitby et al. (2018) determined the binding constants of two Cu binding ligands in the NE Pacific Ocean: the first ligand, L1, had a binding constant of 15.0-16.5, while the second ligand, L2, exhibits a binding constant of 11.6-13.6. This strongly suggests that dissolved organic ligands in the ocean could have a more significant effect on trace metal cycling and should be considered, along with particulates such as bacteria, clay particles, and iron oxides, as vectors controlling trace metal bioavailability in the oceans.

2.5 Conclusion

This study determined the ability of the marine cyanobacterium *Synechococcus* sp. PCC 7002 to remove biologically important metal cations (Co, Cu, Ni, Zn) from solution by adsorption using a

surface complexation modelling approach. It was demonstrated that this species of cyanobacteria can adsorb considerable quantities of bioessential trace elements from simulated seawater, and importantly, we quantified the effects of competitive adsorption. The data shows that *Synechococcus* has the highest removal capacity for Cu and Zn, followed by Co and Ni. The ability for *Synechococcus* to remove trace metals were broadly consistent with the well-known Irving-Williams stability series for organic-metal complexes.

This data indicates that *Synechococcus* has the potential to be a crucial contributor of the cycling of trace metals in the oceans due to adsorption to the cell surface. Additional mechanisms which may contribute to metal removal include complexation with Cl^- or OH^- species, precipitated as hydroxides or carbonates at high pH, or competition for adsorption by other dissolved ligands, bacteria, or particulate matter in the water column. Nevertheless, this study corroborates the hypothesis that phytoplankton are ideally suited to scavenge trace metals from seawater due to their rapid growth and correspondent cellular turnover rates, high surface area to volume ratio, and highly reactive cell walls.

This study is one of the first to quantitatively investigate competitive adsorption of bioessential trace metals to marine biomass, and future work should focus on assessing additional exit channels for the incorporation of these nutrients into BIF pre-cursor phases such as ferrihydrite and silica, dissolved organic carbon, and bacterial assimilation. By determining the metal binding behaviour of trace elements to particulate matter in seawater, including multi-metal, multi-sorbent systems, models containing multiple sorbents and metals, which more closely represents realistic marine conditions, can be developed. By assessing a range of realistic sorbent and metal concentrations, this competitive SCM approach will allow for further refinement of the role of specific exit pathways on the cycling of trace elements between the water column and sediments in both modern

and ancient marine systems, and ultimately for the identification of transition metal-based biosignatures within the rock record.

References

Achterburg E. P. and Van Den Berg C. M. G. (1997). Chemical speciation of chromium and nickel in the western Mediterranean. *Deep Sea Res. Part 2*, **44**, 693-720.

Alam Md. S., Swaren L., von Gunten, K., Cossio M., Bishop B., Robbins L. J., Hou D., Flynn S. L., Ok Y. S., Konhauser K. O., Alessi D. S. (2018) Application of surface complexation modeling to trace metals uptake by biochar-amended agricultural soils. *App. Geochem.* **88**, 103-112.

Banerjee R. and Ragsdale S. W. (2003) The Many Faces of Vitamin B 12: Catalysis by Cobalamin-Dependent Enzymes. *Annu. Rev. Biochem.* **72**, 209–247.

Bjerrum C. J. and Canfield D. E. (2002) Ocean productivity before about 1.9 Gyr ago limited by phosphorus adsorption onto iron oxides. *Nature* **417**, 159-162

Boiteau R. M., Mende D. R., Hawco N. J., McIlvin M. R., Fitzsimmons J. N., Saito M. A., Sedwick P. N., DeLong E. F. and Repeta D. J. (2016) Siderophore-based microbial adaptations to iron scarcity across the eastern Pacific Ocean. *Proc. Natl. Acad. Sci.* **113**, 14237–14242.

Boyd P. W., Ellwood M. J., Tagliabue A. and Twining B. S. (2017) Biotic and abiotic retention, recycling and remineralization of metals in the ocean. *Nat. Geosci.* **10**, 167–173.

Bruland K. W. (1980) Oceanographic distributions of cadmium, zinc, nickel, and copper in the North Pacific. *Earth Planet. Sci. Lett.* **47**, 176–198.

Bruland K. W. and Lohan M. C. (2003) Controls of Trace Metals in Seawater. In *Treatise on Geochemistry* pp. 19–51. Elsevier Ltd.

Bruland K. W. and Franks R. P. (1983) Mn, Ni, Cu, Zn, and Cd in the western North Atlantic. In *Trace Metals in Seawater*. Plenum, New York. 395-414.

Bruland K. W., Donat J. R. and Hutchins D. A. (1991) Interactive influences of bioactive trace metals on biological production in oceanic waters. *Limnol. Oceanogr.* **36**, 1555–1577.

Bruland K. W., Middag R, and Lohan M. C. (2014) Controls of Trace Metals in Seawater. In *Treatise on Geochemistry: 2nd edition*. 19–51. Elsevier Ltd.

Byrne R. H. (2002) Inorganic speciation of dissolved elements in seawater: the influence of pH on concentration ratios. *Geochem. Trans.* **2**, 11.

Cavet J. S., Borrelly G. P. M. and Robinson N. J. (2003) Zn, Cu and Co in cyanobacteria: Selective control of metal availability. *FEMS Microbiol. Rev.* **27**, 165–181.

Chi Fru E. (2011) Copper biogeochemistry: A cornerstone in aerobic methanotrophic bacterial ecology and activity? *Geomicrobiol. J.* **28**, 601–614.

Chi Fru E., Rodríguez N. P., Partin C. A., Lalonde S. V, Andersson P., Weiss D. J., El Albani A., Rodushkin I. and Konhauser K. O. (2016) Cu isotopes in marine black shales record the Great Oxidation Event. *Proc. Natl. Acad. Sci.* **113**, 4941–4946.

Coale K. H. and Bruland K. W. (1988) Copper complexation in the Northeast Pacific. *Limnol. Oceanogr.* **33**, 1084–1101.

Cox J. S., Smith D. S., Warren L. A., Ferris F. G. (1999). Characterizing heterogeneous bacterial surface functional groups using discrete affinity spectra for proton binding. *Environ. Sci. Technol.* **33**, 4514–4521.

David L. A. and Alm E. J. (2011) Rapid evolutionary innovation during an Archaean genetic expansion. *Nature* **469**, 93–96.

Donat J. R., Lao K. A. and Bruland K. W. (1994) Speciation of dissolved copper and nickel in South San Francisco Bay: a multi-method approach. *Anal. Chim. Acta* **284**, 547–571.

Dupont C. L., Nelson R. K., Bashir S., Moffett J. W. and Ahner B. A. (2004) Novel copper-binding and nitrogen-rich thiols produced and exuded by Emiliania huxleyi. *Limnol. Oceanogr.* **49**, 1754–1762.

Dupont C. L., Yang S., Palenik B. and Bourne P. E. (2006) Modern proteomes contain putative imprints of ancient shifts in trace metal geochemistry. *Proc. Natl. Acad. Sci. U. S. A.* **103**, 17822-17827.

Dupont C. L., Neupane K., Shearer J. and Palenik B. (2008) Diversity, function and evolution of genes coding for putative Ni-containing superoxide dismutases. *Environ. Microbiol.* **10**, 1831–1843.

Dupont C. L., Butcher A., Valas R. E., Bourne P. E. and Caetano-Anollés G. (2010) History of biological metal utilization inferred through phylogenomic analysis of protein structures. *Proc. Natl. Acad. Sci.* **107**, 10567–10572.

Ellwood M. J. and Van den Berg C. M. G. (2001) Determination of organic complexation of cobalt in seawater by cathodic stripping voltammetry. *Mar. Chem.* **75**, 33–47.

Engel A., Thoms S., Riebesell U., Rochelle-Newall E. and Zondervan I. (2004) Polysaccharide aggregation as a potential sink of marine dissolved organic carbon. *Nature* **428**, 929–932.

Falkowski P. G., Barber R. T. and Smetacek V. (1998). Biogeochemical controls and feedbacks on ocean primary production. *Science.* **281**, 200–206.

Fein J. B., Daughney C. J., Yee, N., Davis T. A. (1997) A chemical equilibrium model for metal adsorption onto bacterial surfaces. *Geochim. Cosmochim. Acta.* **61** (16), 3319-3328

Fisher N. S. (1985) Accumulation of metals by marine phytoplankton. *Mar. Biol.* **87**, 137–142.

Fowle D. A. and Fein J. B. (1999) Competitive adsorption of metal cations onto two gram positive bacteria: Testing the chemical equilibrium model. *Geochim. Cosmochim. Acta.* **63**, 3059–3067.

Fowle D. A. and Fein J. B. (2000) Experimental measurements of the reversibility of metal-bacteria adsorption reactions. *Chem. Geol.* **168**, 27–36.

Hausinger R. P. (1987) Nickel utilization by microorganisms. *Microbiol. Rev.* **51**, 22–42.

Herbelin A. L. and Westall J. C. (1999). FITEQL 4.0: A computer program for determination of chemical equilibrium constants from experimental data.

Ho T.-Y., Quigg A., Finkel Z. V., Milligan A. J., Wyman K., Falkowski P. G. and Morel F. M. M. (2003) The elemental composition of some marine phytoplankton. *J. Phycol.* **39**, 1145–1159.

Hunter K. A., Kim J. P. and Croot P. L. (1997) Biological roles of trace metals in natural waters. *Environ. Monit. Assess.* **44**, 103-147.

Irving H. and Williams R. J. P. (1953). The Stability of Transition-metal Complexes. *J. Chem. Soc.* **0**, 3192-3210

Jiang W., Saxena A., Song B., Ward B. B., Beveridge T. J. and Myneni S. C. B. (2004) Elucidation of Functional Groups on Gram-Positive and Gram-Negative Bacterial Surfaces Using Infrared Spectroscopy. *Langmuir* **20**, 11433–11442.

Jiao N., Herndl G. J., Hansell D. A., Benner R., Kattner G., Wilhelm S. W., Kirchman D. L., Weinbauer M. G., Luo T., Chen F. and Azam F. (2010) Microbial production of recalcitrant dissolved organic matter: Long-term carbon storage in the global ocean. *Nat. Rev. Microbiol.* **8**, 593–599.

Konhauser K. O., Fisher Q. J., Fyfe W. S., Longstaffe F. J. and Powell M. A. (1998) Authigenic mineralization and detrital clay binding by freshwater biofilms: The Brahmani river, India. *Geomicrobiol. J.* **15**, 209–222.

Konhauser K. O., Hamade T., Raiswell R., Morris R. C., Ferris F. G., Southam G. and Canfield D. E. (2002) Could bacteria have formed the Precambrian banded iron formations? *Geology.* **30**, 1079-1082

Konhauser K. O., Lalonde S. V., Amskold L. and Holland H. D. (2007) Was There Really an Archean Phosphate Crisis? *Science Brevia* **315**, 1234.

Konhauser K. O., Pecoits E., Lalonde S. V., Papineau D., Nisbet E. G., Barley M. E., Arndt N. T., Zahnle K. and Kamber B. S. (2009) Oceanic nickel depletion and a methanogen famine before the Great Oxidation Event. *Nature* **458**, 750-753.

Konhauser K. O., Lalonde S. V., Planavsky N. J., Pecoits E., Lyons T. W., Mojzsis S. J., Rouxel O. J., Barley M. E., Rosiere C., Fralick P. W., Kump L. R., Bekker A. (2011) Aerobic bacterial pyrite oxidation and acid rock drainage during the Great Oxidation Event. *Nature*. **478**, 369-373.

Konhauser K. O., Robbins L. J., Pecoits E., Peacock C., Kappler A., Lalonde S. V. (2015) The Archean Nickel Famine Revisited. *Astrobiology* **15**, 804-815

Konhauser K. O., Robbins L. J., Alessi D. S., Flynn S. L., Gingras M. K., Martinez R. E., Kappler A., Swanner E. D., Li Y. L., Crowe S. A., Planavsky N. J., Reinhard C. T. and Lalonde S. V. (2018) Phytoplankton contributions to the trace-element composition of Precambrian banded iron formations. *Bull. Geol. Soc. Am.* **130**, 941–951.

Lalonde S. V., Dafoe L. T., Pemberton S. G., Gingras M. K. and Konhauser K. O. (2010) Investigating the geochemical impact of burrowing animals: Proton and cadmium adsorption onto the mucus lining of Terebellid polychaete worms. *Chem. Geol.* **271**, 44–51.

Lalonde S. V., Smith D. S., Owttrim G. W., Konhauser K. O. (2008b) Acid-base properties of cyanobacterial surfaces I: Influences of growth phase and nitrogen metabolism on cell surface reactivity. *Geochim. Cosmochim. Acta* **72**, 1257–1268.

Lalonde S. V., Smith D. S., Owttrim G. W., Konhauser K. O. (2008a) Acid-base properties of cyanobacterial surfaces. II: Silica as a chemical stressor influencing cell surface reactivity. *Geochim. Cosmochim. Acta* **72**, 1269–1280.

Leão P. N., Vasconcelos M. T. S. D. and Vasconcelos V. M. (2007) Role of marine cyanobacteria in trace metal bioavailability in seawater. *Microb. Ecol.* **53**, 104–109.

Lipscomb W. N. and Sträter N. (1996) Recent advances in zinc enzymology. *Chem. Rev.* **96**, 2375–2433.

Liu Y., Alessi D. S., Owttrim G. W., Petrash D. A., Mloszewska A. M., Lalonde S. V., Martinez R. E., Zhou Q. and Konhauser K. O. (2015) Cell surface reactivity of Synechococcus sp. PCC 7002: Implications for metal sorption from seawater. *Geochim. Cosmochim. Acta* **169**, 30–44.

Mishra B., Boyanov M., Bunker B. A., Kelly S. D., Kemner K. M. and Fein J. B. (2010) High- and low-affinity binding sites for Cd on the bacterial cell walls of Bacillus subtilis and Shewanella oneidensis. *Geochim. Cosmochim. Acta* **74**, 4219–4233.

Morel F. M. M., Milligan A. J. and Saito M. A. (2014) Marine Bioinorganic Chemistry: The Role of Trace Metals in the Oceanic Cycles of Major Nutrients. in *Treatise on Geochemistry: 2nd edition.* 123–150. Elsevier Ltd.

Morel F. M. M., Reinfelder J. R., Roberts S. B., Chamberlain C. P., Lee J. G. and Yee D. (1994) Zinc and carbon co-limitation of marine phytoplankton. *Nature* **369**, 740–742.

Morel F.M. M. and Price N. (2003). The biogeochemical cycles of trace metals in the ocean. *Science* **300**, 944–947.

Mullen M. D., Wolf D. C., Ferris F. G., Beveridge T. J., Flemming C. A. and Bailey G. W. (1989) Bacterial sorption of heavy metals. *Appl. Environ. Microbiol.* **55**, 3143–3149.

Neilands J. B. (1995) Siderophores: Structure and Function of Microbial Iron Transport Compounds. *J. Biol. Chem.* **270**, 26723–26726.

Nell R. M. and Fein J. B. (2017) Influence of sulfhydryl sites on metal binding by bacteria. *Geochim. Cosmochim. Acta* **199**, 210–221.

Partin C. A., Lalonde S. V., Planavsky N. J., Bekker A., Rouxel O. J., Lyons T. W. and Konhauser K. O. (2013a) Uranium in iron formations and the rise of atmospheric oxygen. *Chem. Geol.* **362**, 82-90.

Partin C. A., Bekker A., Planavsky N. J., Scott C. T., Gill B. C., Li C., Podkovyrov V., Maslov A., Konhauser K. O., Lalonde S. V., Love G. D., Poulton S. W. and Lyons T. W. (2013b) Large-scale fluctuations in Precambrian atmospheric and oceanic oxygen levels from the record of U in shales. *Earth Planet. Sci. Lett.* **369-370**, 284-293.

Petrash D. A., Lalonde S. V, Gingras M. K. and Konhauser K. O. (2011) A Surrogate Approach to Studying the Chemical Reactivity of Burrow Mucous Linings in Marine Sediments. *Palaios* **26**, 594–600.

Playter T., Konhauser K., Owttrim G., Hodgson C., Warchola T., Mloszewska A. M., Sutherland B., Bekker A., Zonneveld J. P., Pemberton S. G. and Gingras M. (2017) Microbe-clay interactions as a mechanism for the preservation of organic matter and trace metal biosignatures in black shales. *Chem. Geol.* **459**, 75–90.

Price, N. M. and Morel, F. M. M. (1990) Cadmium and cobalt substitution for zinc in a marine diatom. *Nature* **344**, 658–660.

Robbins L. J., Lalonde S. V., Saito M. A., Planavsky N. J., Mloszewska A. M., Pecoits E., Scott C., Dupont C. L., Kappler A., Konhauser K. O. (2013) Authigenic iron oxide proxies for marine zinc over geological time and implications for eukaryotic metallome evolution. *Geobiol.* **11**, 295-306.

Robbins L. J., Lalonde S. V., Planavsky N. J., Partin C. A., Reinhard C. T., Kendall B., Scott C., Hardisty D. S., Gill B. C., Alessi D. S., Dupont C. L., Saito M. A., Crowe S. A., Poulton S. W., Bekker A., Lyons T. W. and Konhauser K. O. (2016) Trace elements at the intersection of marine biological and geochemical evolution. *Earth-Science Rev.* **163**, 323–348.

Saito M. A. and Moffett J. W. (2001) Complexation of cobalt by natural organic ligands in the Sargasso Sea as determined by a new high-sensitivity electrochemical cobalt speciation method suitable for open ocean work. *Mar. Chem.* **75**, 49–68.

Saito M. A. and Moffett J. W. (2002) Temporal and spatial variability of cobalt in the Atlantic Ocean. *Geochim. Cosmochim. Acta* **66**, 1943–1953.

Saito M. A., Sigman D. M. and Morel F. M. M. (2003) The bioinorganic chemistry of the ancient ocean: The co-evolution of cyanobacterial metal requirements and biogeochemical cycles at the Archean-Proterozoic boundary? *Inorganica Chim. Acta* **356**, 308–318.

Scott C., Lyons T. W., Bekker A., Shen Y., Pouton S. W., Chu X. and Anbar A. D. (2008) Tracing the stepwise oxygenation of the Proterozoic ocean. *Nature*. **452**, 456-459.

Scott C., Planavsky N. J., Dupont C. L., Kendall B., Gill B. C., Robbins L. J., Husband K. F., Arnold G. L., Wing B. A., Poulton S. W., Bekker A., Anbar A. D., Konhauser K. O. and Lyons T. W. (2013) Bioavailability of zinc in marine systems through time. *Nat. Geosci.* **6**, 125–128.

Stevens S. E. and Porter R. D. (1980) Transformation in *Agmenellum quadriplicatum. Proc. Natl. Acad. Sci. U.S.A.* **77**, 6052-6056.

Stevens S. and Van Baalen C. (1973) Characteristics of nitrate reductions in a mutant of the blue-green alga *Agmenellum quadruplicatum. Plant Physiol.* **51**, 350-356.

Sunda, W. G. (2012) Feedback interactions between trace metal nutrients and phytoplankton in the ocean. *Frontiers in Microbiology.* **3** (1-22).

Sunda W. G. and Huntsman S. A. (1995) Cobalt and zinc interreplacement in marine phytoplankton: Biological and geochemical implications. *Limnol. Oceanogr.* **40**, 1404–1417.

Swanner E. D., Planavsky N. J., Lalonde S. V., Robbins L. J., Bekker A., Rouxel O. J., Saito M. A., Kappler A., Mojzsis S. J. and Konhauser K. O. (2014) Cobalt and marine redox evolution. *Earth Planet. Sci. Lett.* **390**, 253–263.

Van Den Berg C. M. G. and Nimmo M. (1987) Determination of interactions of nickel with dissolved organic material in seawater using cathodic stripping voltammetry. *Sci. Total Environ.* **60**, 185–195.

Warchola T. J., Flynn S. L., Robbins L. J., Liu Y., Gauger T., Kovalchuk O., Alam Md. S., Wei S., Myers R., Bishop B., Lalonde S. V, Gingras M. K., Kappler A., Alessi D. S. and Konhauser K. O. (2017) Field-and Lab-Based Potentiometric Titrations of Microbial Mats from the Fairmont Hot Spring. *Geomicrobiol. J.* **34**, 851-863.

Warchola T., Lalonde S. V., Pecoits E., Gunten K. von, Robbins L. J., Alessi D. S., Philippot P. and Konhauser K. O. (2018) Petrology and Geochemistry of the Boolgeeda Iron Formation, Hamersley Basin, Western Australia. *Precambrian Res.*

Whitby H., Posacka A. M., Maldonado M. T. and van den Berg C. M. G. (2018) Copper-binding ligands in the NE Pacific. *Mar. Chem.* **204**, 36–48.

Yee N., Benning L. G., Phoenix V. R. and Ferris F. G. (2004) Characterization of Metal-Cyanobacteria Sorption Reactions: A Combined Macroscopic and Infrared Spectroscopic Investigation. *Environ. Sci. Technol.* **38**, 775–782.

Zehr, J. P. and Ward, B. B. (2002). Nitrogen cycling in the ocean: new perspectives on processes and paradigms. *Appl. Environ. Microbiol.* **68**, 1015–1024.

Chapter 3

Surface reactivity of cyanobacterial cell lysates: An analogue for marine dissolved organic carbon

3.1 Marine cycling of dissolved organic carbon

Dissolved organic carbon (DOC) is ubiquitous throughout the ocean, holding an estimated 662 Pg of C; similar to the amount of carbon contained in the atmosphere (Hansell et al., 2009) and significantly higher than the estimated 2.2 Pg of carbon in marine prokaryotes (Whitman et al., 1998). The majority of marine DOC is thought to be produced autochthonously by photosynthetic plankton in the photic zone, with the majority of produced DOC being labile in nature (Hansell et al., 2009). As previously mentioned in chapter 1, dissolved organic carbon is generally divided into three classes based on biological availability: labile, semi-labile, and refractory (or recalcitrant) compounds, with each having distinct residence times and compositions (Jiao et al., 2010; Carlson and Hansell, 2014). The majority of the DOC produced by photosynthetic bacteria is labile and can be remineralized or assimilated by microbes on the order of minutes to days (Jiao et al., 2010; Carlson and Hansell, 2014).

Semi-labile dissolved organic carbon (SLDOC) can be preserved in the water column for months to years, and makes up the bulk of the DOC flux from surface waters to greater depths (Jiao et al., 2010). This class of DOC is composed mainly of carbohydrates which have similar chemical properties throughout the ocean; with similar elemental ratios of carbon, nitrogen, and phosphorus being observed, allowing for SLDOC to be traced through the water column (Hansell et al., 2009),

Refractory DOC (RDOC) makes up the dominant fraction of dissolved carbon because it is highly resistant to decomposition in the water column. The average residence time of the most refractory compounds was found to be approximately 6000 years (Williams and Druffel, 1987). Although more recently, this class of organic compounds has been further subdivided into fractions based on their residence times including: semi-refractory (~20 years), refractory (~16000 years), and ultra-refractory (~40000 years) (Hansell et at., 2012). Approximately 50% of the photosynthetically produced POC is transformed into DOC through processes such as, excretion, zooplankton grazing, microbial ectohydrolases, and importantly, viral lysis (Anderson and Tang, 2010). Amon and Benner (1994) studied the relative bioavailabilities of low- and high-molecular weight DOM molecules in seawater and observed that bacterial growth and respiration rates were higher in the presence of high-molecular weight DOM. This implies that the bulk of RDOM is composed of small molecules which cycle slowly and are intrinsically recalcitrant and cannot be degraded by marine microbes. However, contrary to this view, the dilution hypothesis by Arrieta et al. (2015) postulates that the concentrations of refractory DOC in the deep ocean are too dilute for bacterial use, and therefore, the energetic investments required for uptake and degradation is higher than the energetic output. Dittmar and Paeng (2009) determined that a large amount of DOC in the ocean shows evidence of being thermally altered, either in deep sediments or through combustion on land and this thermal alteration may be a factor in RDOM being highly resistant to bacterial decomposition.

Jiao et al. (2010) proposed the microbial carbon pump (MCP) as a process which helps to understand the role of microbes in the production of RDOC. The main driver of the MCP is regenerated production, where the processing of DOM by the MCP transforms some of the reactive, more labile organic compounds, into refractory compounds. This process also transforms

low concentrations of highly reactive carbon compounds into high concentrations of refractory carbon with low reactivity. Furthermore, it changes the chemical composition of DOM, for instance the ratios of carbon, nitrogen, and phosphorus as observed by the selective remineralization of P (Clark et al., 1998) and decreasing ratios of N and P ratios at depth relative to C (Hopkinson and Vallino, 2005). Hence, the MCP transfers more carbon, relative to nitrogen and phosphorus, from labile DOM to RDOM, as well as releasing inorganic N and P into the water column as nutrients which can then be re-used by other organisms (Jiao et al., 2010). Those same authors further classified the recalcitrant DOC compounds into two classes. The first being $RDOC_t$, which is composed of compounds which are intrinsically refractory in an environmental context, while the second class is $RDOC_c$ which is composed of a vast array of molecules whose concentrations are below the uptake thresholds for microbes. However, Jiao et al. (2010) still believe the MCP is a major source of RDOC to seawater as it can produce both $RDOC_t$ and $RDOC_c$.

Cell wall and cell surface macromolecules could be important sources of RDOC once released by viral lysis (Jiao et al., 2010). Based on the research presented in Chapter 1, these cell wall macromolecules are highly surface reactive and can adsorb trace metals from seawater, therefore it is also likely that once released, they can affect the cycling of nutrients in the ocean. By studying the surface reactivity of *Synechococcus* lysate which includes these cell wall macromolecules, the effects of DOC on trace metal cycling in the ocean can be better understood.

3.2 Methods

3.2.1 Cyanobacterial growth and lysate preparation

Lysate from the marine cyanobacterium *Synechococcus* sp. PCC 7002 was selected as an analogue for DOC because *Synechococcus* type cells are ubiquitous in the open ocean and are representative of marine cyanobacterial populations. Furthermore, previous studies have postulated that marine bacteria could be a source of marine DOC (e.g., Aluwihare and Repeta, 1999; Ogawa, 2001; Suttle 2007; Jiao et al. 2014). Briefly, *Synechococcus* cells were cultured aerobically on A+ agar plates until suitable colonies developed, at which point a colony was inoculated in 50 mL of A+ liquid media for 3 days. In order to grow sufficient biomass for the experiments, the cells were transferred to an additional 350 mL of A+ for 10 further days, until the stationary growth phase was achieved. Aeration was provided via bubbling with humidified air for the duration of the growth. Cells were harvested by centrifugation at 10000 g for five minutes and washed with 0.56 M NaCl five times to remove residual growth media and remove competing metals from the cell wall. The bacteria were then suspended in fresh electrolyte for each wash cycle. Following centrifugation, the supernatant was discarded, and the weight mass of bacteria was determined, then re-suspended in 0.56 M NaCl for a final concentration of 10 g/L.

Bacterial lysis was performed by sonication, as this technique does not introduce chemicals which could interfere with the surface reactivity of the bacteria. 10 mL aliquots of washed cell suspension were partitioned into 15 mL polypropylene falcon tubes and sonicated at 160 MHz for 30 seconds each, and then placed into an ice-water bath between cycles to inhibit protein denaturing due to the heat produced by sonication. Eight cycles of sonication were performed on each sample, and lysis was confirmed by conducting cell counts by light microscopy. In order to

separate the dissolved from the particulate fraction, lysed samples were centrifuged at 10000 g for 5 min and then filtered through 0.45 μm nylon membranes.

3.2.2 Fourier Transform Infrared (FTIR) spectroscopy

Fourier Transform Infrared (FTIR) spectroscopy was performed to determine the presence and composition of organic ligands in the *Synechococcus* lysate, which assists in assigning organic functional groups to the titration surface complexation model (SCM). The *Synechococcus* lysate was prepared as described above, and FTIR was performed on both the bulk (unfiltered) lysate, and the dissolved fraction which had been filtered through 0.45 μm nylon membranes. The unfiltered and filtered samples were partitioned into 15 mL polypropylene tubes and freeze dried for 48 h to remove moisture. Following the freeze-drying step, 1 mg of the dried lysate was combined with KBr powder in a 1:150 (wt/wt) ratio and pressed into a pellet. The lysate-KBr pellet was then analyzed using a Deuterated Tri Glycine Sulfate (DTGS) detector coupled to a FTIR spectrometer (Thermo Nicolet 8700). The infrared spectra were examined within a range of 4000-450 cm^{-1} in absorbance mode with 32 scans being collected for each spectrum at a resolution of 4 cm^{-1}.

3.2.3 Non-purgeable organic carbon analysis

Non-purgeable organic carbon (NPOC) analysis was performed in order to determine the amount of total organic carbon, total carbon, and total nitrogen present in the bulk and filtered lysates. NPOC analysis was performed using the Shimadzu NPOC Combustion Catalyst method on a TOC-V CHN analyzer (Shimadzu). Each sample was diluted 10x, while TOC samples were acidified with 1 M HCl. TOC calibrations were performed using a 7-point 50 ppm calibration,

while TN calibrations were performed using an 8-point 5 ppm calibration. Each sample was sparged with N_2 for 6 minutes prior to analysis.

3.2.4 Potentiometric titrations of the lysate

All glass and plasticware used in the titration were soaked in 10% HCl for 24 hours, rinsed 3 times with 18.2 MΩ•cm water (ultra-pure water), and air-dried while inverted. Prior to each titration, *Synechococcus* lysate, and lysate filtered through a 0.45 µm nylon membrane were diluted to 1 g/L in 50 mL of 0.56 M NaCl background electrolyte and purged with N_2 before, and during the titration to ensure CO_2 did not enter the system. Titrations were performed from pH 3-10 by first acidifying the solution the pH to 3 with 0.1 M HCl, followed by increasing the pH to 10 by addition of 0.1M NaOH ("up" titration), and then decreasing the pH to 3 by adding 0.1 M HCl ("down" titration). "Up" and "down" titrations were performed to determine the reversibility of proton binding, and to identify hysteresis which could be caused by either cell damage, or dissolution of organic molecules in the lysate. The pH was measured throughout the titration using a glass electrode (Metrohm), calibrated in advance with commercially available pH 3, 7, and 10 buffers (Thermo Fisher Scientific). The amount of titrant added, as well as the change in pH was measured for each titration step.

Potentiometric titrations were performed on the lysed *Synechococcus* cells to determine the proton reactivity of the cell lysate. The resulting titration data was modeled in terms of excess charge by subtracting the reactivity of the background electrolyte from the lysate using MATLAB as per Lalonde et al. (2010), with the resulting data modeled using the software program FITEQL (Herbelin and Westall, 1999) to calculate site pK_a values and corresponding concentrations in terms of the moles of base added to deprotonate the surface.

3.2.5 Dynamic light scattering

Dynamic light scattering (DLS) analysis was performed to determine the size distribution of the *Synechococcus* cell lysate. Sizes were determined for intact cells, lysed cells, and lysate filtered through a 0.45 µm nylon membrane. The size of the particles was obtained similar to Safari et al. (2014), using a Malvern Instrument Zetasizer Nano ZS equipped with a 633 nm laser (Westborough, Massachusetts, USA), and measured in 173° backscatter mode.

3.3 Results

3.3.1 Total organic carbon and nitrogen analysis

Results from the NPOC analysis are summarized in Table 3.1 and are the mean of 3 of 4 injections. From the results, the filtration only removes approximately 20% of the TC, TOC, and TN, respectively, indicating that the majority of each of these elements are associated with the dissolved fraction. The results show that approximately 90% of carbon in the lysate is in organic form, and there is no change in the C:N ratio between the bulk and filtered lysates.

These results are the basis for determining the concentration of DOC in the filtered lysate for the titrations, as the centrifugation method would not be sufficient as many of the dissolved compounds would not be incorporated into the pellet due to their low masses.

Sample	TC (ppm)	NPOC (ppm)	TN (ppm)	C:N
Bulk Lysate	423.6	372.3	106.7	3.970009372
Dissolved fraction	332.4	296	82.6	4.024213075

Table 3.1: Total carbon, non-purgeable organic carbon, and total nitrogen analysis for the bulk lysate and dissolved fraction.

3.3.2 Dynamic light scattering (DLS) analysis

The data for the dynamic light scattering analysis is presented in Figure 3.1. According to the DLS intensity-based size analysis, it was observed that the majority of the intact cells had sizes greater than 5000 nm, whereas the unfiltered lysate had a much lower size distribution of about 350 nm with a long tail towards the intact cells, indicating there were some intact cells still present. The filtered lysate showed a lower overall size of 142 nm with some aggregates (~3 µm). The lower overall size may be due to the removal of intact cells and larger cell fragments which would have been present in the cell lysate, while larger aggregates could have formed after filtration due to the ionic strength. All samples show broad size distribution indicating polydispersity of particles. Number-based size analysis shows a similar particle size trend with no aggregates in the lysate and filtered lysate, which means aggregates observed in intensity-based size distribution are statistically insignificant. Note intensity-based size analysis is used in determining particle size, while number-based size analysis is used to determine relative proportion of each particle size.

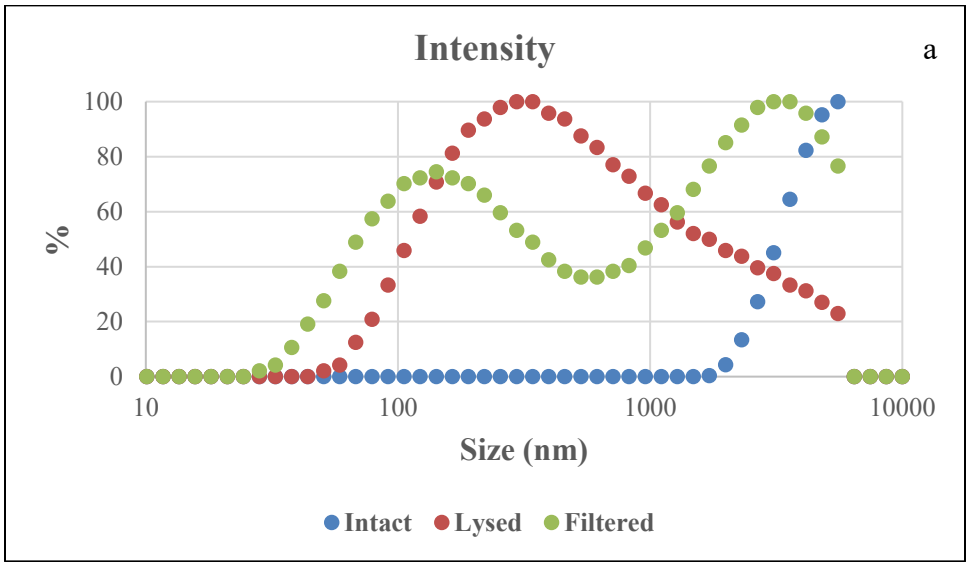

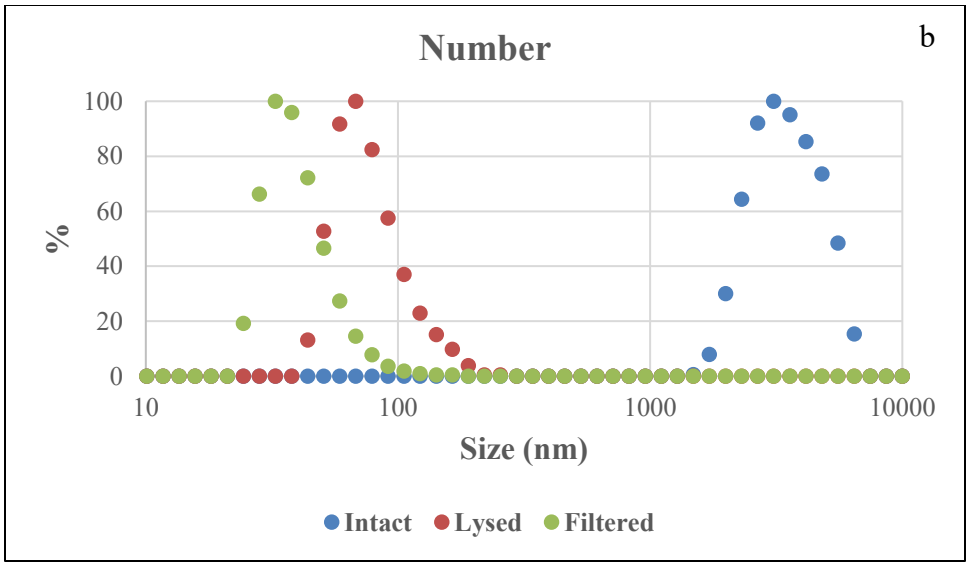

Figure 3.1 (a, b): Dynamic light scattering intensity (a) and number (b) graphs for intact *Synechococcus* cells, bulk lysate, and the dissolved fraction showing the intensity and distribution of the sizes of each.

3.3.3 Fourier Transform Infrared (FTIR) spectroscopy

Fourier Transform Infrared (FTIR) spectroscopic analyses were performed on the bulk and filtered lysate to distinguish differences in organic functional groups between the cell wall, lysate, and dissolved fraction. The infrared bands determined by FTIR are indicative of numerous biochemical molecules including proteins, lipids, and carbohydrates. The specific functional groups present in both lysate fractions and the intact *Synechococcus* cells are nearly identical based on comparison of the FTIR spectra, including the most noticeable peaks between 1000-1200 cm^{-1} which are characteristic of C-O-C, C-O-P, and P-O-P stretching (Coates, 2000; Naumann, 2000) in lipopolysaccharides (Yee et al., 2004). There was also a strong, broad peak at 3414 cm^{-1} due to O-H vibrations (Coates, 2000; Naumann, 2000). Further sharp absorption peaks were observed at 1655 and 1534 cm^{-1}, indicative of amide I group α helical structures and amide II groups, respectively (Naumann, 2000), which are characteristic of the outer membranes of cyanobacteria which contain lipopolysaccharides and proteins (Benning et al., 2004). Adsorption peaks between 2800-3000 cm^{-1} are suggestive of C-H stretching of $-CH_3$ and $>CH_2$ functional groups, which could be related to the fatty acid components of phospholipids (Yee et al., 2004). The smaller

absorption band at 1234 cm^{-1} is consistent with P=O stretching of $>PO_2^-$ phosphodiesters, which is characteristic of nucleic acid or phorylated polysaccharides (Yee et al., 2004), and the band at 1395 cm^{-1} could be due to C=O stretching of COO^- groups (Naumann, 2000; Benning et al., 2004).

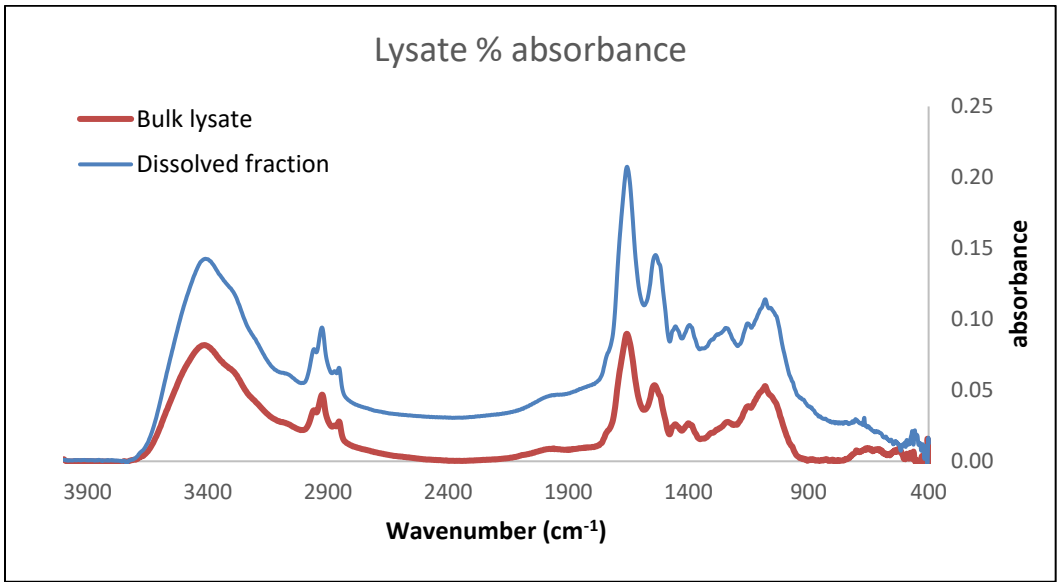

Figure 3.2: FTIR spectra for bulk lysate and dissolved fraction in terms of absorbance.

3.3.4 Proton reactivity

Titration data for 2 g/L *Synechococcus* lysate and the dissolved fraction (0.45 µm filtered lysate) in 0.56 M NaCl are presented in terms of excess charge per gram of biomass versus pH (Figure 3.3 and Table 3.2). It was observed that the cell lysate has a strong buffering capacity in the circumneutral pH range, with the highest changes in excess charge occurring at low and high pH values where a small addition of base induces a large change in excess charge. The background electrolyte was subtracted from the titration as per Lalonde et al. (2008) to ensure the only buffering effects were a result of the biomass and not the NaCl solution. The number of pK_a values is fixed by the user in FITEQL (Herbelin and Westall, 1999), which then simultaneously optimizes the value of each pK_a and the corresponding site concentrations. Protonation models with 2-4 sites

were tested for the cell lysate, and a model where 3 proton active sites were invoked provided the best fit to the data.

By combining spectroscopic studies with titration data, the specific functional groups can be assigned to each of the proton active sites determined by the titration data. FTIR analysis shows the presence of carboxyl, phosphoryl, amine, and hydroxyl groups, each of which deprotonates under different pH conditions (Fein et al., 1997). Carboxyl groups generally deprotonate under acidic conditions (pH 3-6), in which case site 1 is likely composed of carboxyl groups and deprotonates as given by reaction 1:

$$R{>}COOH + OH^- = R{>}COO^- + H_2O \quad [1]$$

Phosphoryl groups typically have pK_a values in the neutral pH range between 5-8, as such site 2 can be assigned a phosphoryl site as given by reaction 2.

$$R{>}PO_4H_2 + OH^- = R{>}PO_4H^- + H_2O \quad [2]$$

Amine and hydroxyl groups usually have alkaline pK_a values in the pH 8-10 range, and therefore, compose the surface functional groups for the 3rd proton active site, given by equations 3 and 4, respectively.

$$R{>}NH_3^+ + OH = R{>}NH_2 + H_2O \quad [3]$$

$$R{>}OH^- + OH^- = R{>}O^- + H_2O \quad [4]$$

Although proton active sites which deprotonate under alkaline conditions can be interpreted as both amine and hydroxyl groups (Fein et al., 1997), the hydroxyl group is generally associated with phenol groups (Cox et al., 1999). Thus, more information is required to definitively assign a functional group to this site.

Based on the titration data, Site 1 has similar densities of proton active carboxyl sites for both the bulk lysate and the dissolved fraction. The bulk lysate has approximately 3 times more

hydroxyl groups (Site 3) than were calculated for the dissolved lysate. However, the largest disparity between the two samples is shown in the 2nd site, where the dissolved fraction has ~60 times more phosphoryl groups than the bulk lysate for an equivalent amount of biomass.

Each of these site concentrations are higher on a per-gram basis than intact *Synechococcus* cells compared to studies by both Liu et al (2015) and the results from Chapter 2. Furthermore, the site pK_a values are also lower for the DOC analogue, meaning the proton-active sites begin to deprotonate at a lower pH than the intact cells, which provides the DOC with an overall negative charge at lower pH values. As such, the *Synechococcus* lysate and the dissolved fraction are more reactive than the intact cells, which is to be expected because of the greatly increased ligand availability to solution due to the sonication. For these reasons, the increased number of negatively charged sites coupled with lower pK_a values would likely allow for the lysate to complex more protons and metals than an equivalent mass of intact cells.

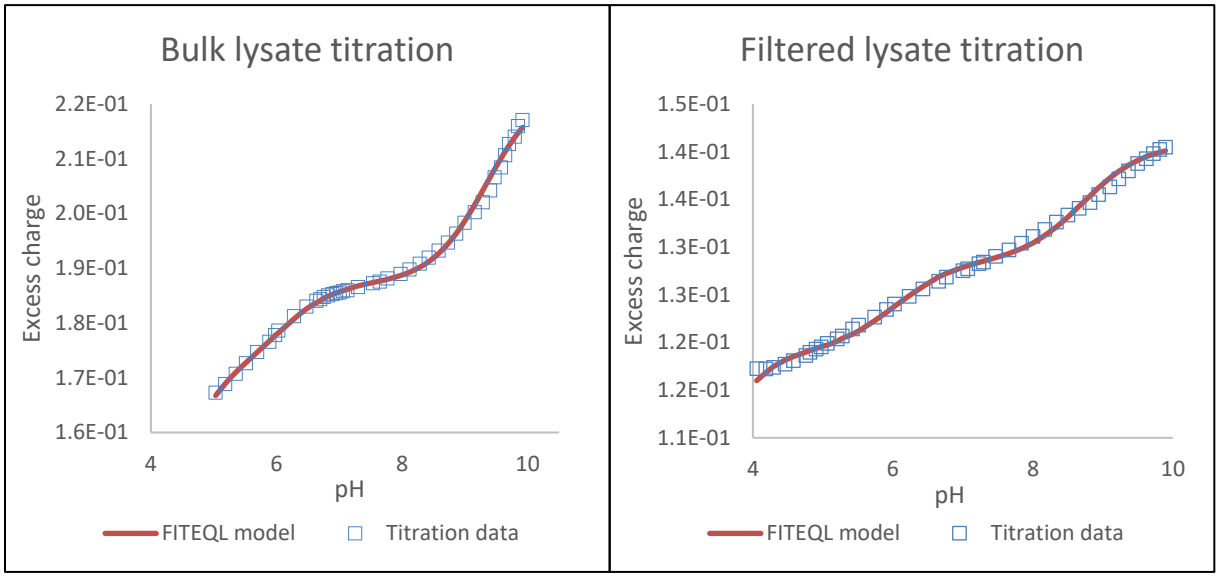

Figure 3.3 (a&b): Titration data in terms of excess charge per gram of biomass for the bulk lysate (a) and the dissolved fraction (b) plotted alongside the FITEQL protonation model.

Site	Sample	1	2	3
pKa	Bulk lysate	3.578	6.389	9.498
	Dissolved	2.504	6.028	8.720
Site density (mol/g)	Bulk lysate	0.149	0.0151	0.0372
	Dissolved	0.110	0.936	0.0123

Table 3.2: Titration data for the bulk lysate and dissolved fraction.

3.4 Discussion

3.4.1 Surface reactivity of the DOC analogue

Neihof et al. (1972) determined by electrophoresis that many natural particles in seawater, such as bacteria, small algae, and clays have a net negative surface charge. This notion is corroborated by the results here as it was determined that the lysate has many proton-active sites that deprotonate with increasing pH, with these negatively charged sites then being able to electrostatically attract cations from solution. Although the lysate possesses the same surface organic functional groups as intact *Synechococcus* cells, as evidenced by their nearly identical FTIR spectra, the pK_a values of the DOC analogue are generally lower, especially for the carboxyl and phosphoryl sites. Furthermore, the lysate contains more moles of proton active functional groups on a per gram basis than the intact cells which could be due to the increased site availability due to the lysis of the bacteria.

Bioessential trace elements, such as Fe, Co, Ni, Cu, Zn, and Mo, are required as co-factors in a multitude of metalloenzymes required in many cellular processes like photosynthesis, respiration, and DNA and RNA synthesis (Robbins et al., 2016). However, it has been estimated that >99% of total Fe and Cu, approximately 98% of Zn, >90% of Co, and ~80% of Cd in the

oceans are bound to strong metal-binding ligands based on studies employing stripping voltammetric analysis (see Bruland et al. (2014) and references therein).

Numerous studies have explored the complexation of trace elements to organic ligands. For example, Gonzalez-Davila et al. (1995) demonstrated that the marine phytoplankton *Dunaliella teriolecta,* and its exudates, can both complex Cu from seawater, showing that extracellular ligands play an important role in sequestering trace cations. Humic substances compose 5-25% of DOC in seawater (Benner, 2002), and therefore, many workers are now exploring their effect on trace metal cycling. Yang and van den Berg (2009) determined the stability constants of Cu, Zn, Co, and Al with humic and fulvic acids using a two-site metal binding model. They determined the major functional groups involved in metal binding were carboxyl and phenol (hydroxyl group attached to a benzene ring) groups. Yang and van den Berg (2009) further hypothesized that humic substances in seawater might be an important metal binding compound, a notion later confirmed by Whitby and van den Berg (2015) who studied the complexation of Cu by humic substances in coastal and estuarine waters. Further work exploring humic substance-Cu complexation by Abualhaija et al. (2015), found that humic substances make up the major Cu and Fe binding ligands in the Mersey estuary (England) and nearly the entire inventory of Fe binding ligands is represented by humic substances, while it is likely that a second ligand also plays a role in Cu complexation. Whitby et al. (2018) explored Cu binding in the NE Pacific, and substantiated the finding that Cu is bound by two major ligands; a strong ligand class of low concentration, and a weaker Cu-binding ligand of higher concentration. Research by Bundy et al. (2015) proposed that humic substances may be an important vector in the transferring of organically bound trace metals from estuaries to the coastal waters.

These studies show that although humic substances are an important compound in complexation trace metals, the major functional involved in binding trace metals are carboxyl (Yang and Van Den Berg, 2009; Bundy et al., 2015) and phenol (Yang and Van Den Berg, 2009) groups. These ligands were the same organic functional groups determined in this study by the titration data modelling in tandem with the FTIR spectra. The work performed in Chapter 2 demonstrated that the organic ligands on *Synechococcus* cells, specifically carboxyl groups, can adsorb appreciable quantities of trace metals from simulated seawater; hence, it is highly likely that bacterially-derived organic molecules would have a considerable impact on trace metal cycling because of the similarity in ligand type, lower pK_a values, and marine abundances.

3.4.2 Marine DOC and trace metal cycling

Many bioessential trace elements exhibit nutrient like profiles in the ocean, with decreased concentrations in the pelagic zone due to uptake by bacteria and adsorption to organic ligands, with the trace metals returning to solution in deeper waters due to remineralization (Sunda, 2012). DOM shows a similar profile with low concentrations in surface waters and high concentrations in deeper waters, although the profile varies with lability.

Labile DOC is unlikely to be an important mechanism for transporting trace metals out of the water column and into the sediment due to its short residence time. However, it is likely important in the recycling of trace metals as the organic compounds with their associated trace metals are quickly consumed in the pelagic zone. By contrast, SLDOC is a major contributor for trace metal transport out of the photic zone as it is responsible for the largest flux of DOC into deeper waters (Carlson et al, 2004). Based on nuclear magnetic resonance spectroscopy and ultra-high-resolution mass spectrometry, a large fraction of SLDOC is composed of carboxyl-rich

alicyclic molecules (CRAM) and are thought to contain a ligand which a strong affinity for metal binding (Hertkorn et al., 2006). Based on previous work focusing on metal-ligand interactions in cyanobacteria as well as the structure of CRAM molecules, it is likely that this ligand is a carboxyl group. Therefore, since CRAM molecules in SLDOC molecules are highly surface reactive, they may be one of the first vectors in transferring adsorbed trace metals from the pelagic zone into deeper waters and may be important for longer-term trace metal sequestration than labile DOC.

Refractory compounds persist in the oceans for thousands of years (Williams and Druffel, 1987; Druffel et al., 2016), and could have an even larger effect on the long term cycling of trace metals than SLDOC due to the long residence times and immense reservoir size. However, the refractory aspect of DOC can be contextual. For example, an organic compound could be recalcitrant to a microbe if the latter lacks the necessary enzyme to break down the molecule (Jiao et al., 2014). Since the DOC reservoir is composed of potentially billions of different molecules (Koch et al., 2005), the concentration of individual species is extremely low, below the threshold to be accessed by microbes. This notion has been termed the "dilution hypothesis" by Arrieta et al. (2015).

Ultra-refractory DOC (URDOC) is composed of polycyclic aromatic hydrocarbons, known as has residence times of 2500-13900 years based on ^{14}C analysis (Ziolkowski and Druffel, 2010), and is partly composed of thermogenic black carbon, or polycyclic aromatic hydrocarbons (Dittmar and Paeng, 2009). In order to fully understand the effects different classes of DOC have on the adsorption and cycling of trace metals, more work needs to be undertaken to determine the composition and structure of these molecules, followed by exploration of their metal binding capabilities.

3.4.3 Viral lysis and the coupled cycling of DOC and trace elements

In this study, the effects of viral lysis were simulated by sonication to study the reactivity of dissolved organic carbon derived from cyanobacteria. It was determined that the cell lysate, as an analogue for DOC, is highly surface reactive and has many negatively charged functional groups at seawater pH which have the potential to adsorb trace elements. The adsorption of trace elements could affect the cycling of trace elements through the water column as viral lysis produces vast amounts of DOC through the viral shunt (Jiao et al., 2010). The viral shunt diverts carbon from the POC pool to the DOC pool (Wilhelm and Suttle, 1999), and consequently, a large proportion of DOC is not transferred to higher trophic levels, but is recycled through the microbial loop (Azam et al., 1983). Furthermore, the viral shunt reduces the C:N:P ratio, sequestering more C relative to N and P, allowing the N and P to be accessed as nutrients by other organisms (Suttle, 2007).

A major assumption about viral infection on marine microbial populations is that the viruses affect all members of the prokaryotic community equally, however, it is possible that viruses preferentially infect certain populations (Suttle, 2007). This could have a significant effect on nutrient and carbon cycling in the ocean if the viruses were to specifically target the fastest growing populations, such as *Synechococcus*. If a virus were to quickly spread through a *Synechococcus* bloom, large amounts of DOM would be released, with these molecules being able to adsorb or compete with other ligands for free trace metals, creating a localized area of extremely low nutrient concentrations. This, in turn, could prevent proliferation growth of microbial communities until nutrients are replenished through diffusion and upwelling currents, or the dissolved organic molecules are remineralized with the trace metals returning to solution.

3.4.4 Organic carbon removal processes

Although there are many processes that produce DOM as described in section 1.3, DOM concentrations are maintained within a narrow range of 34-80 μm kg^{-1} C throughout the oceans, and hence, many efficient removal processes must exist (Hansell et al., 2009). Through these processes, which are both biotic and abiotic, the dissolved carbon molecules and their associated trace metals are processed many times where they are either recycled through the water column, or eventually incorporated into the sediment.

DOM can be removed biotically, through chemoheterotrophy by some bacteria and archaea that use organic matter as both a carbon source and electron donor (Carlson and Hansell, 2014). Bacterioplankton (heterotrophic prokaryotes) are one of the major consumers of marine DOM, and can transform DOM to POM through the microbial loop, which is the return of DOM to higher trophic levels through consumption by bacteria (Azam et al., 1983). Eukaryotes can remove colloidal DOM containing carbohydrates and proteins directly from seawater (First and Hollibaugh, 2009). Abiotic processes can also alter the composition of DOM in the water column, including phototransformation into CO_2 and CO, sorption onto sinking particles, condensation to marine microgels, and hydrothermal circulation (Carlson and Hansell, 2014).

Engel et al (2004) demonstrated through experimental and modelling studies that polysaccharides formed during phytoplankton blooms can form aggregates, converting dissolved organic carbon into particulate organic carbon. These particles can then settle gravitationally through the water column. Since polysaccharides provide strong binding sites for trace metals, this aggregation may be an important processes in controlling race metal residence times in the surface ocean (Engel et al., 2004). DLS analysis performed on the *Synechococcus* lysate shows that the organic molecules within the lysate can form aggregates in solution, similar to what was

demonstrated by the Engel et al (2014) study. Therefore, it is possible that DOC molecules with their adsorbed metals could aggregate and sink out of the water column. This, combined with viral lysis of a plankton bloom, could cause a major, localized sink of nutrients. If a large bloom were infected and lysed as described above, the vast amount of quickly produced DOM could adsorb the free trace element inventory, aggregate into larger particles, and sink out of the water column to be incorporated in the sediment. Another sink for DOM and adsorbed trace metals could be due to association with clays. Clay particles are also highly surface reactive and have the ability to adsorb trace metals (e.g. Spark et al., 1995; Playter et al., 2017; Hao et al., 2018). Theoretically, if DOM molecules had adsorbed divalent cations, they could act as a cation bridge between the negatively charged surface of clay and the negatively charged DOM molecules. These DOM-metal-clay particulates would then quickly settle out of solution, acting as another potential exit channel for trace metals from seawater.

3.4.5 Impacts on the Proterozoic carbon cycle

Changes in the long-term carbon cycle has the ability to greatly influence the evolution of both the biosphere and geosphere, as these changes in the carbon cycle are recorded in the isotopic compositions of ancient carbonate and organic carbon sediments. An extremely large DOC pool in the Precambrian ocean could have important implications for the earliest trace metal and biogeochemical cycles, oxygenation of the atmosphere, and the termination of BIF deposition. The oxidation of organic matter can act as a marine oxygen sink, since the oxygen content of deep ocean waters is controlled by the balance between the supply of downwelling oxygen, and oxygen consumption by the decomposition of organic debris (Sarmiento et al., 1988). However, deep-ocean anoxia could occur by either a decrease of downwelling oxygen, or an influx of nutrients

leading to increased primary productivity releasing more organic matter to be subjected to decomposition (Sarmiento et al., 1988). Canfield (1998) proposed that increased sulphate reduction in restricted basins in the Proterozoic ocean could have produced enough sulfide to remove dissolved ferrous iron, thus preventing the further creation of BIF and limiting the accumulation of trace nutrients in the water column. This sulfate reduction was a by-product of reduced oxygenation due to the oxidation of organic matter which would allow euxinic conditions to persist (Canfield, 1998). However, limited evidence for this theory has been found in the rock record (Planavsky et al., 2011; Poulton and Canfeld, 2011). In contrast to this hypothesis, modelling studies determined that the organic carbon content of the Neoproterozoic ocean was at least 2-3 orders of magnitude greater than that of modern oceans (Rothman et al., 2003). These organic-rich oceans were stratified, with shallow oxygenated waters overlying deep anoxic waters where most of the organic matter remained in suspension. Oxygen which had not escaped to the atmosphere would have been consumed by respiration in surface waters, with a deep pool of organic matter buffering against a buildup of deep-ocean oxygen (Rothman et al., 2003). Therefore, an increased DOM pool in the Precambrian could have delayed the buildup of oxygen in the ocean and atmosphere

The size and lability of the Precambrian marine DOM pool could greatly affect Precambrian ocean chemistry. A large DOM pool could theoretically prevent oxygen from building up in the ocean because of oxygen consumption due to the oxidation of organic matter. The size of the Precambrian DOC reservoir could be controlled by primary production, which is further controlled by the input of nutrients into the ocean due to continental weathering and hydrothermal inputs. Although enough oxygen could be present in surface waters and the atmosphere to promote continental weathering, the decomposition of organic matter could prevent

oxygenation of deeper waters. Jiao et al. (2014) proposed that the microbial carbon pump (MCP) may have been an important process in creating a huge RDOC reservoir in a Precambrian ocean. However, this may not necessarily decrease the amount of oxygen in the atmosphere if these organic compounds were highly recalcitrant and thus resistant to decomposition. This RDOC reservoir could, however, complex trace elements and affect their bioavailability in the water column, delaying the proliferation of some life forms in the ocean. Furthermore, a large DOC pool could complex the free Fe^{2+} in solution inhibiting its oxidation to the less soluble Fe^{3+} and preventing the deposition of laterally extensive banded iron formations. Regardless of the lability of the Precambrian DOM pool, its presence in the early ocean would have an influence on the early ocean chemistry, whether it be a sink for oxygen through decomposition, or by chelating trace metals and reducing their bioavailability.

3.5 Conclusion

This study was one of the first to utilize a surface complexation modelling approach to determine the surface reactivity of marine DOC. Cyanobacterial cell lysate, as an analogue for marine DOC, was shown to be highly reactive, containing more proton-active sites and lower pK_a values than intact *Synechococcus* cells, while the truly dissolved fraction of the lysate was shown to have a higher number of proton-active sites than both intact cells and the bulk lysate. FTIR analysis determined that the dissolved fraction, bulk lysate, and intact cells all contain similar functional groups, and previous studies have found that these groups (carboxyl and phosphoryl) have the ability to adsorb trace metals from seawater. Therefore, dissolved organic molecules derived from cyanobacteria would likely have a greater influence in the complexation of trace metals than cyanobacteria.

Viruses can quickly spread through marine organisms, including cyanobacteria, are a major contributor to mortality in the ocean causing a turnover of 20-50% of marine biomass per day (Suttle, 2007). Lysis can release and abundance of organic molecules which can quickly cycle through the water column. These organic molecules can then form aggregates which sink to the seafloor, carrying with them the trace metals which could then be incorporated into the sediment. However, the type of molecule does play a role in trace metal sequestration. Some compounds, such as CRAM, contain many carboxyl groups and could impart a greater influence on trace metal cycling than other bacterially-derived molecules. The recalcitrance of a molecule will also affect its contribution to trace metal cycling, the more recalcitrant molecules are more resistant to degradation and will affect trace metal cycling on longer time scales than labile compounds.

Dissolved organic matter can also influence marine chemistry in the Precambrian oceans. A large DOM reservoir could affect the buildup of oxygen in the atmosphere through decomposition of organic matter, complexation of iron in the ocean keeping it soluble and preventing the deposition of BIF, or complexation of bioessential trace metals which could delay evolution of the marine biosphere. Further work investigating which of these possible scenarios could have been possible during the Precambrian is necessary to determine the extent to which DOM could have affected ocean chemistry.

Based on this study, it is clear that the surface properties of DOM has the potential to have a profound effect on the cycling of trace elements in the ocean. However, the mechanisms and extent to which DOM affects it remains to be completely explained, and further studies should explore the metal binding of DOM molecules in more depth, specifically which molecules are the most important for metal adsorption. This will give marine geochemists and oceanographers a

better understanding of trace metal cycling throughout not only the modern ocean, but also oceans of the past.

References

Abualhaija M. M., Whitby H. and van den Berg C. M. G. (2015) Competition between copper and iron for humic ligands in estuarine waters. *Mar. Chem.* **172**, 46–56.

Aluwihare L. I. and Repeta D. J. (1999) A comparison of the chemical characteristics of oceanic DOM and extracellular DOM produced by marine algae. *Mar. Ecol. Prog. Ser.* **186**, 105–117.

Amon R. M. W. and Benner R. (1994) Rapid cycling of high-molecular-weight dissolved organic matter in the ocean. *Nature* **369**, 549–552.

Anderson T. R. and Tang K. W. (2010) Carbon cycling and POC turnover in the mesopelagic zone of the ocean: Insights from a simple model. *Deep. Res. Part II Top. Stud. Oceanogr.* **57**, 1581–1592.

Arrieta J. M., Mayol E., Hansman R. L., Herndl G. J., Dittmar T. and Duarte C. M. (2015) Dilution limits dissolved organic carbon utilization in the deep ocean. *Science.* **348**, 331–333.

Azam F., Fenchel T., Field J., Gray J., Meyer-Reil L. and Thingstad F. (1983) The Ecological Role of Water-Column Microbes in the Sea. *Mar. Ecol. Prog. Ser.* **10**, 257–263.

Benner R. (2002) Chemical composition and reactivity. In: *Biogeochemistry of marine dissolved organic matter.* Elsevier Inc. 59–90.

Benning L. G., Phoenix V. R., Yee N. and Konhauser K. O. (2004) The dynamics of cyanobacterial silicification: An infrared micro-spectroscopic investigation. *Geochim. Cosmochim. Acta* **68**, 743–757.

Boiteau R. M., Mende D. R., Hawco N. J., McIlvin M. R., Fitzsimmons J. N., Saito M. A., Sedwick P. N., DeLong E. F. and Repeta D. J. (2016) Siderophore-based microbial adaptations to iron scarcity across the eastern Pacific Ocean. *Proc. Natl. Acad. Sci.* **113**, 14237–14242.

Bruland K. W. and Lohan M. C. (2003) Controls of Trace Metals in Seawater. In *Treatise on Geochemistry* pp. 19–51.

Bundy R. M., Abdulla H. A. N., Hatcher P. G., Biller D. V., Buck K. N. and Barbeau K. A. (2015) Iron-binding ligands and humic substances in the San Francisco Bay estuary and estuarine-influenced shelf regions of coastal California. *Mar. Chem.* **173**, 183–194.

Canfield D. E. (1998) A new model for Proterozoic ocean chemistry. *Nature* **396**, 450–453.

Carlson C. A. and Hansell D. A. (2014) *DOM Sources, Sinks, Reactivity, and Budgets* in Biogeochemistry of Marine Dissolved Organic Matter: Second Edition. Elsevier Inc.

Carlson C. A., Giovannoni S. J., Hansell D. A., Goldberg S. J., Parsons R. and Vergin K. (2004) Interactions among dissolved organic carbon, microbial processes, and community structure in the mesopelagic zone of the northwestern Sargasso Sea. *Limnol. Oceanogr.* **49**, 1073–1083.

Clark L. L., Ingal E. D. and Benner R. (1998) Marine phorphorus is selectively remineralized. *Nature* **393,** 426

Coates J. (2000) Interpretation of Infrared Spectra, A Practical Approach. *Encycl. Anal. Chem.*, 10815–10837.

Cox J. S., Smith D. S., Warren L. A. and Ferris F. G. (1999) Characterizing heterogeneous bacterial surface functional groups using discrete affinity spectra for proton binding. *Environ. Sci. Technol.* **33**, 4514–4521.

Dittmar T. and Stubbins A. (2014) Dissolved Organic Matter in Aquatic Systems. In *Treatise on Geochemistry*: *2nd Ed*., Elsevier Ltd.

Dittmar T. and Paeng J. (2009) A heat-induced molecular signature in marine dissolved organic matter. *Nat. Geosci.* **2**, 175–179.

Druffel E. R. M., Griffin S., Coppola A. I. and Walker B. D. (2016) Radiocarbon in dissolved organic carbon of the Atlantic Ocean. *Geophys. Res. Lett.* **43**, 5279–5286.

Engel A., Thoms S., Riebesell U., Rochelle-Newall E. and Zondervan I. (2004) Polysaccharide aggregation as a potential sink of marine dissolved organic carbon. *Nature* **428**, 929–932.

Fein J. B., Daughney C. J., Yee N. and Davis T. A. (1997) A chemical equilibrium model for metal adsorption onto bacterial surfaces. *Geochim. Cosmochim. Acta* **61**, 3319–3328.

First, M.R. and Hollibaugh, J.T. (2009). The model high molecular weight DOC compound, dextran, is ingested by the benthic ciliate Uronema marinum but does not supplement ciliate growth. *Aquat. Microb. Ecol*. **57**, 79.

Gonzalez-Davila M., Magdalena Santana-Casiano J., Perez-Peña J. and Millero F. J. (1995) Binding of Cu(II) to the Surface and Exudates of the Alga Dunaliella tertiolecta in Seawater. *Environ. Sci. Technol.* **29**, 289–301.

Hansell D. A., Carlson C. A. and Schlitzer R. (2012) Net removal of major marine dissolved organic carbon fractions in the subsurface ocean. *Global Biogeochem. Cycles* **26**, 1–9.

Hansell D., Carlson C., Repeta D. and Schlitzer R. (2009) Dissolved Organic Matter in the Ocean: A Controversy Stimulates New Insights. *Oceanography* **22**, 202–211.

Herbelin A. L. and Westall J. C. (1999). FITEQL 4.0: A computer program for determination of chemical equilibrium constants from experimental data.

Hertkorn N., Benner R., Frommberger M., Schmitt-Kopplin P., Witt M., Kaiser K., Kettrup A. and Hedges J. I. (2006) Characterization of a major refractory component of marine dissolved organic matter. *Geochim. Cosmochim. Acta* **70**, 2990–3010.

Hao W., Flynn S. L., Alessi D. S. and Konhauser K. O. (2018) Change of the point of zero net proton charge (pHPZNPC) of clay minerals with ionic strength. *Chem. Geol.* **493**, 458–467.

Hopkinson C. S. and Vallino J. J. (2005) Efficient export of carbon to the deep ocean through dissolved organic matter. *Nature* **433**, 142–145.

Jiao N., Herndl G. J., Hansell D. A., Benner R., Kattner G., Wilhelm S. W., Kirchman D. L., Weinbauer M. G., Luo T., Chen F. and Azam F. (2010) Microbial production of recalcitrant dissolved organic matter: Long-term carbon storage in the global ocean. *Nat. Rev. Microbiol.* **8**, 593–599.

Jiao N., Robinson C., Azam F., Thomas H., Baltar F., Dang H., Hardman-Mountford N. J., Johnson M., Kirchman D. L., Koch B. P., Legendre L., Li C., Liu J., Luo T., Luo Y. W., Mitra A., Romanou A., Tang K., Wang X., Zhang C. and Zhang R. (2014) Mechanisms of microbial carbon sequestration in the ocean; Future research directions. *Biogeosciences* **11**, 5285–5306.

Koch B. P., Witt M., Engbrodt R., Dittmar T. and Kattner G. (2005) Molecular formulae of marine and terrigenous dissolved organic matter detected by electrospray ionization Fourier transform ion cyclotron resonance mass spectrometry. *Geochim. Cosmochim. Acta* **69**, 3299–3308.

Lalonde S. V., Dafoe L. T., Pemberton S. G., Gingras M. K. and Konhauser K. O. (2010) Investigating the geochemical impact of burrowing animals: Proton and cadmium adsorption onto the mucus lining of Terebellid polychaete worms. *Chem. Geol.* **271**, 44–51.

Lalonde S. V., Smith D. S., Owttrim G. W., Konhauser K. O. (2008) Acid-base properties of cyanobacterial surfaces I: Influences of growth phase and nitrogen metabolism on cell surface reactivity. *Geochim. Cosmochim. Acta* **72**, 1257–1268.

Liu Y., Alessi D. S., Owttrim G. W., Petrash D. A., Mloszewska A. M., Lalonde S. V., Martinez R. E., Zhou Q. and Konhauser K. O. (2015) Cell surface reactivity of Synechococcus sp. PCC 7002: Implications for metal sorption from seawater. *Geochim. Cosmochim. Acta* **169**, 30–44

Naumann D. (2000) Infrared Spectroscopy in Microbiology. *Encycl. Anal. Chem.*, 1–32.

Neihof R. A. and Loeb G. I. (1972) The Surface Charge of Particulate Matter in Seawater. *Limnol. Oceanogr.* **17**, 7–16.

Ogawa H., Amagai Y., Koike I., Kaiser K. and Benner R. (2001) Production of refractory dissolved organic matter by bacteria. *Science.* **292**, 917–920.

Planavsky N. J., McGoldrick P., Scott C. T., Li C., Reinhard C. T., Kelly A. E., Chu X., Bekker A., Love G. D. and Lyons T. W. (2011) Widespread iron-rich conditions in the mid-Proterozoic ocean. *Nature* **477**, 448–451.

Playter T., Konhauser K., Owttrim G., Hodgson C., Warchola T., Mloszewska A. M., Sutherland B., Bekker A., Zonneveld J. P., Pemberton S. G. and Gingras M. (2017) Microbe-clay interactions as a mechanism for the preservation of organic matter and trace metal biosignatures in black shales. *Chem. Geol.* **459**, 75–90.

Poulton S. W. and Canfeld D. E. (2011) Ferruginous conditions: A dominant feature of the ocean through Earth's history. *Elements* **7**, 107–112.

Robbins L. J., Lalonde S. V., Planavsky N. J., Partin C. A., Reinhard C. T., Kendall B., Scott C., Hardisty D. S., Gill B. C., Alessi D. S., Dupont C. L., Saito M. A., Crowe S. A., Poulton S. W., Bekker A., Lyons T. W. and Konhauser K. O. (2016) Trace elements at the intersection of marine biological and geochemical evolution. *Earth-Science Rev.* **163**, 323–348.

Rothman D. H., Hayes J. M. and Summons R. E. (2003) Dynamics of the Neoproterozoic carbon cycle. *Proc. Natl. Acad. Sci.* **100**, 8124–8129.

Safari S., Sheikhi A. and van de Ven T. G. M. (2014) Electroacoustic characterization of conventional and electrosterically stabilized nanocrystalline celluloses. *J. Colloid Interface Sci.* **432**, 151–157.

Sarmiento J. L., Herbert T. D. and Toggweiler J. R. (1988) Causes of anoxia in the world ocean. *Glob. Biogeochem. Cycles1* **2**, 115–128.

Spark K. M., Wells J. D. and Johnson B. B. (1995) Characterizing trace metal adsorption on kaolinite. *Eur. J. Soil Sci.* **46**, 633–640.

Sunda W. G. (2012) Feedback interactions between trace metal nutrients and phytoplankton in the ocean. *Front. Microbiol.* **3**.

Suttle C. A. (2007) Marine viruses - Major players in the global ecosystem. *Nat. Rev. Microbiol.* **5**, 801–812.

Whitby H. and van den Berg C. M. G. (2015) Evidence for copper-binding humic substances in seawater. *Mar. Chem.* **173**, 282–290.

Whitby H., Posacka A. M., Maldonado M. T. and van den Berg C. M. G. (2018) Copper-binding ligands in the NE Pacific. *Mar. Chem.* **204**, 36–48.

Whitman W. B., Coleman D. C. and Wiebe W. J. (1998) Prokaryotes: The unseen majority. *Proc. Natl. Acad. Sci.* **95**, 6578–6583.

Wilhelm S. W. and Suttle C. A. (1999) Viruses and Nutrient Cycles in the Sea. *Bioscience* **49**,

781–788.

Williams P. M. and Druffel E. R. M. (1987) Radiocarbon in dissolved organic matter in the central North Pacific Ocean. *Nature* **330**, 246–248.

Yang R. and Van Den Berg C. M. G. (2009) Metal complexation by humic substances in seawater. *Environ. Sci. Technol.* **43**, 7192–7197.

Yee N., Benning L. G., Phoenix V. R. and Ferris F. G. (2004) Characterization of Metal-Cyanobacteria Sorption Reactions: A Combined Macroscopic and Infrared Spectroscopic Investigation. *Environ. Sci. Technol.* **38**, 775–782.

Ziolkowski L. A. and Druffel E. R. M. (2010) Aged black carbon identified in marine dissolved organic carbon. *Geophys. Res. Lett.* **37**, 1–4.

Chapter 4

The net effects of marine ligands on trace metal cycling and future directions

4.1 Interactions between cyanobacteria, DOC, and trace metals

The research presented here highlights the effects that both cyanobacteria and cyanobacteria-derived dissolved organic carbon can impart on marine trace metal cycling. In Chapter 2, the proton reactivity of *Synechococcus* and its ability to bind bioessential trace elements was determined employing titration and pH metal adsorption experiments, which were then used to develop a predictive surface complexation model. *Synechococcus* has three distinct proton-binding sites, composed of carboxyl, phosphoryl, and hydroxyl/amine organic functional groups with pK_a values of 5.59, 7.61, and 9.24, respectively. These values were consistent with previous studies that explored the surface properties of bacteria in both terrestrial and marine environments (e.g. Fein et al. 1997; Daughney et al. 1998; Yee et al. 2001; Borrok et al. 2005; Kaulbach et al. 2005; Lalonde et al. 2007; Liu et al. 2015; Martinez et al. 2016). With regards to trace metal adsorption, Zn exhibited the highest total adsorption, followed by Cu, Ni, and Co; the expected pattern as it follows the Irving-Williams stability series (Irving and Williams, 1953). Binding of metals invoked two of the three sites determined in the protonation model, the carboxyl and phosphoryl sites, and it was determined that the phosphoryl site had a higher affinity for metals than the carboxyl site. Furthermore, the SCM was able to accurately predict the adsorption behaviour in a competitive system when all four metals were present.

The values determined from the metal adsorption data were then used to estimate the impacts *Synechoccocus* could impart on trace metal cycling in the marine photic zone. It was determined that a *Synechococcus* bloom could theoretically adsorb all of the free Co, Ni, Cu, and Zn present in an equivalent volume of seawater. However, this did not take into account

competition among trace metals and between sorbents, such as dissolved organic carbon which has been shown to more strongly bind trace metals based on their thermodynamic binding constants (e.g.: Whitby et al. 2018).

Accordingly, Chapter 3 built upon the cell wall proton reactivity and metal binding properties determined for *Synechococcus* in Chapter 2, by assessing the proton and metal reactivities of the *Synechococcus* lysate, which was used as an analogue for marine DOC. The lysate was chosen as a DOC analogue because much of the marine DOC pool is produced autochthonously through direct release and viral lysis of these cells. Titrations, FTIR, NPOC, and DLS analyses were performed on the bulk lysate and the dissolved fraction to determine proton reactivity, surface functional groups, amount of organic carbon present in the lysate, and the size distribution, respectively. The titration data and subsequent SCM demonstrated that the lysate contains 3 surface functional groups, each of them having a lower pK_a value and higher site concentrations per equivalent mass than the intact *Synechococcus* cells. The composition of the functional groups on the *Synechococcus* cell wall and its lysate are similar based on FTIR analysis, which determined the presence of carboxyl, phosphoryl, hydroxyl, and amine groups. However, the SCM determined that both the bulk lysate and dissolved fraction contained approximately 100 x more carboxyl and hydroxyl/amine groups while the bulk lysate had approximately 10 x more phosphoryl sites and the dissolved fraction had about 100 x more phosphoryl sites than the *Synechococcus* cell wall.

The organic ligands derived from *Synechococcus* in this study are proton-active and can adsorb bioessential trace metals from seawater. This has important implications for the cycling of marine nutrients since these ligands can act as a sink for trace metals and alter their bioavailability. Cyanobacteria require trace metals as cofactors in metalloenzymes for a number of cellular

processes and rely on adsorption as the first step in acquiring them from seawater, followed by transfer across the cell membrane. However, there is a relationship between cyanobacteria and DOC as they both affect the cycling of marine trace metals, with a key link between cyanobacteria and DOC being viral cell lysis. The majority of trace metals in the ocean are heavily complexed by dissolved organic ligands (Bruland et al., 2014), many of which are produced by bacteria through either vial lysis, direct release, or feeding processes. The interaction between cyanobacteria and DOC could depend on the lability of the metal binding ligands in the ocean. Previous studies have determined that trace metals are more strongly bound to dissolved ligands (e.g. Whitby et al., 2018), than to cyanobacterial cell walls, as described in detail at the end of Chapter 2. However, it could also be possible that the cyanobacteria need not compete with the ligands for trace metals but instead consume the labile DOC with adsorbed trace metals to meet both their micro and macro nutrient needs concurrently, and then passively release the excess nutrients back into the environment. On the other hand, if the trace metals are strongly absorbed to more recalcitrant compounds, cyanobacteria may need to develop a process to compete with the DOC, as these DOC molecules could not be consumed by microbes. Because of their long residence times in the ocean, the RDOC compounds would have a more long-term effect on trace metal cycling. In this case, the cyanobacteria could overcome this competition through producing high metal affinity ligands such as sulfhydryl groups (Mishra et al., 2010; Nell and Fein, 2017; Yu et al., 2018). Therefore, the specific compounds that the metals are most strongly bound to, as well as their labilities, will need to be investigated in further studies employing techniques such as GC-MS.

Many studies have explored the trace element inventories of ancient black BIF and black shales (see references in Chapter 2), however understanding the processes by which trace metals

were included in these sediments is important for understanding ancient ocean chemistry. Adsorption to cyanobacteria and DOC are two such processes. Based on DLS analysis, DOC can aggregate to form POC which can then sink through the water column along with *Synechococcus* cells, carrying adsorbed trace metals to the seafloor where they can become incorporated in the sediment, as described in Section 3.4.4. If the Precambrian ocean contained a large DOC pool, this could affect the bioavailability of trace metals including Fe, preventing the deposition of BIF. If the bioavailability of trace metals in ancient oceans were low either due to low supply or strong sinks, the evolution of some metalloenzymes would be delayed if the concentration of trace metal cofactors were below a certain threshold. Furthermore, previous studies have indicated that silica-containing oxyhydroxides have a point of zero charge (PZC) in the pH range of 5.3-7.5 (Schwertmann and Fechter, 1982), which falls within the pH range of Archean seawater (6.5-7) (Halevy and Bachan, 2017). Therefore, silica-containing oxyhydroxides would likely be neutrally, or only slightly negatively charged compared to *Synechococcus*, which remain negatively charged above pH 4 (Liu et al., 2015). The *Synechococcus* would then be able to attract positively charged ions from seawater and could be a more efficient sink for trace metals than silica-containing oxyhydroxides, which could make them one of the most important sinks for trace metals into ancient chemical sediments.

4.2 Limitations to this study

Although the surface complexation modelling was performed in accordance with previously published protocols, some limitations still exist. For instance, a non-electrostatic model was applied to the data, so although the data presented here is applicable to high ionic strength environments such as the oceans, this model might not be accurate under comparatively low ionic

strengths. In such a case, an electrostatic approach such as the constant capacitance model (CCM) could be a better alternative, as it would be able to account for changes in the bacterial electric field as a function of ionic strength. However, CCM models require an electrostatic fitting parameter and information on the surface area of the sorbent, both of which usually need to be estimated which would lead to inherent error. Furthermore, the SCM only provides a model of best fit to the data. As such, the pK_a values and site concentrations are not necessarily reflective of reality, therefore caution should be used when making direct assumptions and calculations from this data.

Unrealistically high metal concentrations were used for the pH edge experiments in order to be within detection limits of the ICP-MS. This could be problematic because a set of relatively low concentration but high affinity sites on the *Synechoccocus* cell walls or lysates could control the removal of trace metals, in which case the more abundant carboxyl, hydroxyl, and phosphoryl groups may not be at seawater metal concentrations. For example, due to their generally low concentrations, sulfhydryl groups were not taken into account in the SCM, although if present, they would be expected to have the highest affinity for trace metals, as determined by Nell and Fein (2017) and Yu et al. (2018).

Metal binding experiments were not performed using the lysate due to technical limitations, as separating the lysates with the bound metals from the free metal species could not be performed by filtration alone. Various solid phase extraction (SPE) techniques (e.g. C18 and Strata X columns (Phenomenex)) were used to remove the organics from solution, however the SPE cartridges also removed some free metal as observed in blank experiments. In this case, IC-ICP-MS or HPLC-ICP-MS techniques may be used to overcome this problem as they would be able to analyze for

free metal concentrations, as well as the quantifying the amount of trace metals associated with each functional group.

4.3 Future directions

Future work exploring the effects organic ligands impart on trace metal cycling should include high resolution work using techniques such as FT-ICR-MS, HPLC-Orbitrap-MS or HPLC-ICP-MS, combined with SCM using realistic concentrations of biomass and trace metals could give better insights into the mechanisms of adsorption in seawater including their binding strengths to various ligand types and the type of complexes that they form. The investigation of different ligand types, including sulfhydryl, phenol, and silanol groups would further our understanding of metal-bacteria interactions, and allow for the assigning of relative binding strengths to each of these groups.

The adsorption behaviour of other nutrients could also be examined including divalent cations, and oxyanions in the presence of cations to observe the effects of cation bridging. Adsorption of macro-nutrients such as N and P should be investigated as these can heavily influence primary productivity in the oceans. Other sorbents should also be considered such as ferrihydrite, clay minerals, and silica in the ocean to compare their adsorption capacities with that of cyanobacteria.

More in-depth characterization of the lysate is also required, utilizing techniques such as FT-ICR-MS to determine the classes and identities of organic molecules present in the lysate. These molecules could then be compared to other studies where the composition of DOM was determined for marine samples. If the analogue DOC showed similarities to previously discovered RDOC compounds, then it is possible that RDOC can be directly produced by microbes, as

opposed to their formation being a function of decomposition of more labile molecules in the water column. Further analysis, including GC-MS or NMR could be used to target specific organic molecules, such as carboxyl rich alicyclic molecules, to determine their concentrations in lysate and their affinity for trace metals.

Viruses are an important element in the production of DOC, however their metal binding abilities are very poorly understood despite their abundance and importance in microbial food webs. Future studies could investigate the surface reactivity of viruses as well as the impacts of viruses on the cycling of trace elements caused by cellular lysis.

Increased nutrient and contaminant supplies to aquatic environments due to anthropogenic activities will also need to be considered in future studies, as this will continue to change the way oceanographic models are interpreted. Furthermore, global climate change will affect the interactions between the oceans, atmosphere, geosphere, and biosphere by turning former nutrients sinks into sources, as is the case for marine CO_2.

Although there is a great deal of studies focusing on the trace element inventories of ancient sediments including BIF and black shales to determine the presence of oxygen and timing of the GOE, more work needs to be done to constrain trace metal abundances throughout the Precambrian. These studies can be supplemented by proteomic and genomic studies to determine the utilization of trace elements in metabolisms through time to find a connection between the geochemistry of the oceans and how this influenced the evolution of metalloenzymes, and by extension, life.

Ultimately, the goal of these studies is to increase our understanding of marine processes in modern settings which will allow us to determine the relationships between abiotic and biotic factors. These studies are also important for studying deep time and the Precambrian oceans, as

the famous geologist Charles Lyell first put forward, “The present is the key to the past.” Therefore, by understanding current processes, we will be able to better understand ancient earth processes and it how led to important events in geological history such as the Great Oxidation Event and the proliferation of life.

References

Borrok D., Turner B. F. and Fein J. B. (2005) A universal surface complexation framework for modeling proton binding onto bacterial surfaces in geologic settings. *Am. J. Sci.* **305**, 826–853.

Bruland K. W., Middag R. and Lohan M. C. (2014) *Controls of Trace Metals in Seawater*. 2nd ed., Elsevier Ltd. Available at: http://dx.doi.org/10.1016/B978-0-08-095975-7.00602-1.

Daughney C. J., Fein J. B. and Yee N. (1998) A comparison of the thermodynamics of metal adsorption onto two common bacteria. *Chem. Geol.* **144**, 161–176.

Fein J. B., Daughney C. J., Yee N. and Davis T. A. (1997) A chemical equilibrium model for metal adsorption onto bacterial surfaces. *Geochim. Cosmochim. Acta* **61**, 3319–3328.

Halevy I. and Bachan A. (2017) The Geologic History of Seawater. *Science.* **355**, 1069–1071.

Irving H. and Williams R. J. P. (1953) The Stability of Transition-metal Complexes.

Kaulbach E. S., Szymanowski J. E. S. and Fein J. B. (2005) Surface complexation modeling of proton and Cd adsorption onto an algal cell wall. *Environ. Sci. Technol.* **39**, 4060–4065.

Lalonde S. V., Amskold L. A., Warren L. A. and Konhauser K. O. (2007) Surface chemical reactivity and metal adsorptive properties of natural cyanobacterial mats from an alkaline hydrothermal spring, Yellowstone National Park. *Chem. Geol.* **243**, 36–52.

Liu Y., Alessi D. S., Owttrim G. W., Petrash D. A., Mloszewska A. M., Lalonde S. V., Martinez R. E., Zhou Q. and Konhauser K. O. (2015) Cell surface reactivity of Synechococcus sp. PCC 7002: Implications for metal sorption from seawater. *Geochim. Cosmochim. Acta* **169**, 30–44.

Martinez R. E., Konhauser K. O., Paunova N., Wu W., Alessi D. S. and Kappler A. (2016) Surface reactivity of the anaerobic phototrophic Fe(II)-oxidizing bacterium Rhodovulum iodosum: Implications for trace metal budgets in ancient oceans and banded iron formations. *Chem. Geol.* **442**, 113–120.

Mishra B., Boyanov M., Bunker B. A., Kelly S. D., Kemner K. M. and Fein J. B. (2010) High- and low-affinity binding sites for Cd on the bacterial cell walls of Bacillus subtilis and Shewanella oneidensis. *Geochim. Cosmochim. Acta* **74**, 4219–4233.

Nell R. M. and Fein J. B. (2017) Influence of sulfhydryl sites on metal binding by bacteria. *Geochim. Cosmochim. Acta* **199**, 210–221.

Schwertmann, U., and Fechter, H., 1982, The point of zero charge of natural and synthetic ferrihydrites and its relation to adsorbed silicate. *Clay Minerals*, **17**, 471–476.

Whitby H., Posacka A. M., Maldonado M. T. and van den Berg C. M. G. (2018) Copper-binding ligands in the NE Pacific. *Mar. Chem.* **204**, 36–48.

Yee N. and Fein J. (2001) Cd adsorption onto bacterial surfaces: A universal adsorption edge? *Geochim. Cosmochim. Acta* **65**, 2037–2042.

Yu Q., Boyanov M. I., Liu J., Kemner K. M. and Fein J. B. (2018) Adsorption of Selenite onto *Bacillus subtilis*: The Overlooked Role of Cell Envelope Sulfhydryl Sites in the Microbial Conversion of Se(IV). *Environ. Sci. Technol.*, acs.est.8b02280

References

Abualhaija M. M., Whitby H. and van den Berg C. M. G. (2015) Competition between copper and iron for humic ligands in estuarine waters. *Mar. Chem.* **172**, 46–56.

Achterburg E. P. and Van Den Berg C. M. G. (1997). Chemical speciation of chromium and nickel in the western Mediterranean. *Deep Sea Res. Part 2*, **44**, 693-720.

Alam Md. S., Swaren L., von Gunten, K., Cossio M., Bishop B., Robbins L. J., Hou D., Flynn S. L., Ok Y. S., Konhauser K. O., Alessi D. S. (2018) Application of surface complexation modeling to trace metals uptake by biochar-amended agricultural soils. *App. Geochem.* **88**, 103-112.

Alessi D. S., Henderson J. M., Fein J. B. (2010) Experimental Measurement of Monovalent Cation Adsorption onto Bacillus subtilis Cells. *Geomicrobiol. J.* **27**, 464–472.

Aluwihare L. I. and Repeta D. J. (1999) A comparison of the chemical characteristics of oceanic DOM and extracellular DOM produced by marine algae. *Mar. Ecol. Prog. Ser.* **186**, 105–117.

Amon R. M. W. and Benner R. (1994) Rapid cycling of high-molecular-weight dissolved organic matter in the ocean. *Nature* **369**, 549–552.

Anderson T. R. and Tang K. W. (2010) Carbon cycling and POC turnover in the mesopelagic zone of the ocean: Insights from a simple model. *Deep. Res. Part II Top. Stud. Oceanogr.* **57**, 1581–1592.

Arrieta J. M., Mayol E., Hansman R. L., Herndl G. J., Dittmar T. and Duarte C. M. (2015) Dilution limits dissolved organic carbon utilization in the deep ocean. *Science.* **348**, 331–333.

Azam F., Fenchel T., Field J. G., Gray J. S., Meyer-Reil L. A. and Thingstad F. (1983) The Ecological Role of Water-Column Microbes in the Sea. *Mar. Ecol. Prog. Ser.* **10**, 257–263.

Banerjee R. and Ragsdale S. W. (2003) The Many Faces of Vitamin B 12: Catalysis by Cobalamin-Dependent Enzymes. *Annu. Rev. Biochem.* **72**, 209–247.

Benner R. (2002) Chemical composition and reactivity. In *Biogeochemistry of marine dissolved organic matter.* Elsevier Inc. pp. 59–90.

Benner R. and Amon R. M. W. (2015) The Size-Reactivity Continuum of Major Bioelements in the Ocean. *Ann. Rev. Mar. Sci.* **7**, 185–205.

Benner R., Pakulski J. D., Mccarthy M., Hedges J. I. and Hatcher P. G. (1992) Bulk Chemical Characteristics of Dissolved Organic Matter in the Ocean. *Science.* **255**, 1561–1564.

Benning L. G., Phoenix V. R., Yee N. and Konhauser K. O. (2004) The dynamics of

cyanobacterial silicification: An infrared micro-spectroscopic investigation. *Geochim. Cosmochim. Acta* **68**, 743–757.

Beveridge T. J. and Murray R. G. E. (1980) Sites of metal deposition in the cell wall of Bacillus subtilis. *J. Bacteriol.* **141**, 876–887.

Bjerrum C. J. and Canfield D. E. (2002) Ocean productivity before about 1.9 Gyr ago limited by phosphorus adsorption onto iron oxides. *Nature* **417**, 159-162

Bjørnsen P. K. (1988). Phytoplankton exudation of organic matter: why do healthy cells do it? *Limnol. Oceanogr.* **33**, 151-154.

Boiteau R. M., Mende D. R., Hawco N. J., McIlvin M. R., Fitzsimmons J. N., Saito M. A., Sedwick P. N., DeLong E. F. and Repeta D. J. (2016) Siderophore-based microbial adaptations to iron scarcity across the eastern Pacific Ocean. *Proc. Natl. Acad. Sci.* **113**, 14237–14242.

Boiteau R. M., Mende D. R., Hawco N. J., McIlvin M. R., Fitzsimmons J. N., Saito M. A., Sedwick P. N., DeLong E. F. and Repeta D. J. (2016) Siderophore-based microbial adaptations to iron scarcity across the eastern Pacific Ocean. *Proc. Natl. Acad. Sci.* **113**, 14237–14242.

Borrok D., Turner B. F. and Fein J. B. (2005) A universal surface complexation framework for modeling proton binding onto bacterial surfaces in geologic settings. *Am. J. Sci.* **305**, 826–853.

Boyd P. W., Ellwood M. J., Tagliabue A. and Twining B. S. (2017) Biotic and abiotic retention, recycling and remineralization of metals in the ocean. *Nat. Geosci.* **10**, 167–173.

Bruland K. W. (1980) Oceanographic distributions of cadmium, zinc, nickel, and copper in the North Pacific. *Earth Planet. Sci. Lett.* **47**, 176–198.

Bruland K. W., Middag R, and Lohan M. C. (2014) Controls of Trace Metals in Seawater. In *Treatise on Geochemistry: 2nd edition*. 19–51. Elsevier Ltd.

Bruland K. W. and Lohan M. C. (2003) Controls of Trace Metals in Seawater. In *Treatise on Geochemistry* pp. 19–51.

Bruland K. W., Donat J. R. and Hutchins D. A. (1991) Interactive influences of bioactive trace metals on biological production in oceanic waters. *Limnol. Oceanogr.* **36**, 1555–1577.

Bruland K. W. and Franks R. P. (1983) Mn, Ni, Cu, Zn, and Cd in the western North Atlantic. In *Trace Metals in Seawater*. Plenum, New York. 395-414.

Bundy R. M., Abdulla H. A. N., Hatcher P. G., Biller D. V., Buck K. N. and Barbeau K. A. (2015) Iron-binding ligands and humic substances in the San Francisco Bay estuary and estuarine-influenced shelf regions of coastal California. *Mar. Chem.* **173**, 183–194.

Byrne R. H. (2002) Inorganic speciation of dissolved elements in seawater: the influence of pH on concentration ratios. *Geochem. Trans.* **2**, 11.

Canfield D. E. (1998) A new model for Proterozoic ocean chemistry. *Nature* **396**, 450–453.

Carlson C. A. and Hansell D. A. (2014) *DOM Sources, Sinks, Reactivity, and Budgets* in Biogeochemistry of Marine Dissolved Organic Matter: Second Edition. Elsevier Inc.

Carlson C. A., Giovannoni S. J., Hansell D. A., Goldberg S. J., Parsons R. and Vergin K. (2004) Interactions among dissolved organic carbon, microbial processes, and community structure in the mesopelagic zone of the northwestern Sargasso Sea. *Limnol. Oceanogr.* **49**, 1073–1083.

Cavet J. S., Borrelly G. P. M. and Robinson N. J. (2003) Zn, Cu and Co in cyanobacteria: Selective control of metal availability. *FEMS Microbiol. Rev.* **27**, 165–181.

Chi Fru E. (2011) Copper biogeochemistry: A cornerstone in aerobic methanotrophic bacterial ecology and activity? *Geomicrobiol. J.* **28**, 601–614.

Chi Fru E., Rodríguez N. P., Partin C. A., Lalonde S. V, Andersson P., Weiss D. J., El Albani A., Rodushkin I. and Konhauser K. O. (2016) Cu isotopes in marine black shales record the Great Oxidation Event. *Proc. Natl. Acad. Sci.* **113**, 4941–4946.

Clark L. L., Ingal E. D. and Benner R. (1998) Marine phorphorus is selectively remineralized. *Nature* **393,** 426

Coale K. H. and Bruland K. W. (1988) Copper complexation in the Northeast Pacific. *Limnol. Oceanogr.* **33**, 1084–1101.

Coates J. (2000) Interpretation of Infrared Spectra, A Practical Approach. *Encycl. Anal. Chem.*, 10815–10837.

Cox J. S., Smith D. S., Warren L. A. and Ferris F. G. (1999) Characterizing heterogeneous bacterial surface functional groups using discrete affinity spectra for proton binding. *Environ. Sci. Technol.* **33**, 4514–4521.

Daughney C. J., Fein J. B. and Yee N. (1998) A comparison of the thermodynamics of metal adsorption onto two common bacteria. *Chem. Geol.* **144**, 161–176.

David L. A. and Alm E. J. (2011) Rapid evolutionary innovation during an Archaean genetic expansion. *Nature* **469**, 93–96.

Dittmar T. and Stubbins A. (2014) Dissolved Organic Matter in Aquatic Systems. In *Treatise on Geochemistry 2nd ed*. 125-156. Elsevier Ltd.

Dittmar T. and Paeng J. (2009) A heat-induced molecular signature in marine dissolved organic matter. *Nat. Geosci.* **2**, 175–179.

Dittrich M. and Sibler S. (2005) Cell surface groups of two picocyanobacteria strains studied by zeta potential investigations, potentiometric titration, and infrared spectroscopy. *J. Colloid and Interface Sci.* **286**, 487–495.

Donat J. R., Lao K. A. and Bruland K. W. (1994) Speciation of dissolved copper and nickel in South San Francisco Bay: a multi-method approach. *Anal. Chim. Acta* **284**, 547–571.

Druffel E. R. M., Griffin S., Coppola A. I. and Walker B. D. (2016) Radiocarbon in dissolved organic carbon of the Atlantic Ocean. *Geophys. Res. Lett.* **43**, 5279–5286.

Du H., Chen W., Cai P., Rong X., Feng X. and Huang Q. (2016) Competitive adsorption of Pb and Cd on bacteria–montmorillonite composite. *Environ. Pollut.* **218**, 168–175.

Dupont C. L., Butcher A., Valas R. E., Bourne P. E. and Caetano-Anollés G. (2010) History of biological metal utilization inferred through phylogenomic analysis of protein structures. *Proc. Natl. Acad. Sci.* **107**, 10567–10572.

Dupont C. L., Neupane K., Shearer J. and Palenik B. (2008) Diversity, function and evolution of genes coding for putative Ni-containing superoxide dismutases. *Environ. Microbiol.* **10**, 1831–1843.

Dupont C. L., Yang S., Palenik B. and Bourne P. E. (2006) Modern proteomes contain putative imprints of ancient shifts in trace metal geochemistry. *Proc. Natl. Acad. Sci. U. S. A.* **103**, 17822-17827.

Dupont C. L., Nelson R. K., Bashir S., Moffett J. W. and Ahner B. A. (2004) Novel copper-binding and nitrogen-rich thiols produced and exuded by Emiliania huxleyi. *Limnol. Oceanogr.* **49**, 1754–1762.

Ellwood M. J. and Van den Berg C. M. G. (2001) Determination of organic complexation of cobalt in seawater by cathodic stripping voltammetry. *Mar. Chem.* **75**, 33–47.

Engel A., Thoms S., Riebesell U., Rochelle-Newall E. and Zondervan I. (2004) Polysaccharide aggregation as a potential sink of marine dissolved organic carbon. *Nature* **428**, 929–932.

Falkowski P. G., Barber R. T. and Smetacek V. (1998). Biogeochemical controls and feedbacks on ocean primary production. *Science.* **281**, 200–206.

Fatayer S., Coppola A. I., Schulz F., Walker B. D., Broek T. A., Meyer G., Druffel E. R. M., McCarthy M. and Gross L. (2018) Direct Visualization of Individual Aromatic Compound Structures in Low Molecular Weight Marine Dissolved Organic Carbon. *Geophys. Res. Lett.*, 1–9.

Fein J. B. (2017) Advanced biotic ligand models: Using surface complexation modeling to quantify metal bioavailability to bacteria in geologic systems. *Chem. Geol.* **464**, 127–136.

Fein J. B. (2006) Thermodynamic Modeling of Metal Adsorption onto Bacterial Cell Walls: Current Challenges. *Adv. Agron.* **90**, 179–202.

Fein J. B., Daughney C. J., Yee, N., Davis T. A. (1997) A chemical equilibrium model for metal adsorption onto bacterial surfaces. *Geochim. Cosmochim. Acta.* **61** (16), 3319-3328

First, M.R. and Hollibaugh, J.T. (2009). The model high molecular weight DOC compound, dextran, is ingested by the benthic ciliate Uronema marinum but does not supplement ciliate growth. *Aquat. Microb. Ecol*. **57**, 79.

Fisher N. S. (1985) Accumulation of metals by marine phytoplankton. *Mar. Biol.* **87**, 137–142.

Flynn S. L., Szymanowski J. E. S. and Fein J. B. (2014) Modeling bacterial metal toxicity using a surface complexation approach. *Chem. Geol.* **374**–**375**, 110–116.

Fogg G. (1983). The ecological significance of extracellular products of phytoplankton. *Bot. Mar.* **26**. 3-14

Fogg G. (1966). The extracellular products of algae. *Oceanogr. Mar. Bio. Annu. Rev.* **4**, 195-212

Fowle D. A. and Fein J. B. (2000) Experimental measurements of the reversibility of metal-bacteria adsorption reactions. *Chem. Geol.* **168**, 27–36.

Fowle D. A. and Fein J. B. (1999) Competitive adsorption of metal cations onto two gram positive bacteria: Testing the chemical equilibrium model. *Geochim. Cosmochim. Acta.* **63**, 3059–3067.

Gardner WD, Mishonov AV, Richardson MJ. (2006). Global POC concentrations from in-situ and satellite data. *Deep-Sea Res. II.* **53,** 718–740

Gélabert A., Pokrovsky O. S., Schott J. and Feurtet-Mazel A. (2018) Surface complexation modeling of interactions between freshwater and marine diatom species and trace elements (Mo, W, Cr, Ge, Ga, Al). *Chem. Geol.* **494**, 117–126.

Gonzalez-Davila M., Magdalena Santana-Casiano J., Perez-Peña J. and Millero F. J. (1995) Binding of Cu(II) to the Surface and Exudates of the Alga Dunaliella tertiolecta in Seawater. *Environ. Sci. Technol.* **29**, 289–301.

Hadjoudja, S., Deluchat, V. and Baudu, M. (2010). Cell surface characterization of *Microcystis aeruginosa* and *Chlorella vulgaris*. *J. Colloid Interface Sci.* **342,** 293-299.

Halevy I. and Bachan A. (2017) The Geologic History of Seawater. *Science.* **355**, 1069–1071.

Hansell D. A., Carlson C. A. and Schlitzer R. (2012) Net removal of major marine dissolved organic carbon fractions in the subsurface ocean. *Global Biogeochem. Cycles* **26**, 1–9.

Hansell D., Carlson C., Repeta D. and Schlitzer R. (2009) Dissolved Organic Matter in the Ocean: A Controversy Stimulates New Insights. *Oceanography* **22**, 202–211.

Hao W., Flynn S. L., Alessi D. S. and Konhauser K. O. (2018) Change of the point of zero net proton charge (pHPZNPC) of clay minerals with ionic strength. *Chem. Geol.* **493**, 458–467.

Hausinger R. P. (1987) Nickel utilization by microorganisms. *Microbiol. Rev.* **51**, 22–42.

Hedges J. I. (1992) Global Biogeochemical Cycles - Progress and Problems. *Mar. Chem.* **39**, 67–93.

Hedges J. I. (1987) Organic matter in sea water. *Nature* **330**, 205–206.

Hedges J. I., Eglinton G., Hatcher P. G., Kirchman D. L., Arnosti C., Derenne S., Evershed R. P., K.ogel-Knabner I., de Leeuw J. W., Littke R., Michaelis W. and Rullkotter J. (2000) The molecularly uncharacter ized component of nonliving organic matter in natural environments. *Org. Geochem.* **31**, 945–958.

Hedges J. I., Keil R. G. and Benner R. (1997) What happens to terrestrial organic matter in the ocean? *Org. Geochem.* **27**, 195–212.

Herbelin A. L. and Westall J. C. (1999). FITEQL 4.0: A computer program for determination of chemical equilibrium constants from experimental data.

Hertkorn N., Benner R., Frommberger M., Schmitt-Kopplin P., Witt M., Kaiser K., Kettrup A. and Hedges J. I. (2006) Characterization of a major refractory component of marine dissolved organic matter. *Geochim. Cosmochim. Acta* **70**, 2990–3010.

Ho T.-Y., Quigg A., Finkel Z. V., Milligan A. J., Wyman K., Falkowski P. G. and Morel F. M. M. (2003) The elemental composition of some marine phytoplankton. *J. Phycol.* **39**, 1145–1159.

Hopkinson C. S. and Vallino J. J. (2005) Efficient export of carbon to the deep ocean through dissolved organic matter. *Nature* **433**, 142–145.

Hopkinson C. S., Vallino J. J. and Nolin A. (2002) Decomposition of dissolved organic matter from the continental margin. *Deep. Res. Part II Top. Stud. Oceanogr.* **49**, 4461–4478.

Hunter K. A., Kim J. P. and Croot P. L. (1997) Biological roles of trace metals in natural waters. *Environ. Monit. Assess.* **44**, 103-147.

Irving H. and Williams R. J. P. (1953). The Stability of Transition-metal Complexes. *J. Chem. Soc.* **0**, 3192-3210

Jiang W., Saxena A., Song B., Ward B. B., Beveridge T. J. and Myneni S. C. B. (2004) Elucidation of Functional Groups on Gram-Positive and Gram-Negative Bacterial Surfaces Using Infrared Spectroscopy. *Langmuir* **20**, 11433–11442.

Jiao N., Robinson C., Azam F., Thomas H., Baltar F., Dang H., Hardman-Mountford N. J., Johnson M., Kirchman D. L., Koch B. P., Legendre L., Li C., Liu J., Luo T., Luo Y. W., Mitra A., Romanou A., Tang K., Wang X., Zhang C. and Zhang R. (2014) Mechanisms of microbial carbon sequestration in the ocean; Future research directions. *Biogeosciences* **11**, 5285–5306.

Jiao N., Herndl G. J., Hansell D. A., Benner R., Kattner G., Wilhelm S. W., Kirchman D. L., Weinbauer M. G., Luo T., Chen F. and Azam F. (2010) Microbial production of recalcitrant dissolved organic matter: Long-term carbon storage in the global ocean. *Nat. Rev. Microbiol.* **8**, 593–599.

Kaiser K. and Benner R. (2009). Biochemical composition and size distribution of organic matter at the Pacific and Atlantic time-series stations. *Mar. Chem.* **113**, 63–77.

Kaulbach E. S., Szymanowski J. E. S. and Fein J. B. (2005) Surface complexation modeling of proton and Cd adsorption onto an algal cell wall. *Environ. Sci. Technol.* **39**, 4060–4065.

Kim S., Kramer R. W. and Hatcher P. G. (2003) Graphical Method for Analysis of Ultrahigh-Resolution Broadband Mass Spectra of Natural Organic Matter, the Van Krevelen Diagram. *Anal. Chem.* **75**, 5336–5344.

Koch B. P., Witt M., Engbrodt R., Dittmar T. and Kattner G. (2005) Molecular formulae of marine and terrigenous dissolved organic matter detected by electrospray ionization Fourier transform ion cyclotron resonance mass spectrometry. *Geochim. Cosmochim. Acta* **69**, 3299–3308.

Konhauser K. O., Robbins L. J., Alessi D. S., Flynn S. L., Gingras M. K., Martinez R. E., Kappler A., Swanner E. D., Li Y. L., Crowe S. A., Planavsky N. J., Reinhard C. T. and Lalonde S. V. (2018) Phytoplankton contributions to the trace-element composition of Precambrian banded iron formations. *Bull. Geol. Soc. Am.* **130**, 941–951.

Konhauser K. O., Robbins L. J., Pecoits E., Peacock C., Kappler A., Lalonde S. V. (2015) The Archean Nickel Famine Revisited. *Astrobiology* **15**, 804-815

Konhauser K. O., Lalonde S. V., Planavsky N. J., Pecoits E., Lyons T. W., Mojzsis S. J., Rouxel O. J., Barley M. E., Rosiere C., Fralick P. W., Kump L. R., Bekker A. (2011) Aerobic bacterial pyrite oxidation and acid rock drainage during the Great Oxidation Event. *Nature*. **478**, 369-373.

Konhauser K. O., Pecoits E., Lalonde S. V., Papineau D., Nisbet E. G., Barley M. E., Arndt N. T., Zahnle K. and Kamber B. S. (2009) Oceanic nickel depletion and a methanogen famine before the Great Oxidation Event. *Nature* **458**, 750-753.

Konhauser K. O., Lalonde S. V., Amskold L. and Holland H. D. (2007) Was There Really an Archean Phosphate Crisis? *Science Brevia* **315**, 1234.

Konhauser K. O., Hamade T., Raiswell R., Morris R. C., Ferris F. G., Southam G. and Canfield D. E. (2002) Could bacteria have formed the Precambrian banded iron formations? *Geology.* **30**, 1079-1082

Konhauser K. O., Fisher Q. J., Fyfe W. S., Longstaffe F. J. and Powell M. A. (1998) Authigenic mineralization and detrital clay binding by freshwater biofilms: The Brahmani river, India. *Geomicrobiol. J.* **15**, 209–222.

Konhauser K. O., Fyfe W. S., Ferris F. G. and Beveridge T. J. (1993) Metal sorption and mineral precipitation by bacteria in two Amazonian river systems: Rio Solimoes and Rio Negro, Brazil. *Geology* **21**, 1103–1106.

Lalonde S. V., Dafoe L. T., Pemberton S. G., Gingras M. K. and Konhauser K. O. (2010) Investigating the geochemical impact of burrowing animals: Proton and cadmium adsorption onto the mucus lining of Terebellid polychaete worms. *Chem. Geol.* **271**, 44–51.

Lalonde S. V., Smith D. S., Owttrim G. W., Konhauser K. O. (2008a) Acid-base properties of cyanobacterial surfaces. II: Silica as a chemical stressor influencing cell surface reactivity. *Geochim. Cosmochim. Acta* **72**, 1269–1280.

Lalonde S. V., Smith D. S., Owttrim G. W., Konhauser K. O. (2008b) Acid-base properties of cyanobacterial surfaces I: Influences of growth phase and nitrogen metabolism on cell surface reactivity. *Geochim. Cosmochim. Acta* **72**, 1257–1268.

Lalonde S. V., Amskold L. A., Warren L. A. and Konhauser K. O. (2007) Surface chemical reactivity and metal adsorptive properties of natural cyanobacterial mats from an alkaline hydrothermal spring, Yellowstone National Park. *Chem. Geol.* **243**, 36–52.

Lampert W. (1978). Release of dissolved organic carbon by grazing zooplankton. *Limnol. Oceanogr.* **23**, 831-834.

Leão P. N., Vasconcelos M. T. S. D. and Vasconcelos V. M. (2007) Role of marine cyanobacteria in trace metal bioavailability in seawater. *Microb. Ecol.* **53**, 104–109.

Lipscomb W. N. and Sträter N. (1996) Recent advances in zinc enzymology. *Chem. Rev.* **96**, 2375–2433.

Liu Y., Alessi D. S., Owttrim G. W., Petrash D. A., Mloszewska A. M., Lalonde S. V., Martinez R. E., Zhou Q. and Konhauser K. O. (2015) Cell surface reactivity of Synechococcus sp. PCC 7002: Implications for metal sorption from seawater. *Geochim. Cosmochim. Acta* **169**, 30–44

Martinez R. E., Konhauser K. O., Paunova N., Wu W., Alessi D. S. and Kappler A. (2016) Surface reactivity of the anaerobic phototrophic Fe(II)-oxidizing bacterium Rhodovulum iodosum: Implications for trace metal budgets in ancient oceans and banded iron formations. *Chem. Geol.* **442**, 113–120.

Mishra B., Boyanov M., Bunker B. A., Kelly S. D., Kemner K. M. and Fein J. B. (2010) High- and low-affinity binding sites for Cd on the bacterial cell walls of Bacillus subtilis and Shewanella oneidensis. *Geochim. Cosmochim. Acta* **74**, 4219–4233.

Moffett J. W. and Brand L. E. (1996) Production of strong, extracellular Cu chelators by marine cyanobacteria in response to Cu stress. *Limnology and Oceanography.* **41**(3), 388–395.

Moran M. A., Kujawinski E. B., Stubbins A., Fatland R., Aluwihare L. I., Buchan A., Crump B. C., Dorrestein P. C., Dyhrman S. T., Hess N. J., Howe B., Longnecker K., Medeiros P. M., Niggemann J., Obernosterer I., Repeta D. J. and Waldbauer J. R. (2016) Deciphering ocean carbon in a changing world. *Proc. Natl. Acad. Sci.* **113**, 3143–3151.

Morel, F. M. M. (2008) The co-evolution of phytoplankton and trace element cycles in the oceans. *Geobiology* **6**, 318–324.

Morel F. M. M., Milligan A. J. and Saito M. A. (2014) Marine Bioinorganic Chemistry: The Role of Trace Metals in the Oceanic Cycles of Major Nutrients. in *Treatise on Geochemistry: 2nd edition.* 123–150. Elsevier Ltd.

Morel F.M. M. and Price N. (2003) The biogeochemical cycles of trace metals in the ocean. *Science* **300**, 944–947.

Morel F. M. M., Reinfelder J. R., Roberts S. B., Chamberlain C. P., Lee J. G. and Yee D. (1994) Zinc and carbon co-limitation of marine phytoplankton. *Nature* **369**, 740–742.

Morel, F. M. M., Hudson, R. J. M., Price, N. M. (1991) Limitation of productivity by trace metals in the sea. *Limnology and Oceanography.* **36** (8), 1742–1755.

Mullen M. D., Wolf D. C., Ferris F. G., Beveridge T. J., Flemming C. A. and Bailey G. W. (1989) Bacterial sorption of heavy metals. *Appl. Environ. Microbiol.* **55**, 3143–3149.

Nagata T. (2000). Production mechanisms of dissolved organic matter. In: *Microbial Ecology of the Oceans*. Wiley-Liss, New York, pp. 121–152.

Naumann D. (2000) Infrared Spectroscopy in Microbiology. *Encycl. Anal. Chem.*, 1–32.

Neihof R. A. and Loeb G. I. (1972) The Surface Charge of Particulate Matter in Seawater. *Limnol. Oceanogr.* **17**, 7–16.

Neilands J. B. (1995) Siderophores: Structure and Function of Microbial Iron Transport Compounds. *J. Biol. Chem.* **270**, 26723–26726.

Nell R. M. and Fein J. B. (2017) Influence of sulfhydryl sites on metal binding by bacteria. *Geochim. Cosmochim. Acta* **199**, 210–221.

Ogawa H., Amagai Y., Koike I., Kaiser K. and Benner R. (2001) Production of refractory dissolved organic matter by bacteria. *Science (80-.).* **292**, 917–920.

Partin C. A., Lalonde S. V., Planavsky N. J., Bekker A., Rouxel O. J., Lyons T. W. and Konhauser K. O. (2013a) Uranium in iron formations and the rise of atmospheric oxygen. *Chem. Geol.* **362**, 82-90.

Partin C. A., Bekker A., Planavsky N. J., Scott C. T., Gill B. C., Li C., Podkovyrov V., Maslov A., Konhauser K. O., Lalonde S. V., Love G. D., Poulton S. W. and Lyons T. W. (2013b) Large-scale fluctuations in Precambrian atmospheric and oceanic oxygen levels from the record of U in shales. *Earth Planet. Sci. Lett.* **369-370**, 284-293.

Petrash D. A., Lalonde S. V, Gingras M. K. and Konhauser K. O. (2011) A Surrogate Approach to Studying the Chemical Reactivity of Burrow Mucous Linings in Marine Sediments. *Palaios* **26**, 594–600.

Playter T., Konhauser K., Owttrim G., Hodgson C., Warchola T., Mloszewska A. M., Sutherland B., Bekker A., Zonneveld J. P., Pemberton S. G. and Gingras M. (2017) Microbe-clay interactions as a mechanism for the preservation of organic matter and trace metal biosignatures in black shales. *Chem. Geol.* **459**, 75–90.

Poorvin L., Rinta-Kanto J. M., Hutchins D. A. and Wilhelm S. W. (2004) Viral release of iron and its bioavailability to marine plankton. *Limnol. Oceanogr.* **49**, 1734–1741.

Price, N. M. and Morel, F. M. M. (1990) Cadmium and cobalt substitution for zinc in a marine diatom. *Nature* **344**, 658–660.

Robbins L. J., Lalonde S. V., Planavsky N. J., Partin C. A., Reinhard C. T., Kendall B., Scott C., Hardisty D. S., Gill B. C., Alessi D. S., Dupont C. L., Saito M. A., Crowe S. A., Poulton S. W., Bekker A., Lyons T. W. and Konhauser K. O. (2016) Trace elements at the intersection of marine biological and geochemical evolution. *Earth-Science Rev.* **163**, 323–348.

Robbins L. J., Lalonde S. V., Saito M. A., Planavsky N. J., Mloszewska A. M., Pecoits E., Scott C., Dupont C. L., Kappler A., Konhauser K. O. (2013) Authigenic iron oxide proxies for marine zinc over geological time and implications for eukaryotic metallome evolution. *Geobiol.* **11**, 295-306.

Rothman D. H., Hayes J. M. and Summons R. E. (2003) Dynamics of the Neoproterozoic carbon cycle. *Proc. Natl. Acad. Sci.* **100**, 8124–8129.

Safari S., Sheikhi A. and van de Ven T. G. M. (2014) Electroacoustic characterization of conventional and electrosterically stabilized nanocrystalline celluloses. *J. Colloid Interface Sci.* **432**, 151–157.

Saito M. A., Sigman D. M. and Morel F. M. M. (2003) The bioinorganic chemistry of the ancient ocean: The co-evolution of cyanobacterial metal requirements and biogeochemical cycles at the Archean-Proterozoic boundary? *Inorganica Chim. Acta* **356**, 308–318.

Saito M. A. and Moffett J. W. (2002) Temporal and spatial variability of cobalt in the Atlantic Ocean. *Geochim. Cosmochim. Acta* **66**, 1943–1953.

Saito M. A. and Moffett J. W. (2001) Complexation of cobalt by natural organic ligands in the Sargasso Sea as determined by a new high-sensitivity electrochemical cobalt speciation method suitable for open ocean work. *Mar. Chem.* **75**, 49–68.

Sañudo-Wilhelmy, S. A., Tovar-Sanchez, A., Fu, F., Capone, D. G., Carpenter, E. J., Hutchins, D. A. (2004). The impact of surface-adsorbed phosphorus on phytoplankton Redfield stoichiometry. *Nature*. **432**, 897-901.

Sarmiento J. L., Herbert T. D. and Toggweiler J. R. (1988) Causes of anoxia in the world ocean. *Glob. Biogeochem. Cycles1* **2**, 115–128.

Schmidt F., Elvert M., Koch B. P., Witt M. and Hinrichs K.-U. (2009) Molecular characterization of dissolved organic matter in pore water of continental shelf sediments. *Geochim. Cosmochim. Acta* **73**, 3337–3358.

Scott C., Planavsky N. J., Dupont C. L., Kendall B., Gill B. C., Robbins L. J., Husband K. F., Arnold G. L., Wing B. A., Poulton S. W., Bekker A., Anbar A. D., Konhauser K. O. and Lyons T. W. (2013) Bioavailability of zinc in marine systems through time. *Nat. Geosci.* **6**, 125–128.

Scott C., Lyons T. W., Bekker A., Shen Y., Pouton S. W., Chu X. and Anbar A. D. (2008) Tracing the stepwise oxygenation of the Proterozoic ocean. *Nature*. **452**, 456-459.

Schwertmann, U., and Fechter, H., 1982, The point of zero charge of natural and synthetic ferrihydrites and its relation to adsorbed silicate. *Clay Minerals*, **17**, 471–476.

Spark K. M., Wells J. D. and Johnson B. B. (1995) Characterizing trace metal adsorption on kaolinite. *Eur. J. Soil Sci.* **46**, 633–640.

Stevens S. and Van Baalen C. (1973) Characteristics of nitrate reductions in a mutant of the blue-green alga *Agmenellum quadruplicatum. Plant Physiol.* **51**, 350-356.

Stevens S. E. and Porter R. D. (1980) Transformation in *Agmenellum quadriplicatum. Proc. Natl. Acad. Sci. U.S.A.* **77**, 6052-6056.

Sunda W. G. (2012) Feedback interactions between trace metal nutrients and phytoplankton in the ocean. *Front. Microbiol.* **3**, 1-22

Sunda W. G. and Huntsman S. A. (1995) Cobalt and zinc interreplacement in marine phytoplankton: Biological and geochemical implications. *Limnol. Oceanogr.* **40**, 1404–1417.

Suttle C. A. (2007) Marine viruses - Major players in the global ecosystem. *Nat. Rev. Microbiol.* **5**, 801–812.

Swanner E. D., Planavsky N. J., Lalonde S. V., Robbins L. J., Bekker A., Rouxel O. J., Saito M. A., Kappler A., Mojzsis S. J. and Konhauser K. O. (2014) Cobalt and marine redox evolution. *Earth Planet. Sci. Lett.* **390**, 253–263.

Tanoue E., Nishiyama S., Kamo M. and Tsugita' A. (1995) Bacterial membranes: Possible source of a major dissolved protein in seawater. *Geochim. Cosmochim. Acta* **59**, 2643–2648.

Twining B. S. and Baines S. B. (2013) The trace metal composition of marine phytoplankton. *Annual Review of Marine Science.* **5**, 191–215.

Van Den Berg C. M. G. and Nimmo M. (1987) Determination of interactions of nickel with dissolved organic material in seawater using cathodic stripping voltammetry. *Sci. Total Environ.* **60**, 185–195.

Warchola T. J., Flynn S. L., Robbins L. J., Liu Y., Gauger T., Kovalchuk O., Alam Md. S., Wei S., Myers R., Bishop B., Lalonde S. V, Gingras M. K., Kappler A., Alessi D. S. and Konhauser K. O. (2017) Field-and Lab-Based Potentiometric Titrations of Microbial Mats from the Fairmont Hot Spring. *Geomicrobiol. J.* **34**, 851-863.

Warchola T., Lalonde S. V., Pecoits E., Gunten K. von, Robbins L. J., Alessi D. S., Philippot P. and Konhauser K. O. (2018) Petrology and Geochemistry of the Boolgeeda Iron Formation, Hamersley Basin, Western Australia. *Precambrian Res.*

Waterbury J. B., Watson S. W., Guillard R. R. L. and Brand L. E. (1979) Widespread occurrence of a unicellular, marine, planktonic, cyanobacterium. *Nature* **277**, 293–294.

Whitby H., Posacka A. M., Maldonado M. T. and van den Berg C. M. G. (2018) Copper-binding ligands in the NE Pacific. *Mar. Chem.* **204**, 36–48.

Whitby H. and van den Berg C. M. G. (2015) Evidence for copper-binding humic substances in seawater. *Mar. Chem.* **173**, 282–290.

Wilhelm S. W. and Suttle C. A. (1999) Viruses and Nutrient Cycles in the Sea. *Bioscience* **49**, 781–788.

Williams P. J. L. B. (1990). The importance of losses during microbial growth: commentary on

the physiology, measurement and ecologe of the release of dissolved organic material. *Mar. Microb. Food Webs.* **4**, 175-206.

Williams P. M. and Druffel E. R. M. (1987) Radiocarbon in dissolved organic matter in the central North Pacific Ocean. *Nature* **330**, 246–248.

Worms I., Simon D. F., Hassler C. S. and Wilkinson K. J. (2006) Bioavailability of trace metals to aquatic microorganisms: importance of chemical, biological and physical processes on biouptake. *Biochimie* **88**, 1721–1731.

Yang R. and Van Den Berg C. M. G. (2009) Metal complexation by humic substances in seawater. *Environ. Sci. Technol.* **43**, 7192–7197.

Yee N. and Fein J. (2001) Cd adsorption onto bacterial surfaces: A universal adsorption edge? *Geochim. Cosmochim. Acta* **65**, 2037–2042.

Yee N., Benning L. G., Phoenix V. R. and Ferris F. G. (2004) Characterization of Metal-Cyanobacteria Sorption Reactions: A Combined Macroscopic and Infrared Spectroscopic Investigation. *Environ. Sci. Technol.* **38**, 775–782.

Yu Q., Boyanov M. I., Liu J., Kemner K. M. and Fein J. B. (2018) Adsorption of Selenite onto *Bacillus subtilis*: The Overlooked Role of Cell Envelope Sulfhydryl Sites in the Microbial Conversion of Se(IV). *Environ. Sci. Technol.*, acs.est.8b02280

Zark M., Christoffers J. and Dittmar T. (2017) Molecular properties of deep-sea dissolved organic matter are predictable by the central limit theorem: Evidence from tandem FT-ICR-MS. *Mar. Chem.* **191**, 9–15.

Zehr, J. P. and Ward, B. B. (2002). Nitrogen cycling in the ocean: new perspectives on processes and paradigms. *Appl. Environ. Microbiol.* **68**, 1015–1024.

Ziolkowski L. A. and Druffel E. R. M. (2010) Aged black carbon identified in marine dissolved organic carbon. *Geophys. Res. Lett.* **37**, 1–4.

Supplementary Information

Species or phase	Log K	α
$Cu(OH)^{+}$	-8	-1.022
$Cu(OH)_2$	-17.3	-1.022
$Cu(OH)_3^{-}$	-27.8	0
$Cu(OH)_4^{2-}$	-39.6	2.044
$Cu(OH)_2^{2+}$	-10.36	-1.022

From: Baes and Mesmer (1976)

SI Table 1a: Hydrolysis constants of Cu^{2+} cations used in Cu adsorption and multi-element FITEQL models.

Species or phase	Log K	α
$ZnOH^{+}$	-8.96	-1.022
$Zn(OH)_2$	-16.9	-1.022
$Zn(OH)_3^{-}$	-28.4	0
$Zn(OH)_4^{2-}$	-41.2	2.044
Zn_2OH^{3+}	-9.0	1.022
$Zn_2(OH)_6^{2-}$	-57.8	1.022

From: Baes and Mesmer (1976)

SI Table 1b: Hydrolysis constants of Zn^{2+} cations used in Zn adsorption and multi-element FITEQL models.

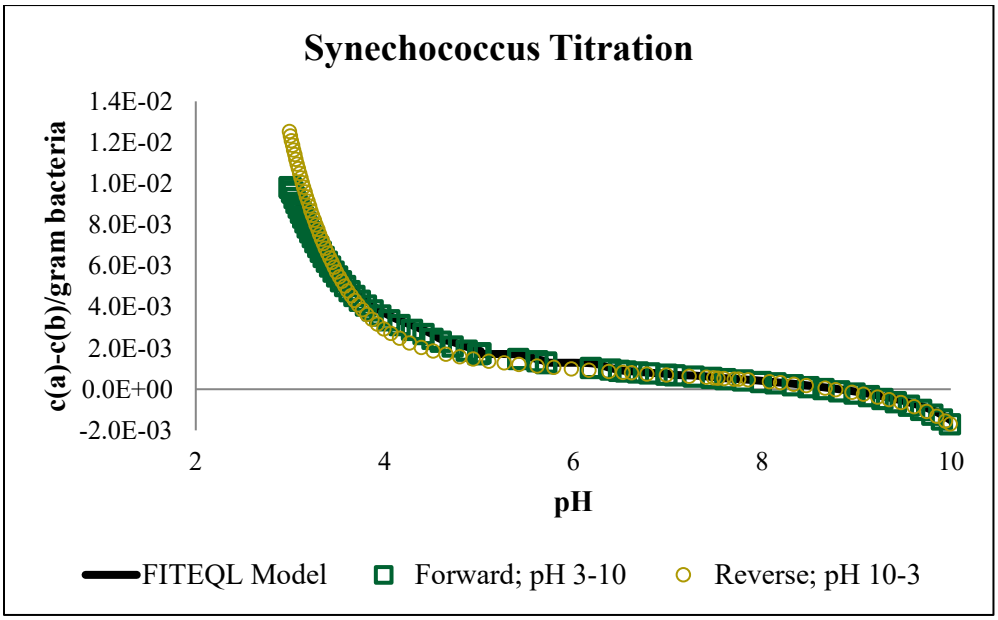

SI Figure 1: Synechococcus titration showing the forward and reverse titrations with the FITEQL model in terms of the concentration of acid added minus the concentration of base added. Forward and reverse titrations are shown to emphasize the limited observed hysteresis between reverse runs.

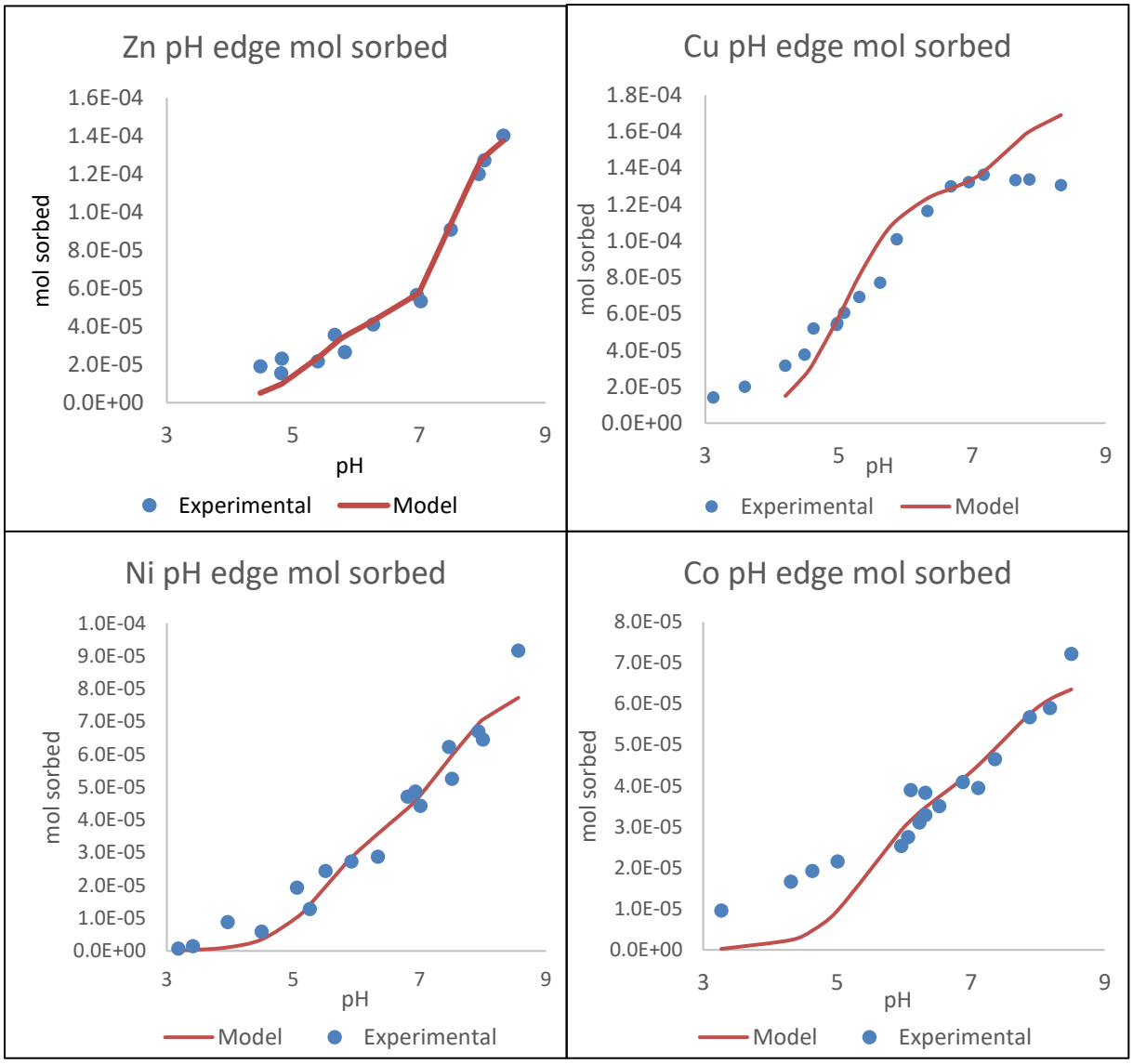

SI Figure 2: Metal adsorption pH edges for *Synechococcus* trace metal experiments in terms of mols of metal adsorbed.